PERFORMANCE AND DESIGN OF PROTOTYPE WOOD-PLASTIC COMPOSITE SECTIONS

By

KEVIN JEROME HAIAR

A thesis submitted in partial fulfillment of
the requirements for the degree of

MASTER OF SCIENCE IN CIVIL ENGINEERING

WASHINGTON STATE UNIVERSITY
Department of Civil and Environmental Engineering

May 2000

CHAPTER 1

INTRODUCTION

1.1 Background and Overview

The benefits of wood as a structural material have long been utilized in marine applications, including fender systems used to protect docking structures and vessels during vessel berthing. In the past, preservative-treated timber has been a commonly used material for structural elements in fender systems. Due to degradation from marine borers and the placement of environmental restrictions on the use of preservative-treated wood, an alternative material is sought to replace the wood members. The U.S. Office of Naval Research funded a project at Washington State University to investigate the use of wood-plastic composite (WPC) lumber as an alternative to the traditional timber members. The benefits of WPC lumber include resistance to marine borers and rot, reduced environmental impact due to the absence of preservative treatments, and members can be produced in hollow net sections. In addition, as manufacturing processes and material composition are refined, reduced production costs will enable the WPC material to become a viable option for many structural applications.

The information presented in this thesis is part of an ongoing comprehensive research project being conducted at Washington State University to develop wood-based composite members for waterfront structures. The project consists of four major components: materials development, structural analysis and design, recycling, and a demonstration component for validation of the technology and products.

The objectives of the structural design and analysis component are to support the materials development by providing estimates for structural demand, identifying components of existing waterfront facilities as targets for application of composite materials, establishing design

criteria, verifying through testing component performance, and facilitating the implementation of both drop-in replacements and complete waterfront systems utilizing engineered wood-plastic composites. The specific contributions to these objectives reported in this thesis include conducting tests of prototype components to characterize performance, developing standard criteria for component evaluation and assignment of design values, providing guidance for design of specific demonstration applications, and developing analytical models for understanding the behavior of WPC structural members.

In order to design with WPC material, strength properties must be quantified and the material behavior must be understood. As the material contains considerable amounts of plastic and is subject to heightened creep during loading, load rates for standard timber strength tests are not appropriate. Standard tests for WPC material were proposed and used to determine material strength properties for structural sections. The proposed test procedures are based primarily on standard methods for determining strength properties in wood and plastic. Tests were conducted on near full-size WPC specimens to determine compression perpendicular-to-extrusion, compression parallel-to-extrusion, modulus of rupture, shear, puncture, and impact resistance strengths for prototype wood-plastic composite members. Allowable design value assignment procedures are proposed for WPC materials and were applied to the experimental results obtained from the tests of near full-size WPC specimens to obtain allowable design values for HDPE and PVC formulations. These allowable design values were used in the design of prototype components for demonstration applications of this project.

A Fortran program (MPHIWPC) was developed to characterize behavior of WPC beam sections. The program uses constitutive stress-strain relations for the WPC material to develop moment-curvature data points as a function of flexural strain in a WPC section. The moment-

curvature data is then used to determine load-displacement behavior for two common test setups. The program enabled an improved understanding of the behavior of WPC sections and will in the future assist in the design of WPC flexural members by providing preliminary strength estimates for proposed sections.

1.2 Objectives

The overall goal of the research presented in this thesis is to characterize the performance of wood-plastic composites for use in fender system component design. The specific objectives are:

1. to develop adequate test procedures for wood-plastic composite materials to determine strength properties;
2. to characterize material behavior and determine strength values for use in design of structural sections using the proposed test procedures;
3. to develop a method to analyze behavior to predict flexural strength for aid in the design of wood-plastic composite members;
4. to determine allowable design values for use in designing WPC deckboards and prototype fender system components for specific naval facilities applications; and
5. to analyze the decking and the support system at the Newport Naval Undersea Weapons Center (NUWC) Pier 171 to provide information needed for a prototype deckboard section design to replace current timber deckboards.

CHAPTER 2

TEST PROCEDURES FOR EVALUATING WOOD-PLASTIC COMPOSITE MATERIALS

2.1 Abstract

Test procedures are developed for establishing performance criteria for prototype wood-plastic components. These procedures are for testing near full-size composite sections and are proposed as standard methods for determining strength properties of wood-plastic structural members. The specific strength properties covered are modulus of rupture (MOR), compression parallel-to-extrusion strength, compression perpendicular-to-extrusion strength, beam shear strength, shear strength parallel and perpendicular to extrusion, shear strength by Iosipescu shear fixture, puncture strength, and resistance to impact.

2.2 Introduction

This chapter presents proposed standard procedures for testing wood-plastic composite (WPC) members and for characterizing strength properties for the material. The development of test methods specific to the WPC material was necessary due to the nonlinear behavior and heightened creep of wood-plastic during loading. Because the WPC formulations proposed for prototype fender system components are wood based, and the sections are similar in size to structural lumber, standard test methods and setups for determination of timber strength properties were used as a basis for development of the test methods for WPC material. The most significant modification to the standard timber tests was load rates, which must be increased to avoid excessive creep during testing. The load rates for the proposed standard procedures were based on load rates from standard test methods for determination of plastic strength properties.

The specific strength properties considered are modulus of rupture (MOR), compression parallel-to-extrusion strength, compression perpendicular-to-extrusion strength, beam shear strength, shear strength parallel and perpendicular to extrusion, shear strength by Iosipescu shear fixture, puncture strength, and resistance to impact by a falling weight. These procedures were developed for wood-plastic composites that contain less than or equal to 50 percent plastic by weight and are therefore proposed only for materials of similar formulations.

2.3 Flexure

2.3.1 Scope

This test method covers the determination of modulus of rupture for structural beams made of wood-plastic material. The method is applicable to beams of rectangular, round, or irregular cross sections. Members may also be slightly cambered. For waterfront structures, this test method may be applied for deckboards, wales and fender piles. These components may be built-up from individual solid or hollow sections.

2.3.2 Summary of Test Method

The test specimen, which may be straight or curved and hollow or solid, is subjected to a bending moment by supporting it near the ends, at locations called reactions, and applying transverse loads symmetrically between the reactions. The test is displacement controlled and load-displacement data is collected until rupture occurs.

The test method, apparatus, and procedure are in accordance with the ASTM D 198 (1997) flexure test. ASTM D 198 is a standard test method used to determine the properties of structural-size lumber. Due to the behavior of plastics and the possibility of hollow sections, two modifications are required.

For the first modification, the speed of testing must be increased to account for the heightened creep of plastic material during loading. Load rates specified by ASTM D 790 (1997) are proposed for use in order to avoid this excessive creep during testing. ASTM D 790 is a standard test method for flexural properties of unreinforced and reinforced plastics. The standard specifies the load rate be employed as a rate of straining in the outer fiber of 0.01 mm/mm/min (0.01 in./in./min).

For the second modification, the test span length should be determined from ratios of length to radius of gyration, l/r, rather than length to depth, l/d, where l is the unsupported span length, r is the least radius of gyration, and d is the depth of the beam. The reason for this modification is to account for hollow sections and nonrectangular sections. In order to reduce displacements due to shear, and thus collect data not influenced by shear deformations, the length must be such that the shear span is relatively long. This is characterized by the l/d ratio for solid rectangular beams, but must be characterized by the l/r ratio for hollow and nonrectangular sections. The procedures for determining span length as functions of the radius of gyration are presented in Appendix A. Figure 2.1 is a sketch of the flexural test setup for four-point bending. Figure 2.2 shows a typical flexural test setup.

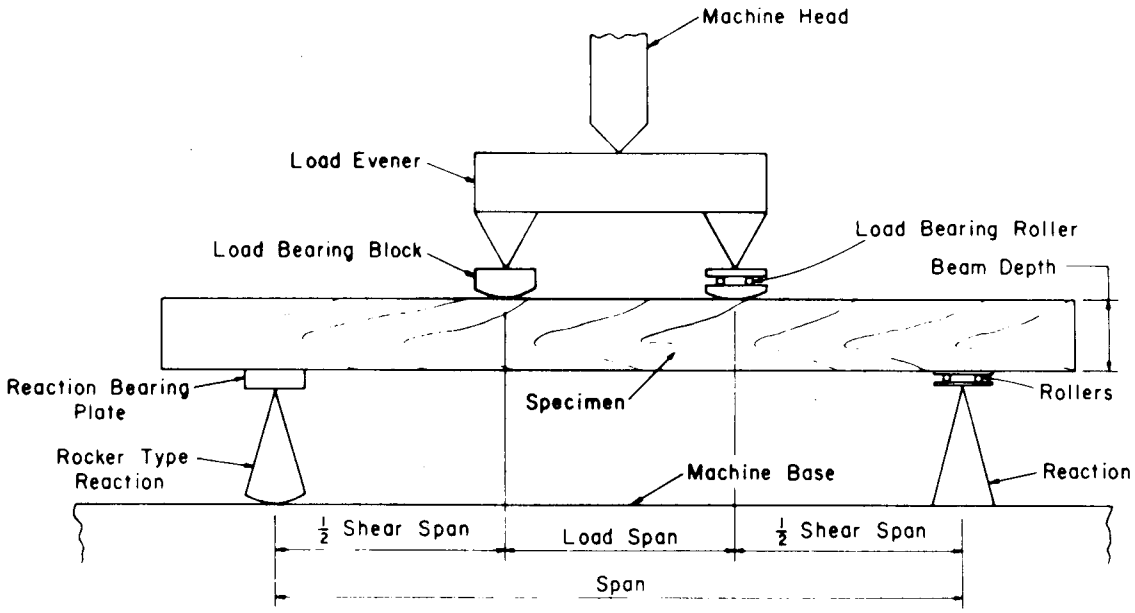

Figure 2.1: General flexural test setup

Figure 2.2: Typical flexural test setup

2.4 Compression Parallel to Extrusion (short column l/r <17)

2.4.1 Scope

This test method covers the determination of compression parallel-to-extrusion strength of members made of wood plastic material. The method is applicable to members of rectangular, round, or irregular cross sections. Test specimens are required to have length/radius of gyration ratios (l/r), less than 17, where r is the least radius of gyration and l is the unsupported length. For waterfront structures, this test method may be applied to chocks and piles. This component may be built-up from individual solid or hollow sections.

2.4.2 Summary of Test Method

The test specimen is subjected to an axial force parallel to the direction of extrusion and uniformly distributed over the contact surface. The test is displacement controlled and load-displacement data is collected until failure occurs.

The test method, apparatus, and procedure are in accordance with the ASTM D 198 (1998) compression parallel-to-grain test. Due to the plastic content of the material, the speed of testing must be increased to account for the heightened creep of plastic material during loading. The compression specimens shall be loaded at a constant displacement rate specified by ASTM D 695 (1998). ASTM D 695 is a standard test method for compressive properties of rigid plastics. The ASTM D 695 load rates are prescribed as 1.3 ± 0.3 mm/min (0.050 ± 0.010 in./min) rate of motion for the crosshead or grips of the machine. Minimum cross-section size shall be 1.0 in. by 1.0 in. Figure 2.3 shows a typical compression parallel-to-extrusion test setup.

Figure 2.3: Typical compression parallel test setup

2.5 Compression Perpendicular to Extrusion

2.5.1 Scope

This test method covers the determination of compression perpendicular-to-extrusion strength of members made of wood plastic material. The method is applicable to members of rectangular, round, or irregular cross sections. For waterfront structures, this test method may be applied to deckboards, wales and fender piles since all can receive lateral loads.

2.5.2 Summary of Test Method

The test specimen is subjected to a force perpendicular to the direction of extrusion and distributed over the middle third of the specimen. The test is displacement controlled and load-displacement data is collected until failure occurs.

The test method, apparatus, and procedure are in accordance with the ASTM D 143 (1998) compression perpendicular to grain test. ASTM D 143 is a standard test method for small clear specimens of timber. This method is modified from the 143 test in that it is proposed that

any size specimen may be tested provided that the middle third of the specimen is loaded in compression. Due to the plastic content of the material the speed of testing must be increased to account for the heightened creep of plastic material during loading. The compression specimens shall be loaded at a constant displacement rate specified by ASTM D 695 (1998). ASTM D 695 is a standard test method for compressive properties of rigid plastics. The ASTM D 695 load rates are prescribed as 1.3 ± 0.3 mm/min (0.050 ± 0.010 in./min) rate of motion for the crosshead or grips of the machine. Load shall be applied normal to the direction of extrusion through a metal bearing plate. The metal bearing plate must be equal to one-third the length of the specimen and shall be placed at right angles to the length. The radius of curvature of the plate edges shall be 2 ± 0.5 mm (0.08 ± 0.02 in.). This is to relieve stress concentration at the edge of the plate in the material and to prevent the plate from cutting into the material causing untimely failure as displacement increases. Figure 2.4 shows a typical compression perpendicular-to-extrusion test setup with the middle third of the specimen loaded in compression.

Figure 2.4: Typical compression perpendicular to extrusion test setup

2.6 Shear

Methods are presented for determining shear strength of WPC materials. The beam shear method is useful because beam shear is generally the most common form of shear loading, and many components of fender systems are subject to beam shear under flexural loading. Because a shear failure cannot always be obtained under flexural loading, shear parallel and perpendicular to extrusion tests and an Iosipescu shear test may be used to determine shear strengths.

2.6.1 Beam Shear

2.6.1.1 Scope

This test method covers the determination of bending shear strength for members made of wood-plastic material. The method is specific to the application of beams and defines the shear strength of a member when loaded normal to the longitudinal axis of the beam. The method is applicable to members of rectangular, round, or irregular cross sections. For waterfront structures, this test method may be applied to deckboards, wales and fender piles.

2.6.1.2 Summary of Test Method

The test specimen is subjected to 5-point bending to induce a shear failure in the beam. The member shall be supported at the ends and at the center while load points are to be located at the quarter points. The test is displacement controlled and load-displacement data is collected until failure occurs.

The test method, apparatus, and procedure are in accordance with the five-point bending test setup developed by the Forest Products Laboratory (Rammer and Soltis 1994). The test uses a five-point flexural loading to investigate shear failures in wood beams. Figure 2.5 shows a sketch of the general test setup. Figure 2.6 shows a typical test setup for the five-point bending shear test. The method is adapted for wood-plastic test specimens by loading pieces in the same

configuration with load rates specified by ASTM D 790 (1998) for flexural tests on plastic materials. ASTM D 790 prescribes a constant rate of strain in the outer fiber of 0.01 in./in./min (0.01 in./in./min).

Each span shall have a length of 5d, with an overall effective beam length of 10d, where d is the actual depth of the specimen. An alternate method for determining span length may be used when approximate shear and bending strength values are available. This method is presented in Appendix B. The alternate method allows for a more accurate determination of a span that will produce a shear failure. This method is preferred when the shear strength to bending strength ratio is relatively high compared to typical ratios for wood. With higher shear strengths a shear failure can be difficult, or even impossible, to achieve under flexural loading.

The loading and middle support plate lengths from Figure 5, b_1 and b_2, respectively, shall be determined based on the perpendicular-to-extrusion compressive strength of the material so as to minimize the amount of local crushing in the material near the supports and loading points.

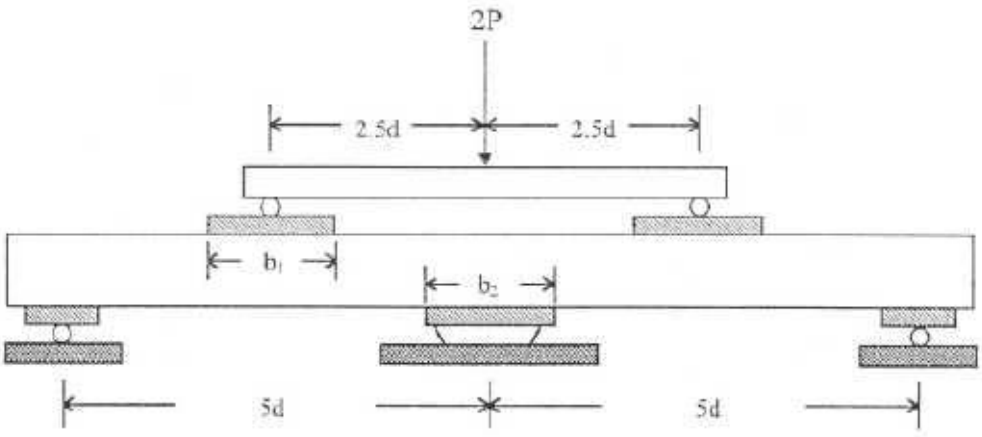

Figure 2.5: General setup for five-point beam shear test

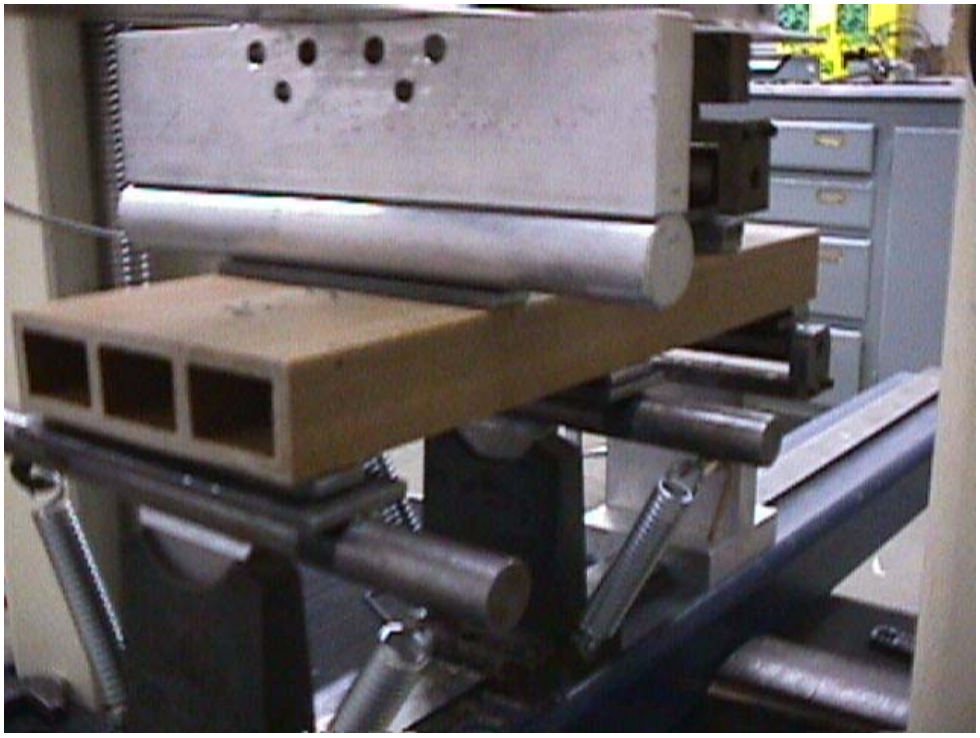

Figure 2.6: Typical five-point bending shear test setup

2.6.2 Shear Parallel to Extrusion and Shear Perpendicular to Extrusion

2.6.2.1 Scope

This test method covers the determination of shear strength parallel or perpendicular to extrusion for members made of wood plastic material. For determining shear strength parallel to extrusion, load shall be applied to produce shear failure along a plane parallel to the longitudinal axis of the member. For determining shear strength perpendicular to extrusion, load shall be applied to produce failure along a plane perpendicular to the longitudinal axis of the member. For waterfront structures, this test method may be applied to deckboards, wales and fender piles.

2.6.2.2 Summary of Test Method

The test specimen, a shear block cut from the structural section of interest, is placed into a shear tool and subjected to continuous loading until failure. The specimen may be solid or hollow. The shear block specimen is shown in Figure 2.7. Only the maximum load is recorded for this test.

The test method, apparatus, and procedure are in accordance with the ASTM D 143 shear parallel-to-grain test. ASTM D 143 is a standard test method for small clear specimens of timber.

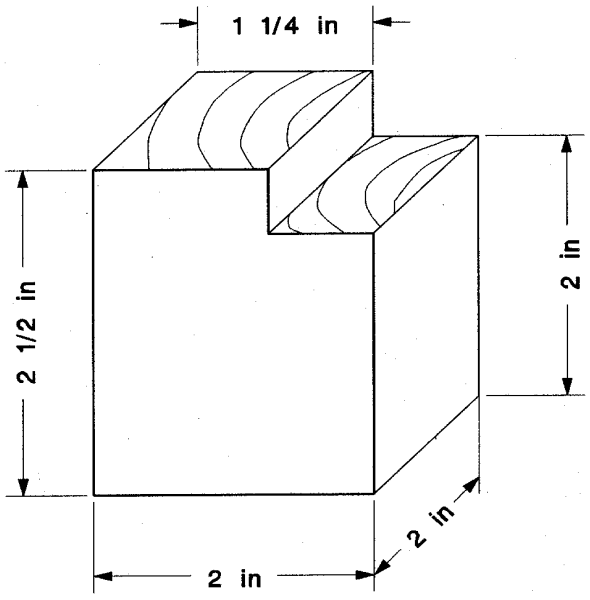

Figure 2.7: Shear block test specimen

2.6.3 Iosipescu Shear Test (ASTM D 5379)

2.6.3.1 Scope

This test method covers the determination of shear strength for materials made of wood plastic material. This method uses an Iosipescu shear fixture to test small specimens in single shear. For waterfront structures, this test method may be applied to deckboards, wales and fender piles.

2.6.3.2 Summary of Test Method

The test method, apparatus, and procedure are in accordance with the ASTM D 5379 shear test. ASTM D 5379 is a standard test method for shear properties of composite materials. The test specimen, a shear block with a 3-in. length, 0.75-in. width, and of any thickness up to 0.50 in., is placed into an Iosipescu shear fixture where the specimen is loaded in single shear. Figure 2.8 shows the test setup for the Iosipescu test. Loading continues until failure occurs on a plane between 90 degree notches on each edge of the specimen.

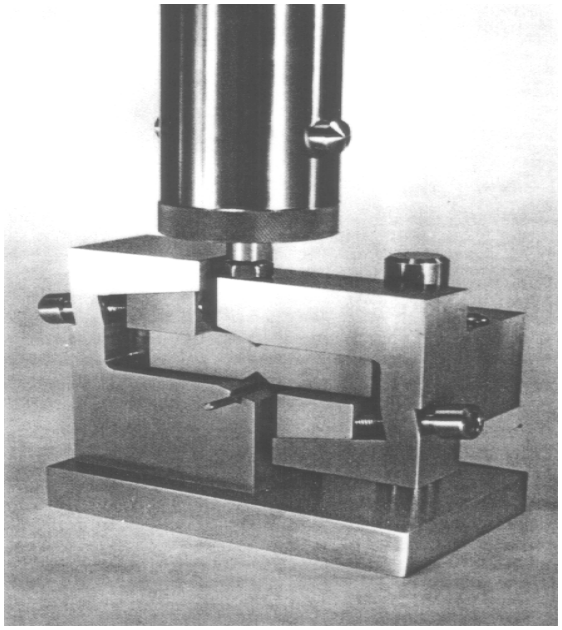

Figure 2.8: Iosipescu shear test setup

2.6.4 Shear Summary

Because a shear failure can be difficult to obtain in some cross-sections, namely solid cross-sections, using the beam shear method, the D 143 shear parallel and perpendicular to grain test or the D 5379 Iosipescu shear test may be applied considering application for the material. Recent research at Washington State University on wood-plastic composites has shown that the D 143 test method produces shear strengths that are lower than those obtained by the D 5379 test method.

2.7 Puncture

2.7.1 Scope

This test method covers the determination of puncture strength for members made of wood plastic material. The method is applicable for test pieces in the form of sheets or molded disks with thickness 0.127 to 12.7 mm (0.050 to 0.500 in.). For waterfront structures, this test method may be applicable to deckboards, chocks, wales and fender piles.

2.7.2 Summary of Test Method

The test specimen is placed into a punch-type tool and is subjected to load by a 1-in. diameter punch. The test is displacement controlled and load-displacement data is collected until failure occurs.

The test method, apparatus, and procedure are in accordance with the ASTM D 732-93 (1998) shear strength by punch tool test. ASTM D 732 is a standard test method for shear strength of plastics by punch tool. Figure 2.9 is a sketch of the punch-type shear tool and Figure 2.10 is a picture of the punch-type shear tool. Figure 2.11 shows a typical test setup with the punch-type shear tool.

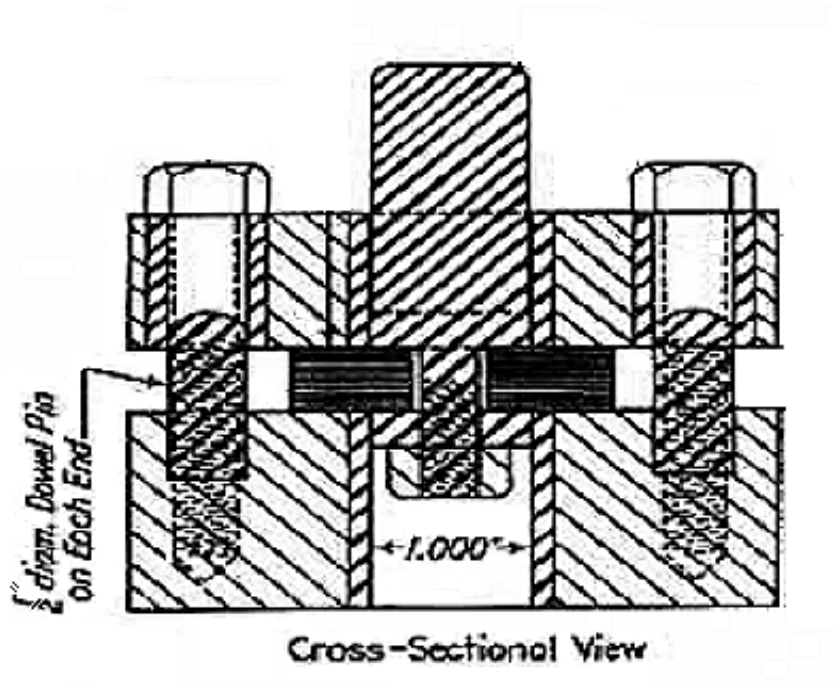

Figure 2.9: Sketch of the punch-type shear tool

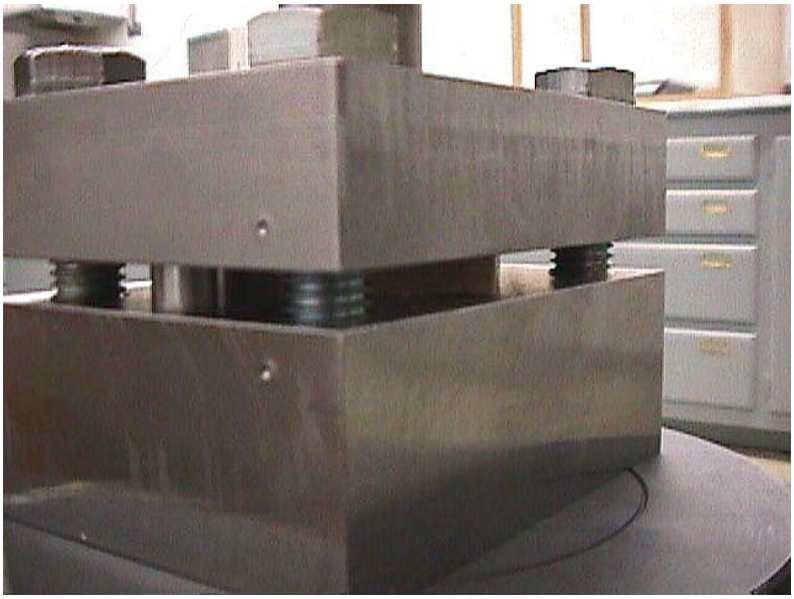

Figure 2.10: Punch-type shear tool

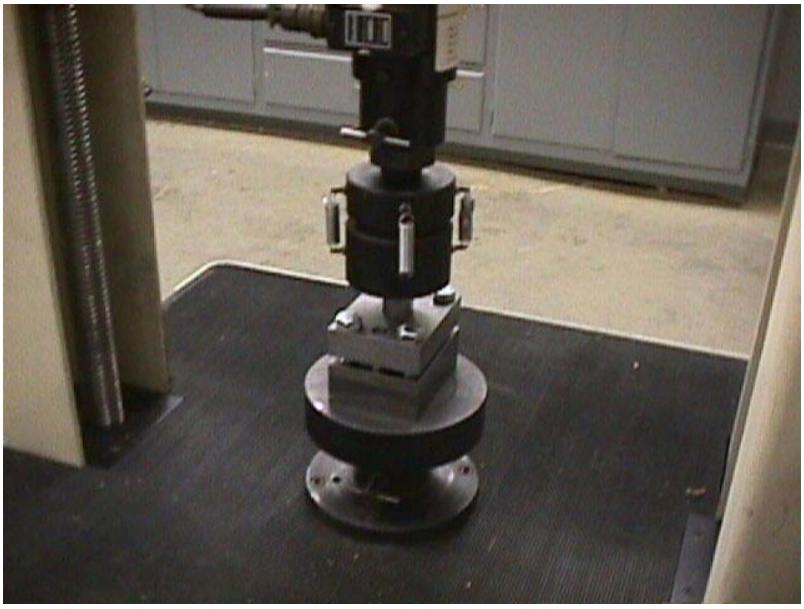

Figure 2.11: Typical puncture test setup

2.8 Impact

2.8.1 Scope

This test method covers the determination of the energy required to crack or break wood-plastic composite profiles. The test method establishes the height from which a standard falling weight will cause failure in at least 50% of specimens tested. The method is applicable for hollow or webbed sections. Solid sections can not be tested using this technique. For waterfront structures, this test method may be applicable to deckboards, chocks and piles.

2.8.2 Summary of Test Method

The test specimen is impacted by a 10-pound weight to generate failure. The test method, apparatus, and procedure are in accordance with the ASTM D 4495-95 (1998) standard impact test for polyvinyl chloride (PVC) profiles. ASTM D 4495 is a standard test method for impact resistance of PVC rigid profiles by means of a falling weight. The testing procedures of ASTM D 4495 were modified so that the diameter of the weight was reduced from 2.5 in. to 1 in.

This modification was made to allow for impact failures to occur between the webs of the box section. Figure 2.12 is a sketch of the impact test setup. Figure 2.13 shows a typical test setup for the impact test.

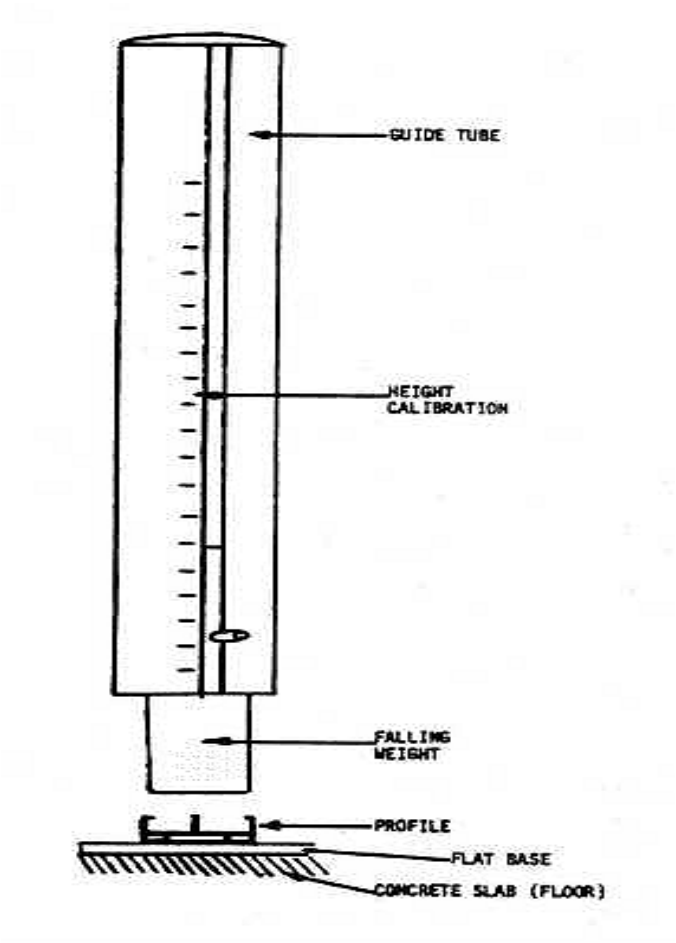

Figure 2.12: Sketch of impact test setup

Figure 2.13: Typical impact test setup

2.9 Conclusions

Test procedures are developed for establishing performance criteria for prototype wood-plastic components. These procedures are for testing near full-size composite sections and are proposed as standard methods for determining strength properties of wood-plastic structural members. The tests were developed for wood-plastic composites that contain less than or equal to 50 percent plastic by weight and are therefore proposed for materials of similar formulation. The specific strength properties covered are modulus of rupture (MOR), compression parallel-to-extrusion strength, compression perpendicular-to-extrusion strength, beam shear strength, shear strength parallel to extrusion, shear strength perpendicular to extrusion, puncture strength, and resistance to impact. Because a shear failure cannot always be obtained using the beam shear method, the D 143 shear parallel and perpendicular to grain test or the D 5379 Iosipescu shear test may be more suited for some applications.

CHAPTER 3

TEST RESULTS OF WOOD-PLASTIC COMPOSITE COMPONENTS

3.1 Abstract

This chapter presents the results from a series of experimental tests conducted on wood-plastic composite (WPC) specimens to characterize material behavior and strength values. Tests were conducted on near full-size sections representative of prototype components for use in fendering systems. The specimens included both polyvinyl chloride (PVC) and high-density polyethylene (HDPE) formulations. Compression, bending, shear, puncture and impact strengths were determined. The test results indicate that specimens formulated using the PVC formulation are stronger and stiffer than specimens using HDPE formulation. However, the PVC specimens displayed more brittle behavior during the tests than did the HDPE specimens. The resulting strength values were used in the design of components for application in specific demonstration projects.

3.2 Introduction

Tests were conducted on near full-size WPC sections to determine compression perpendicular-to-extrusion, compression parallel-to-extrusion, modulus of rupture, shear, puncture, and impact resistance strengths of prototype structural elements. The specimens were selected to be representative of the components expected to be used in fendering systems. Two WPC formulations were evaluated: an HDPE formulation consisting of approximately 70% wood and 30% HDPE, and a PVC formulation consisting of 50% wood and 50% PVC.

The specimens consisted of a rectangular three-cell box section and were tested in both flat-wise (weak-axis) and edge-wise (strong-axis) orientations. Figure 3.1 shows the HDPE and PVC triple-box sections. The section properties of the box section are as follows:

cross-sectional area, A…….5.34 in^2

weak-axis first moment of area, Q ……1.68 in^3

strong-axis moment of inertia……...20.15 in^4

weak-axis moment of inertia…….2.37 in^4

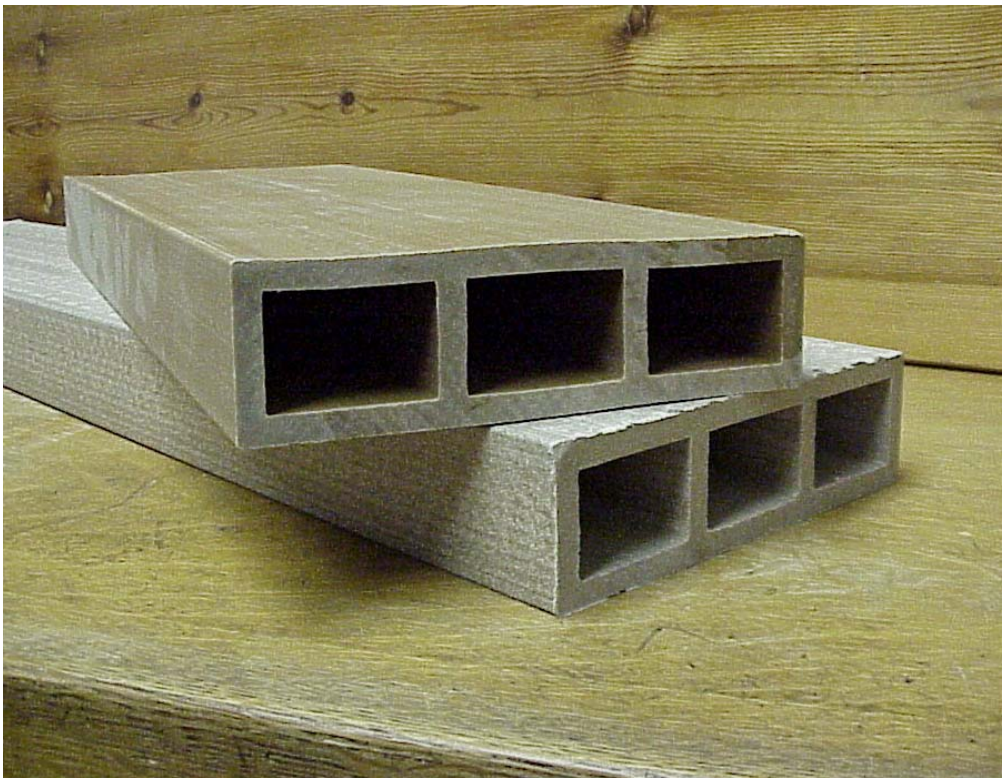

Figure 3.1: HDPE (bottom) and PVC (top) triple-box sections

3.3 Compression Parallel-to-Extrusion Tests

3.3.1 Test Procedures

Five specimens of both HDPE and PVC were tested to determine compression perpendicular-to-extrusion strength by means of ASTM D 198 (1997). ASTM D 198 is a standard test method for determining the strength properties of lumber. One spherical bearing block is used to ensure uniform loading along the vertical axis. The specimens were loaded at a constant displacement rate of 0.05 in./min as specified by ASTM D 695 (1996). ASTM D 695 is a standard test method for compressive properties of rigid plastics. Research conducted previously on wood-based composite materials at the Wood Materials and Engineering Laboratory (WMEL) has indicated that loading rates for plastic materials are more appropriate than load rates specified for wood due to the increased creep rates associated with plastic materials. The specimen dimensions were 6.5 in. x 1.8 in. x 8 in.

Each specimen was tested using an MTS-810 load frame (Figure 3.2) with a hydraulic actuator equipped with a 55-kip load cell that was activated using an MTS-407 controller. The response for each specimen was determined from the load-displacement curve generated during the loading of each specimen. Tests were terminated upon failure of the specimen or shortly after the load began to drop. The software LABVIEW 5.0 was used to collect the test data.

Figure 3.2: Compression parallel test setup

3.3.2 Discussion of Results

The results of the compression-parallel-to-extrusion tests are presented in Table 3.1. Load-displacement curves for the compression parallel tests are shown in Figure 3.3. The average maximum compression-parallel-to-extrusion stress for the HDPE is 999 psi based on the entire gross contact area and 2243 psi based on the net cross-sectional area of the specimen. The average maximum compression-parallel-to-extrusion stress for the PVC is 3663 psi based on the entire gross contact area and 8225 psi based on the net cross-sectional area of the specimen.

The PVC and HDPE test specimens all failed by local crushing near the ends, as shown in Figure 3.4 and Figure 3.5. Comparing the two material types shows that the PVC material exhibits a more linear response until failure and is capable of carrying higher loads.

Table 3.1: Results of the compression parallel-to-extrusion tests

Test No.	Deflection at max. load (in.)	Max. applied load (lbs)	Max. compression para.-to-extr. stress (psi)	Net section max. comp. para.-to-extr. stress (psi)
CPA-1H	0.438	11764	1005	2258
CPA-2H	0.435	10954	936	2102
CPA-3H	0.454	11698	1000	2245
CPA-4H	0.430	12168	1040	2336
CPA-5H	0.449	11838	1012	2272
		Average	**999**	**2243**
		Std. Deviation	**38**	**86**
		Coeff. Of Var.	**4%**	**4%**
CPA-1P	0.136	37832	3233	7261
CPA-2P	0.176	44923	3840	8623
CPA-3P	0.150	41706	3565	8005
CPA-4P	0.177	44868	3835	8612
CPA-5P	0.179	44940	3841	8626
		Average	**3663**	**8225**
		Std. Deviation	**268**	**601**
		Coeff. Of Var.	**7%**	**7%**

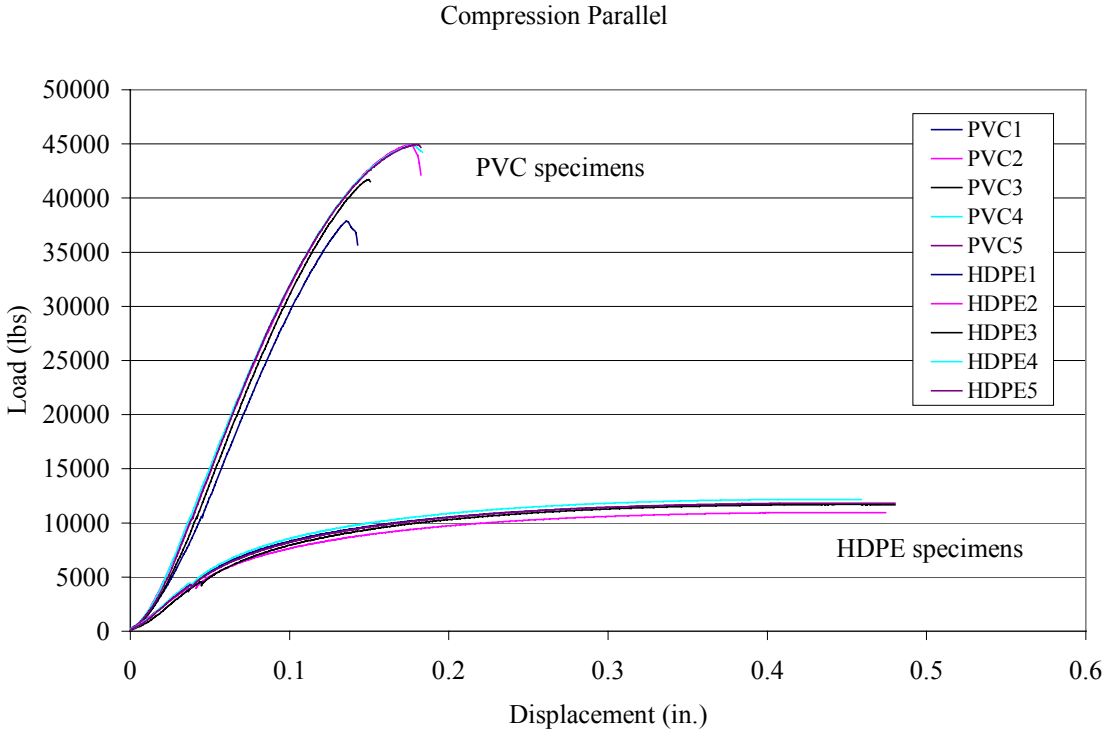

Figure 3.3: Load-displacement curves for compression parallel-to-extrusion tests

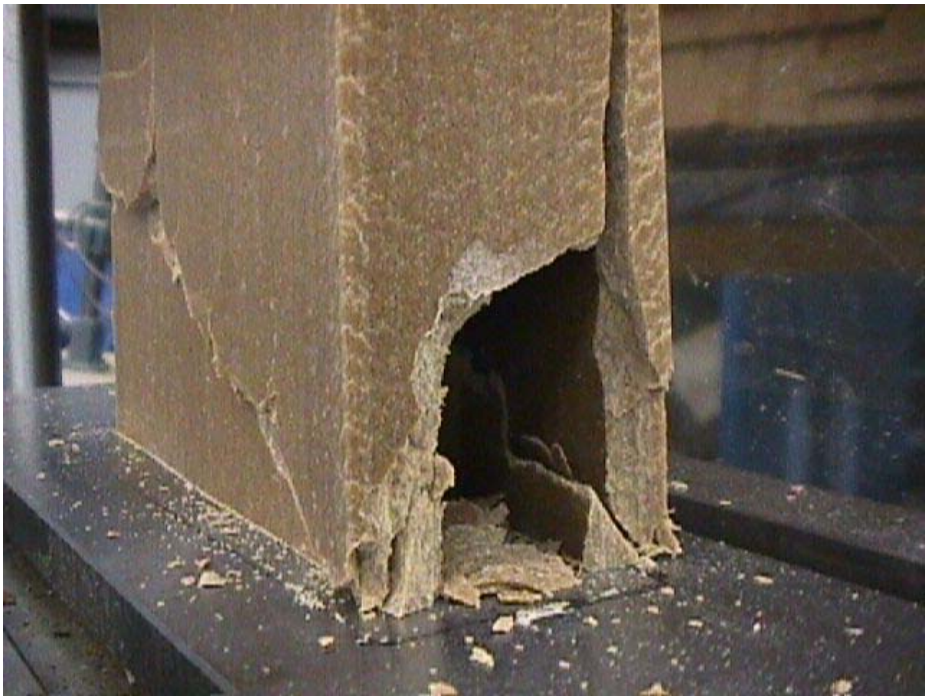

Figure 3.4: PVC compression parallel failure

Figure 3.5: HDPE compression parallel failure

3.4 Flexure Tests

3.4.1 Test Procedures

Five flat-wise and five strong-axis oriented specimens of both HDPE and PVC formulations were tested to determine the modulus of rupture. The strong-axis specimens were assembled with three side-by-side pieces bolted together at the neutral axis in order to provide lateral stability. The specimens were tested in the loading configuration specified by ASTM D 198 (1997). The specimens were loaded at a constant displacement rate of 0.925 in./min for flat-wise bending and 3.390 in./min. for strong-axis bending, as specified by ASTM D 790 (1998). ASTM D 790 is a standard test method for flexural properties of unreinforced and reinforced plastics.

The flat-wise and strong-axis test setups are pictured in Figure 3.6 and Figure 3.7, respectively. The dimensions of the flat-wise specimens were 6.5 in. x 1.8 in. x 36 in. with a span length of 30 in. The dimensions for the built-up strong-axis specimens were 5.25 in. x 6.5 in. x 120 in. with a span length of 108 in. Each flat-wise specimen was tested using a United testing machine equipped with a 20-kip load cell, while the strong-axis specimens were tested using an MTS 55-kip actuator equipped with a 50-kip load cell. The response for each test was determined from the load-displacement curve generated during the loading of each specimen. The tests were terminated upon specimen failure or drop in the applied load the specimen is able to resist. A Linear Variable Displacement Transducer (LVDT) was used to measure displacement of the neutral axis at the mid-span for flat-wise tests. Because larger displacements were expected in the strong-axis tests, potentiometers were used for displacement measurements for these tests. Figure 3.8 and 3.9 show the flat-wise and strong-axis tests during loading.

Figure 3.6: Flat-wise flexural test setup

Figure 3.7: Strong-axis flexural test setup

Figure 3.8: Flat-wise triple-box section during loading

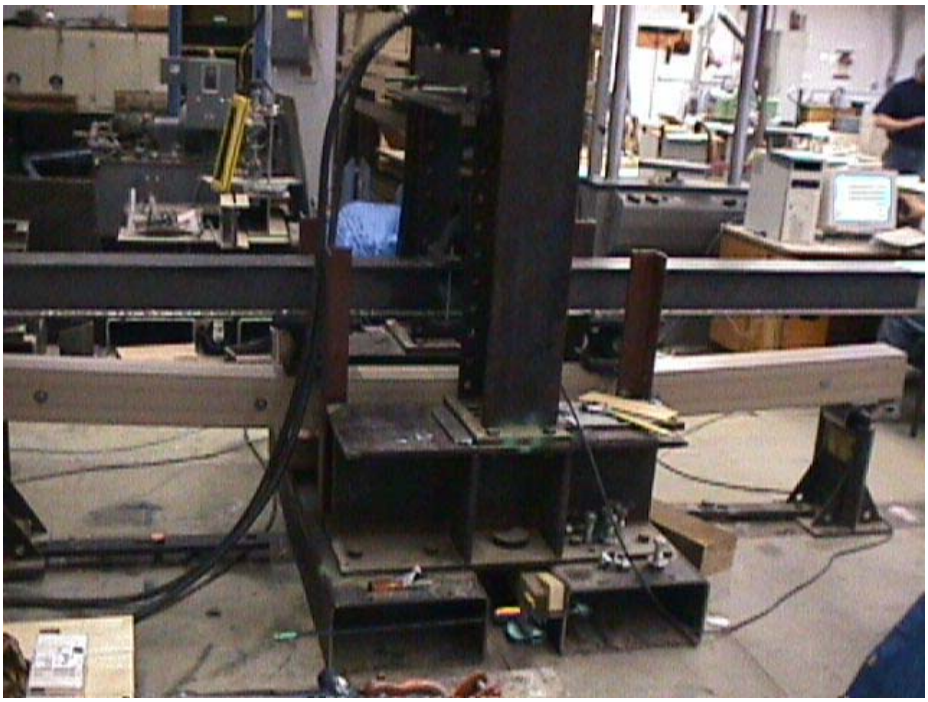

Figure 3.9: Strong-axis triple-box sections during loading

3.4.2 Discussion of Results: Flat-wise Flexure Tests

The results of the flat-wise flexure tests are presented in Table 3.2. Load-displacement curves for the flat-wise flexure tests are shown in Figure 3.10. The average modulus of rupture stress for the HDPE is 1746 psi, and the average modulus of rupture stress for the PVC is 5308 psi.

The beams all failed in tension at the extreme fiber of the specimens. A failed specimen is shown in Figure 3.11. The PVC specimens failed in a brittle manner with little or no warning of failure. The HDPE failures were relatively ductile with large displacements near the maximum load.

Table 3.2: Results of the flat-wise flexure tests

Test No.	Deflection at max load (in.)	Max applied load (lbs)	Max bending moment (lb-in.)	Modulus of rupture (psi)
F-1H	1.14	904	4518	1730
F-2H	1.24	936	4678	1792
F-3H	1.27	937	4686	1794
F-4H	1.32	896	4480	1716
F-5H	1.17	887	4434	1698
		Average	**4559**	**1746**
		Std. Deviation	**116**	**44**
		Coeff. Of Var.	**3%**	**3%**
F-1P	0.78	2669	13347	5112
F-2P	0.67	2811	14057	5383
F-3P	0.71	2563	12813	4907
F-4P	0.73	2914	14568	5579
F-5P	0.74	2903	14515	5559
		Average	**13860**	**5308**
		Std. Deviation	**763**	**292**
		Coeff. Of Var.	**6%**	**6%**

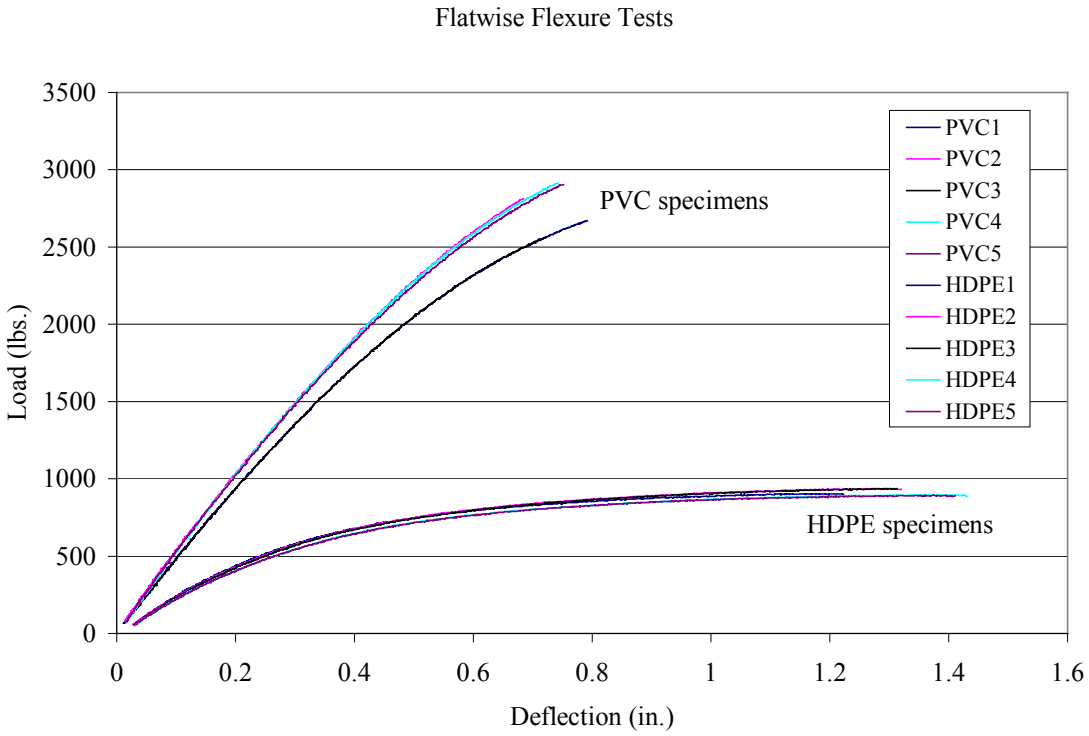

Figure 3.10: Load-displacement curves for flat-wise flexure tests

Figure 3.11: Flat-wise flexural failure

3.4.3 Discussion of Results: Strong-axis Flexure Tests

The results of the strong-axis flexure tests are presented in Table 3.3. Load-displacement curves for the strong-axis flexure tests are shown in Figure 3.12. The average modulus of rupture stress for the HDPE specimens is 1898 psi, and the average modulus of rupture stress for the PVC specimens is 5033 psi.

Similar to the weak-axis results, the strong-axis beams failed in tension at the extreme fiber of the specimens, as seen in Figure 3.13. The general behavior of both the HDPE and PVC specimens in strong-axis bending was similar to that observed in the flat-wise tests. However, the strong-axis specimens all failed through the bolt-hole at the center of each piece.

Table 3.3: Results of the strong-axis flexure tests

Test No.	Deflection at max load (in.)	Max applied load (lbs)	Max bending moment (lb-in.)	Modulus of rupture (psi)
SA-1H	4.04	1978	35604	1809
SA-2H	3.77	2161	38898	1976
SA-3H	3.62	2090	37620	1911
SA-4H	3.65	1999	35982	1828
SA-5H	3.68	2150	38700	1966
		Average	**37361**	**1898**
		Std. Deviation	**1517**	**77**
		Coeff. Of Var.	**4%**	**4%**
SA-1P	2.11	6007	108126	5492
SA-2P	1.90	5460	98280	4992
SA-3P	2.01	5419	97542	4955
SA-4P	1.60	4865	87570	4448
SA-5P	2.04	5770	103860	5276
		Average	**99076**	**5033**
		Std. Deviation	**7749**	**394**
		Coeff. Of Var.	**8%**	**8%**

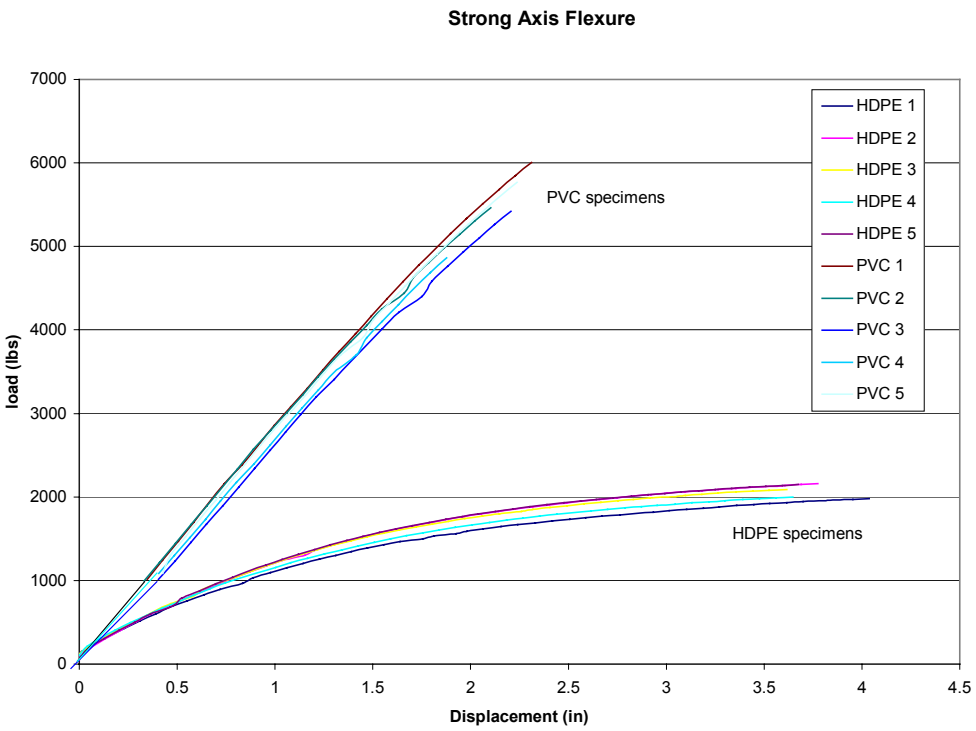

Figure 3.12: Load-displacement curves for strong-axis flexure tests

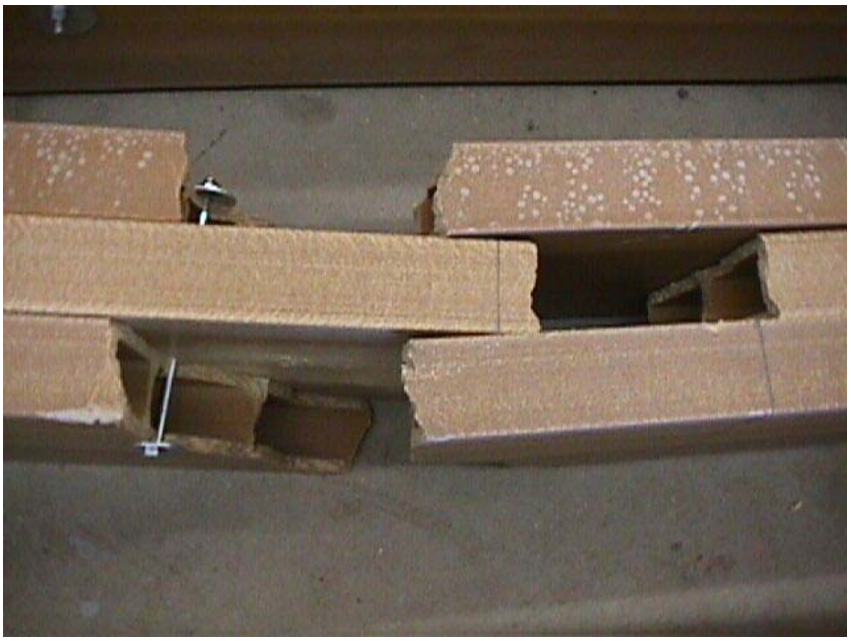

Figure 3.13: Strong-axis flexural failure

3.5 Compression Perpendicular-to-Extrusion Tests

3.5.1 Test Procedures

Five flat-wise and five strong-axis built-up specimens of both HDPE and PVC formulations were tested to determine the compression perpendicular-to-extrusion strengths. The specimens were tested in the loading configuration specified in ASTM D 143 (1994). ASTM D 143 is a standard test method for small clear specimens of timber. The method calls for particular sizes of wood to be loaded by a flat square plate in the middle third of the specimen. Due to the size of the specimens the method was modified to accommodate larger pieces. The flat-wise and strong-axis built-up sections were tested in the same configuration with the middle third of the specimen loaded in compression. The specimens were loaded at a constant rate of 0.05 in./min as specified by ASTM D 695 (1996). ASTM D 695 is a standard test method for compressive properties of rigid plastics.

The test setup is presented in Figure 3.14. The specimen dimensions were 6.5 in. x 1.8 in. x 19.5 in. for flat-wise testing and 5.4 in. x 6.5 in. x 16.2 in. for built-up testing. Each specimen was tested using a Tinius Olsen testing machine equipped with a 400-kip hydraulic actuator. The response for each specimen was determined from the load-displacement curve generated during testing. Each test was terminated upon failure of the specimen or shortly after the load began to drop. Data was collected using the software PCWorkbench.

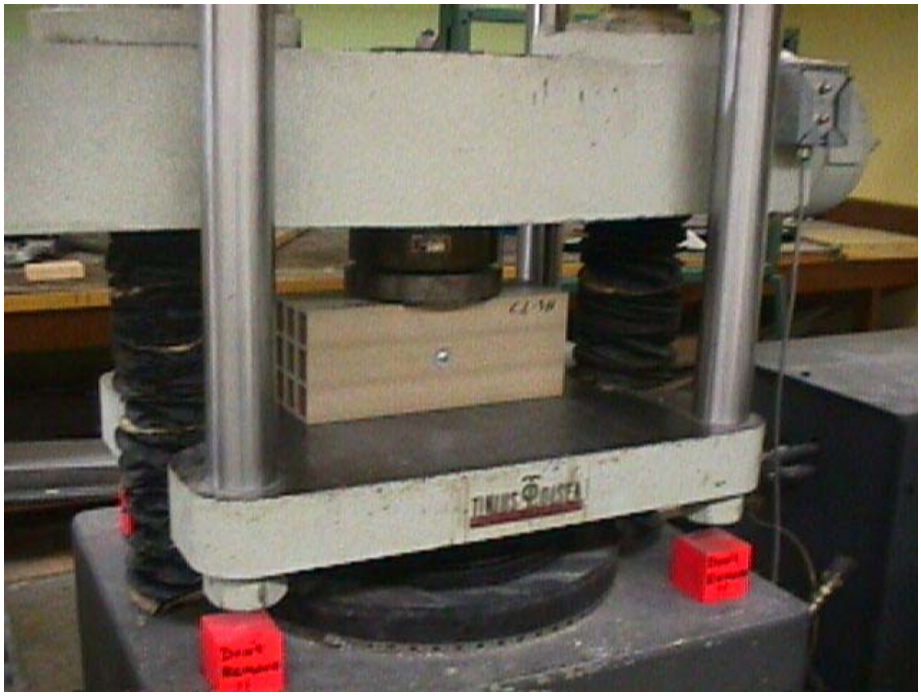

Figure 3.14: Compression perpendicular-to-extrusion test setup

3.5.2 Discussion of Results

The results of the flat-wise and built-up compression-perpendicular-to-extrusion tests are presented in Table 3.4 and Table 3.5. Load-displacement curves for the compression perpendicular tests are presented in Figure 3.15 and Figure 3.16. The average compression-perpendicular-to-extrusion strengths for the flat-wise tests, based upon net web area, are 3334 psi and 8364 psi for the HDPE and PVC specimens, respectively. The average compression-perpendicular-to-extrusion strengths for the built-up specimens, based upon net web area, are 3968 psi and 7702 psi for the HDPE and PVC, respectively. Higher COV's occurred with the built-up test results, when compared to the COV's for the flat-wise tests, as a result of slight irregularities in the formed ends of the sections causing lack of full contact of the applied compression load on the specimen during testing.

The compression perpendicular-to-extrusion specimens all failed near the outer wall of the section. The HDPE failures were relatively ductile with large displacements near the maximum load, while the PVC specimens failed in a brittle manner. Failures in the specimens are shown in Figure 3.17 and Figure 3.18.

Table 3.4: Results of the compression perpendicular-to-extrusion flat-wise tests

Test No.	Deflection at max. load (in.)	Max. applied load (lbs)	Max. compression perp.-to-extr. flat (psi)	Net section max. comp. Perp.-to-extr. flat (psi)
CFL-1H	0.082	25762	634	3303
CFL-2H	0.093	26126	643	3349
CFL-3H	0.093	26071	642	3342
CFL-4H	0.090	26163	644	3354
CFL-5H	0.088	25897	637	3320
		Average	**640**	**3334**
		Std. Deviation	**4**	**22**
		Coeff.of Var.	**1%**	**1%**
CFL-1P	0.093	62440	1536	8005
CFL-2P	0.076	66768	1643	8560
CFL-3P	0.092	66856	1645	8571
CFL-4P	0.090	62857	1547	8059
CFL-5P	0.096	67264	1655	8624
		Average	**1605**	**8364**
		Std. Deviation	**58**	**304**
		Coeff.of Var.	**4%**	**4%**

Table 3.5: Results of the compression perpendicular

Test No.	Deflection at max. load (in.)	Max. applied load (lbs)	Max. compression perp.-to-extr. strong (psi)	Net section max. comp. Perp.-to-extr. strong (psi)
CSA-1H	0.154	30665	755	3931
CSA-2H	0.144	31488	775	4037
CSA-3H	0.144	30480	750	3908
CSA-4H	0.146	30658	754	3930
CSA-5H	0.146	31451	774	4032
		Average	**762**	**3968**
		Std. Deviation	**12**	**62**
		Coeff.of Var.	**2%**	**2%**
CSA-1P	0.112	72826	1792	9337
CSA-2P	0.080	45304	1115	5808
CSA-3P	0.077	51683	1272	6626
CSA-4P	0.097	66319	1632	8502
CSA-5P	0.090	64236	1581	8235
		Average	**1478**	**7702**
		Std. Deviation	**277**	**1444**
		Coeff.of Var.	**19%**	**19%**

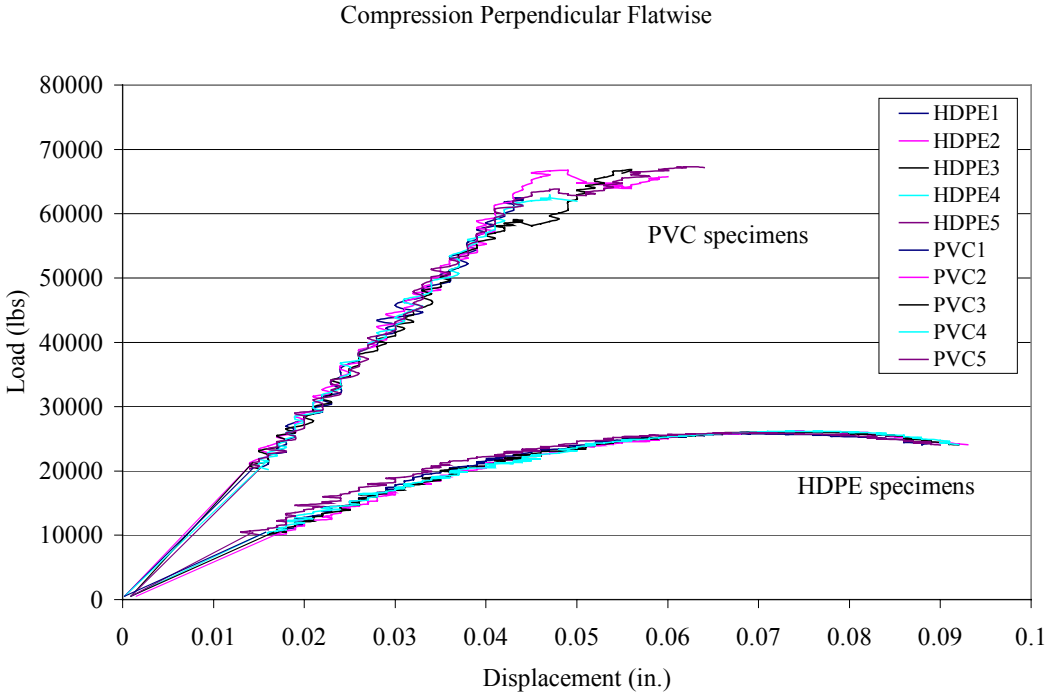

Figure 3.15: Load-displacement curves for compression perpendicular-to-extrusion flat-wise tests

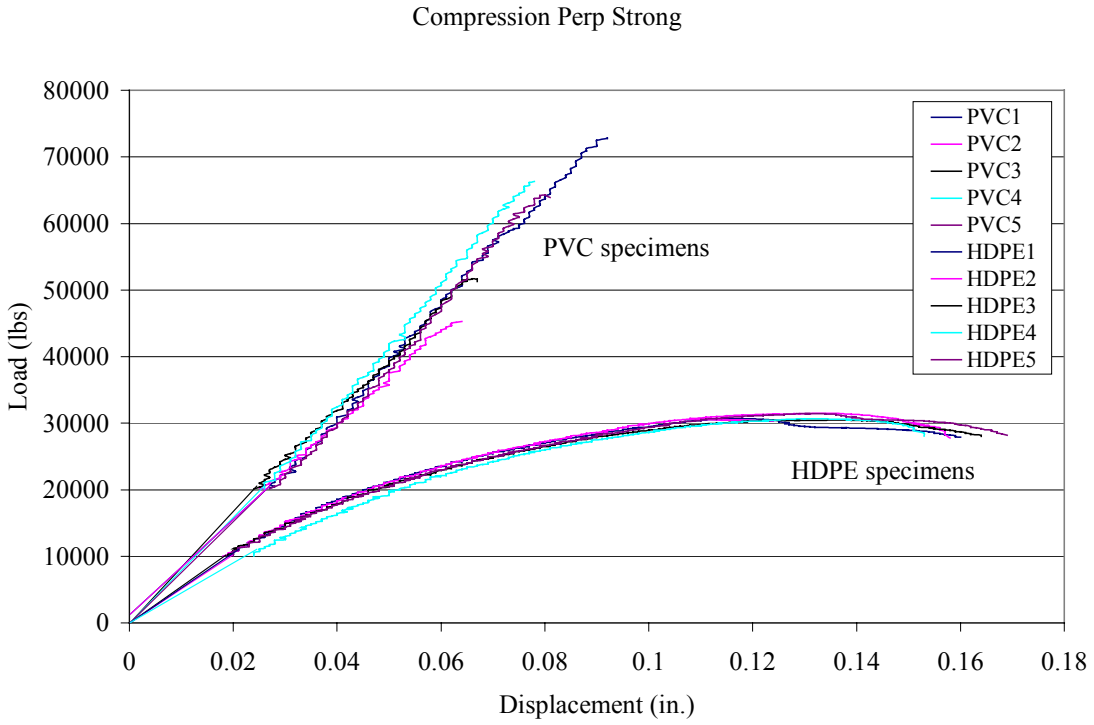

Figure 3.16: Load-displacement curves for compression perpendicular-to-extrusion strong-axis tests

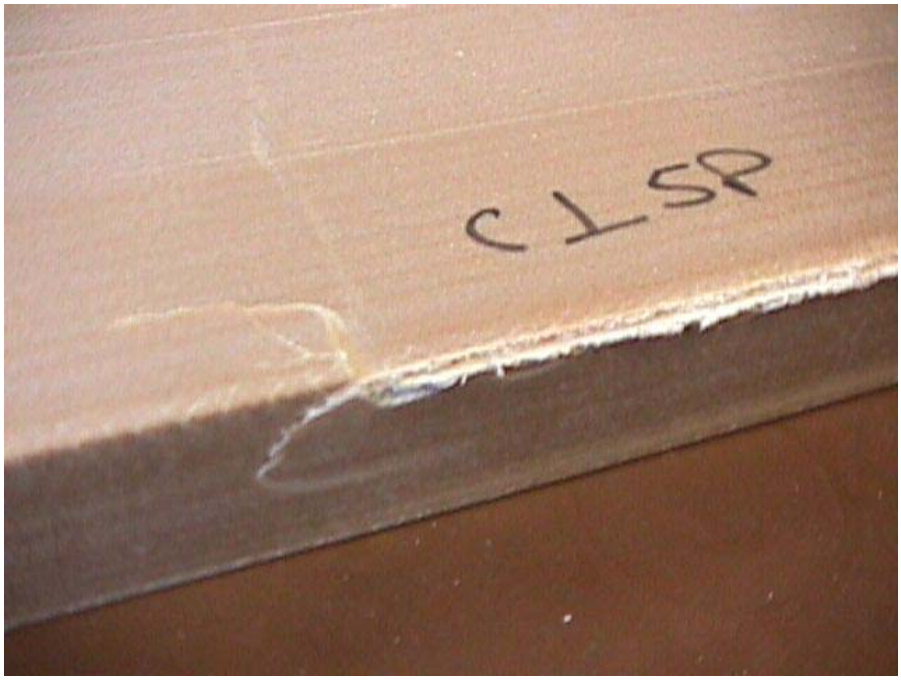

Figure 3.17: Compression perpendicular-to-extrusion flat-wise failure

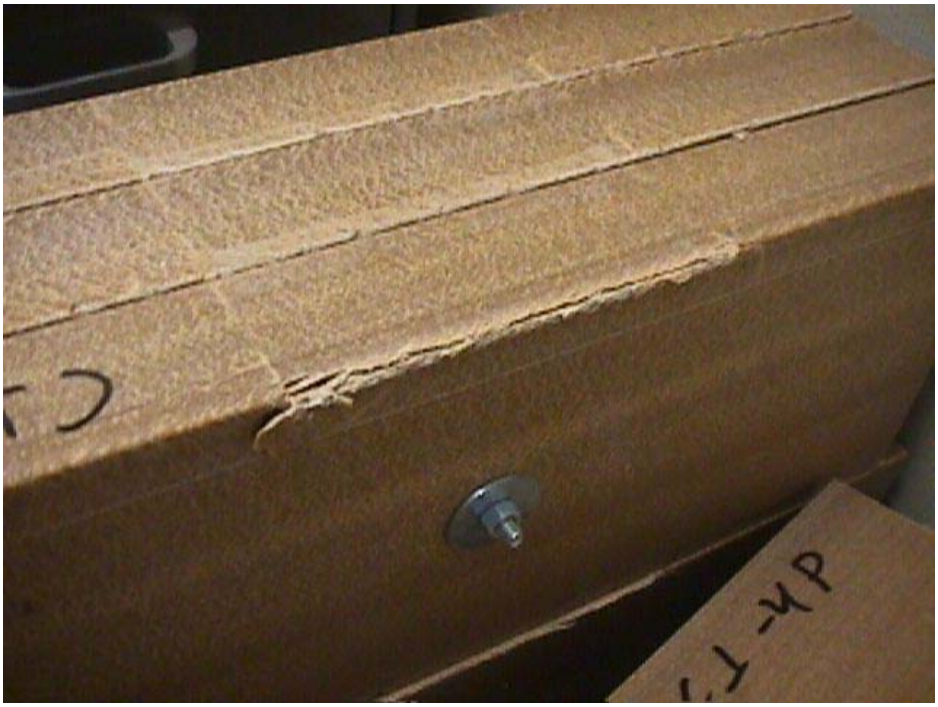

Figure 3.18: Compression perpendicular-to-extrusion strong-axis failure

3.6 Shear Tests

3.6.1 Test Procedures

Five specimens of both HDPE and PVC formulations were tested flat-wise to determine shear strength under bending loading. The specimens were tested in the loading configuration developed previously by the Forest Products Laboratory for timber beams (Rammer and Soltis 1994). The test uses a five-point flexural loading to characterize shear strength. The wood-plastic test specimens were loaded in this configuration at a constant rate of strain of 0.01 in./in./min, as specified by ASTM D 790 (1998). The test setup is presented in Figure 3.19. The specimen dimensions were 6.5 in. x 1.8 in. x 18 in. Each specimen was tested using a United testing machine equipped with a 20-kip load cell. The response for each test was determined

from the load-displacement curve generated during testing for each specimen. Each test was terminated upon failure of the specimen. It was found to not be practical to produce shear failures in the built up, strong-axis specimens; flexural failure controlled even for very short span lengths.

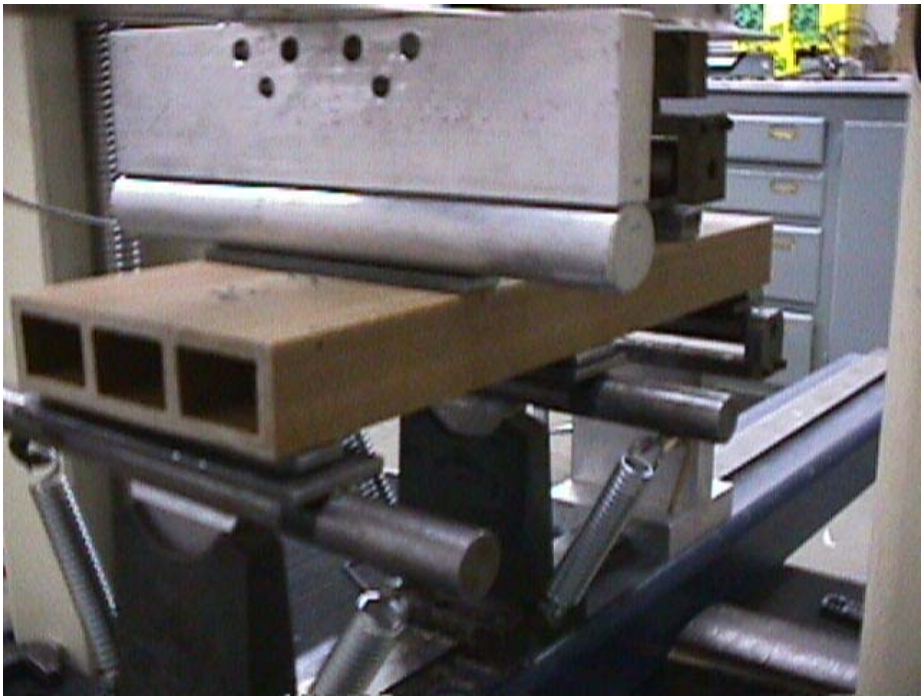

Figure 3.19: Shear test setup

3.6.2 Discussion of Results

The results of the shear tests are presented in Table 3.6. Load-displacement curves for the shear tests are shown in Figure 3.20. The average maximum shear stress for the HDPE is 1133 psi, and the average maximum shear stress for the PVC is 2931 psi. An approximate 45 degree angle was observed with the shear failures, as can been seen in Figure 3.21 and Figure 3.22.

Table 3.6: Results of the shear tests

Test No.	Deflection at max. load (in.)	Max. applied load (lbs)	Max Shear (lbs)	Max. shear stress (psi)
S-1H	0.209	5635	1937	1154
S-2H	0.226	5559	1911	1138
S-3H	0.206	5549	1908	1136
S-4H	0.202	5476	1882	1121
S-5H	0.199	5455	1875	1117
		Average	**1903**	**1133**
		Std. Deviation	**25**	**15**
		Coeff. of Var.	**1%**	**1%**
S-1P	0.213	15845	5447	3245
S-2P	0.214	15149	5207	3102
S-3P	0.204	14429	4960	2955
S-4P	0.185	13403	4607	2745
S-5P	0.174	12726	4375	2606
		Average	**4919**	**2931**
		Std. Deviation	**435**	**259**
		Coeff. of Var.	**9%**	**9%**

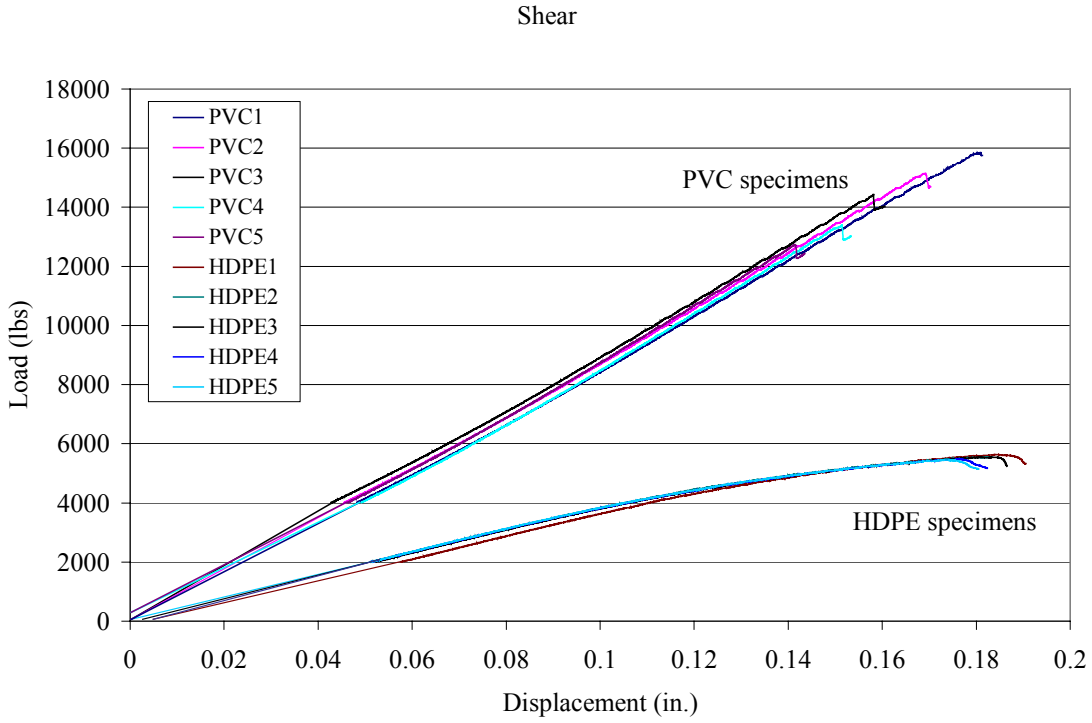

Figure 3.20: Load-displacement curves for shear tests

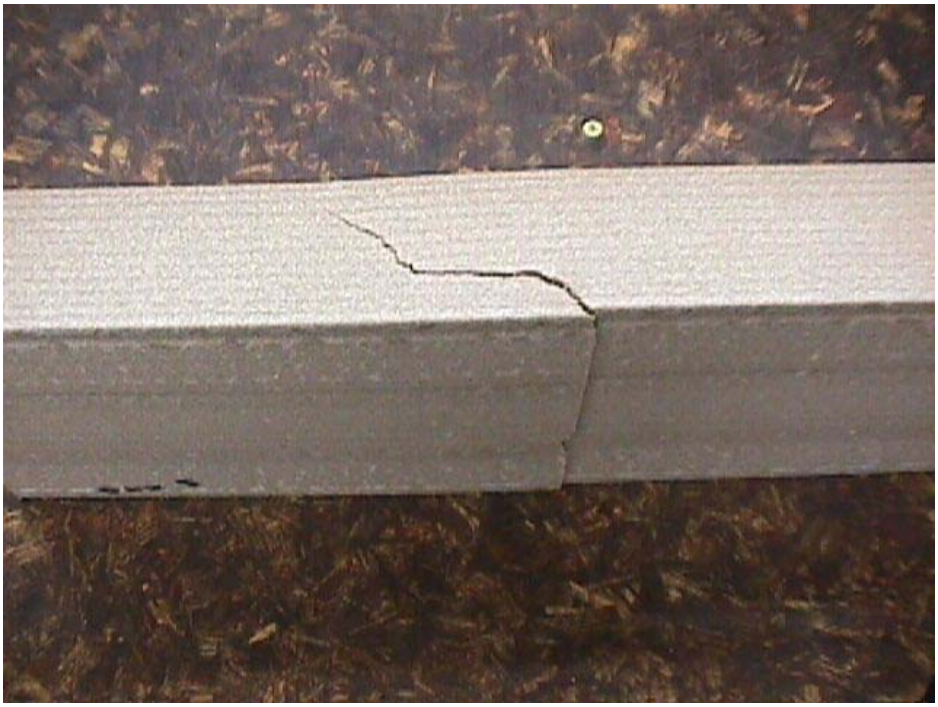

Figure 3.21: HDPE flat-wise shear failure

Figure 3.22: PVC flat-wise shear failure

3.7 Shear Strength by Punch Tool Tests

3.7.1 Test Procedures

Puncture tests of five specimens for each material were carried out in accordance with ASTM D 732 (1993). ASTM D 732 is a standard test method for determining shear strength of plastics using a punching tool. The specimens were tested under a 1-in. diameter punch. The punch-type shear tool is shown in Figure 3.23 and the test setup is shown in Figure 3.24. The specimens were loaded at a constant rate of 0.05 in./min, as specified by ASTM D 695 (1998), using a United testing machine equipped with a 20-kip load cell. The failed specimens are shown in Figure 3.25.

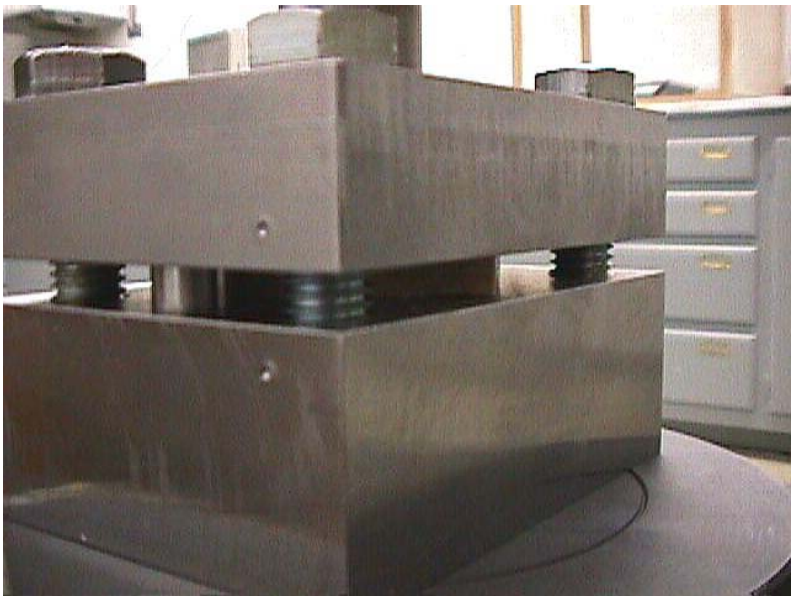

Figure 3.23: Punch-type shear tool

Figure 3.24: Puncture test setup

Figure 3.25: Puncture test failures

3.7.2 Discussion of Results

The results of the puncture tests are presented in Table 3.7. Load-displacement curves for the puncture tests are shown in Figure 3.26. The average maximum shear stress for the HDPE is 2203 psi and the average maximum shear stress for the PVC is 4898 psi. The maximum shear stresses obtained from the puncture tests were much greater than the maximum stresses observed in the beam shear tests. This is due to the configuration of the punch tool and the manner in which the specimens were restrained and supported during testing.

Table 3.7: Results of the puncture tests

Test No.	Deflection at max load (in.)	Max applied load (lbs)	Max shear stress (psi)
P-1H	0.04	2089	2216
P-2H	0.04	2210	2344
P-3H	0.04	2201	2334
P-4H	0.04	1952	2070
P-5H	0.03	1937	2054
		Average	**2203**
		Std. Deviation	**141**
		Coeff. Of Var.	**6%**
P-1P	0.04	4614	4893
P-2P	0.04	4630	4909
P-3P	0.04	4703	4987
P-4P	0.04	4758	5045
P-5P	0.04	4391	4657
		Average	**4898**
		Std. Deviation	**148**
		Coeff. Of Var.	**3%**

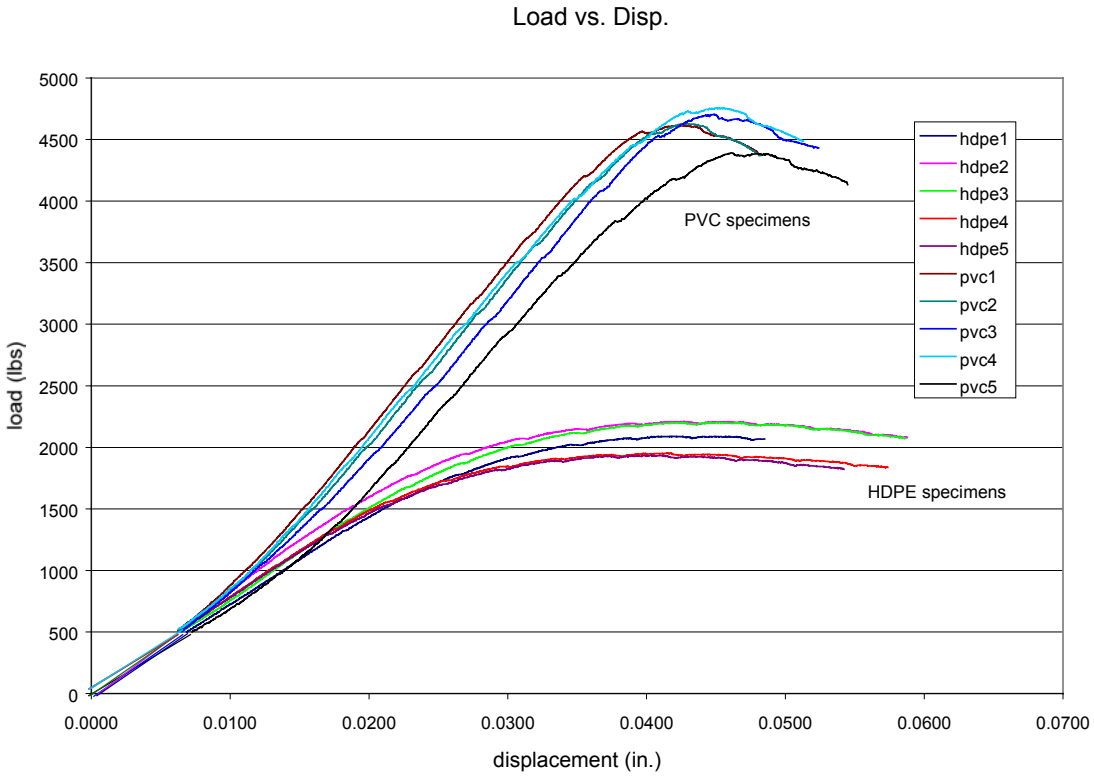

Figure 3.26: Load-displacement curves for puncture tests

3.8 Impact Resistance by Falling Weight Tests

3.8.1 Test Procedures

Impact tests for the HDPE and PVC specimens were carried out in accordance with ASTM D 4495 (1995). ASTM D 4495 is a standard test method for impact resistance of PVC rigid profiles by means of a falling weight. A ten-pound weight is dropped from a vertical drop tube at increments of 2 in. The test determines the mean failure height for which 50% of the specimens experience failure or cracking. The standard specifies that a minimum of five specimens must be tested to yield sufficiently reliable results. The testing procedures of ASTM D 4495 were modified so that the diameter of the weight was reduced from 2.5 in. to 1 in. This modification was made to allow for impact failures to occur between the webs of the box section.

Tests were conducted on specimens with dimensions of 6.5 in. x 1.8 in. x 6 in. The test setup is shown in Figure 3.27.

The impact test was performed on three locations of the sections. First, impact was centered over an open cell creating failure in the flange. Second, impact was centered directly over a web creating failure in the web. Finally, impact was centered over the edge of a web inducing web or flange failure.

Figure 3.27: Impact test setup

3.8.2 Discussion of Results

The results of the impact tests are summarized in Table 3.8. Failure in the flange for the PVC specimens occurred with a lower drop height than for the HDPE specimens. This is reflective of the relatively brittle behavior of the PVC material. However, failure in the web required higher drop heights than the HDPE because of the additional compressive strength of the PVC. The average drop heights for PVC and HDPE flange failure were 4.0 in. and 8.2 in.,

respectively. The average drop height required for failure in the web for PVC was 45.4 in., and for HDPE was 24.6 in. A typical flange failure is illustrated in Figure 3.28. Failure in the webs was generally a result of crushing within the web, which can be seen in Figure 3.29.

Table 3.8: Results of the impact tests

HDPE Drop No.	Flange failure (in.)	Web failure (in.)	Flange or Web failure (in.)
1	9	23	23
2	7	25	21
3	9	23	23
4	7	25	21
5	9	27	23
mean	8.2	24.6	22.2
Stdev	1.10	1.67	1.10
Cov(%)	13	7	5
PVC Drop No.	Flange failure (in.)	Web failure (in.)	Flange or Web failure (in.)
1	4	47	33
2	4	45	35
3	4	43	33
4	4	45	35
5	4	47	33
mean	4	45.4	33.8
Stdev	0	1.67	1.10
Cov(%)	0	4	3

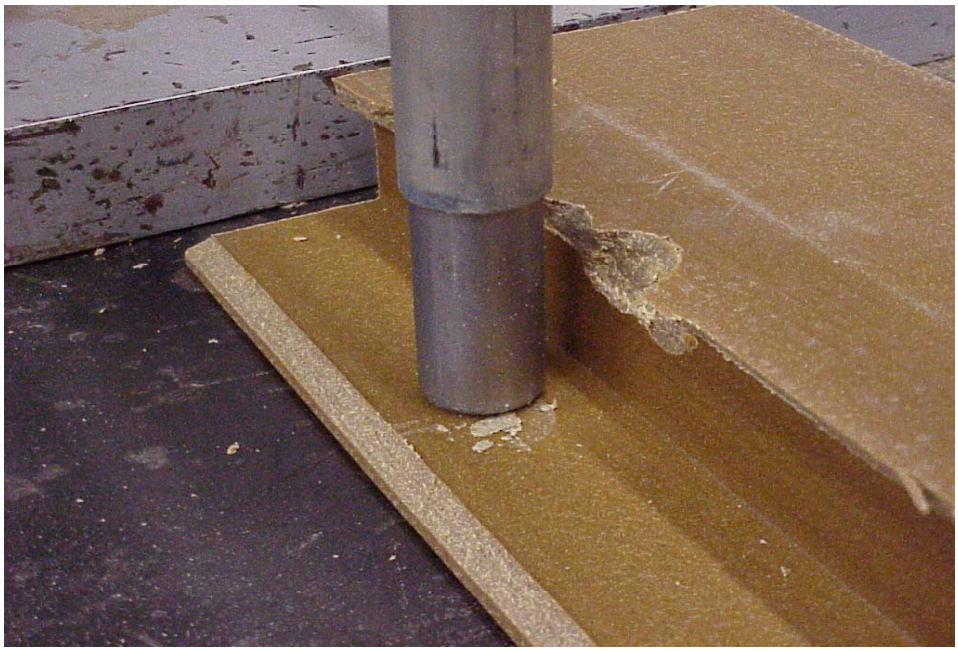

Figure 3.28: Impact failure in PVC flange

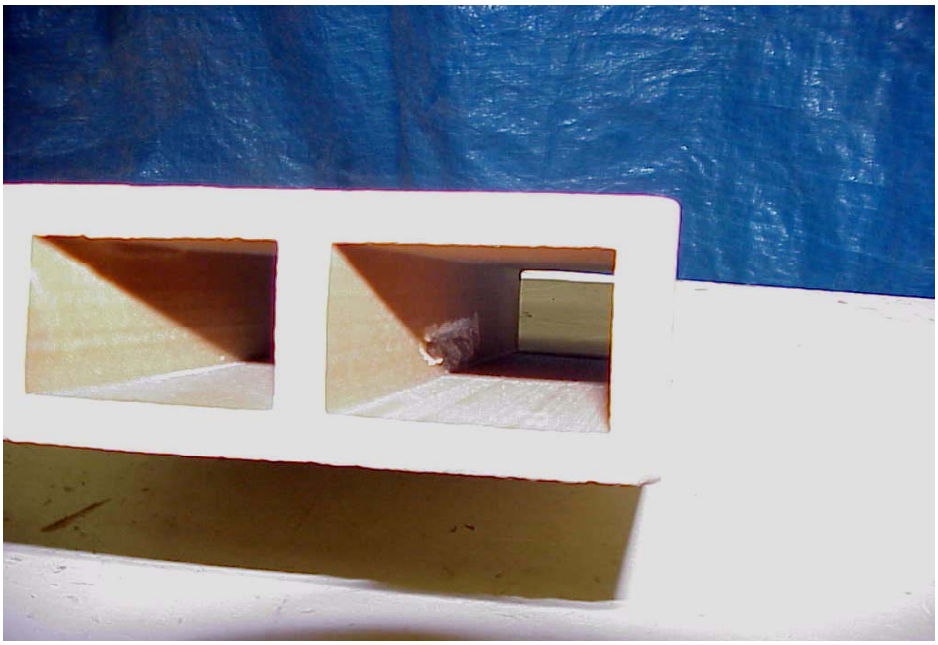

Figure 3.29: Impact failure in PVC web

3.9 Comparison of Material Strength, Stiffness, and Energy Dissipation Characteristics

The test results enable the comparison of strength, apparent stiffness, and the energy dissipated during loading by the HDPE and PVC sections. Table 3.9 presents the relative ratios for the three characteristics. The comparison of ultimate strengths for each test for the two formulations shows that the PVC formulation is from 2 to 4 times stronger than the HDPE formulation. Stiffness comparisons were made with stiffness determined at 40 percent of ultimate strength. Figure 3.30 shows the apparent stiffness for typical flat-wise test sections. Forty percent of ultimate strength is a common basis used for design values (e.g., concrete) allowing safety in capacity and often ductility. The stiffness determined for both formulations using this method is within ten percent of results from previous research in determining apparent modulus of elasticity for WPC material (Lockyear, 1999). The comparison of relative stiffness for each test for the two formulations indicates that the PVC formulation is from 2 to 3 times stiffer than the HDPE formulation.

Computing the area under the load-displacement curves for each test enables a comparison of the energy dissipation capability of the materials. Figure 3.31 illustrates a typical comparison of energy absorbed during shear testing. Due to the apparent ductile response of the HDPE, in the form of large displacements with little increase in load near failure, it might be expected to absorb more energy than the PVC formulation. However, the comparison of energy absorbed for each test for the two formulations shows that the PVC formulation will absorb from 1 to 1.5 times more energy than the HDPE formulation.

Table 3.9: Comparison of strength, stiffness, and energy dissipation for HDPE and PVC formulations

	Relative Strength Ratio P_{Ult} / P_{Ult} PVC / HDPE	Relative Stiffness Ratio (at 0.4P_{Ult}) PVC / HDPE	Energy Ratio (area under load-disp. curve) PVC / HDPE
Flexure (flatwise)	3.3	2.1	1.3
Flexure (edgewise)	2.7	1.8	1.2
Shear	2.4	1.8	1.7
Comp. Perp. (flatwise)	2.4	2.8	1.4
Comp. Perp. (edgewise)	2.1	1.8	0.7
Comp. Parallel	3.8	3.1	0.9

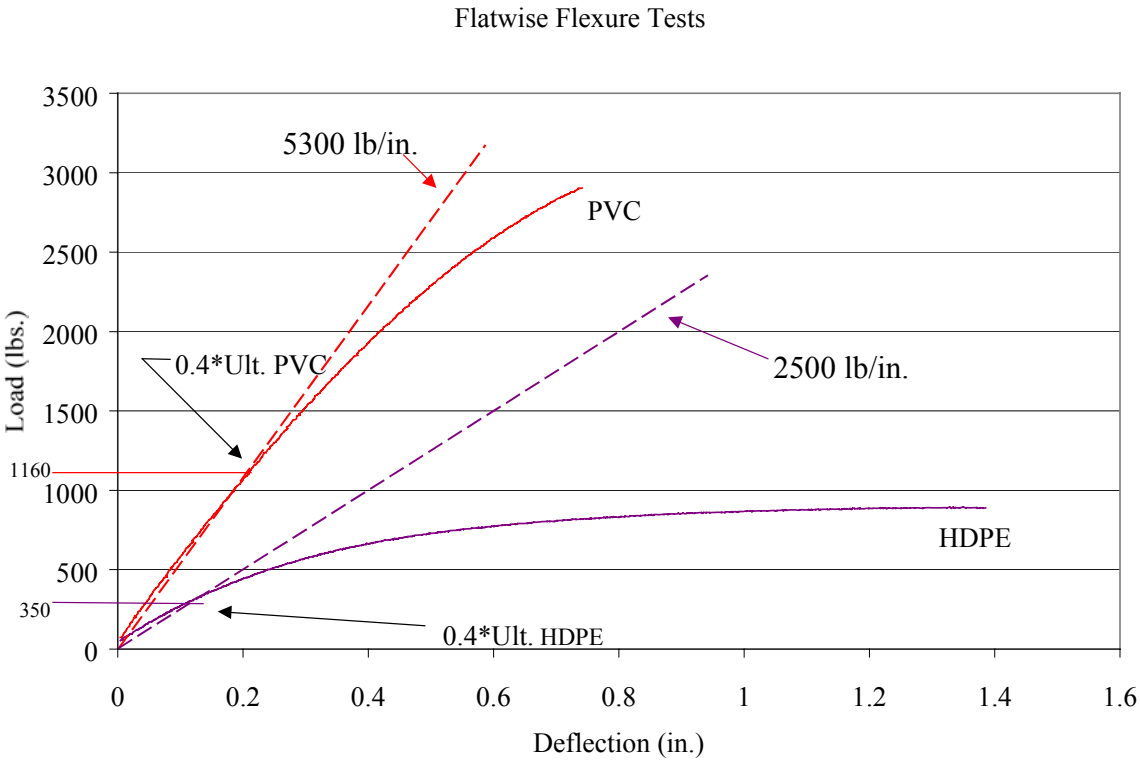

Figure 3.30: Relative stiffness for HDPE and PVC sections

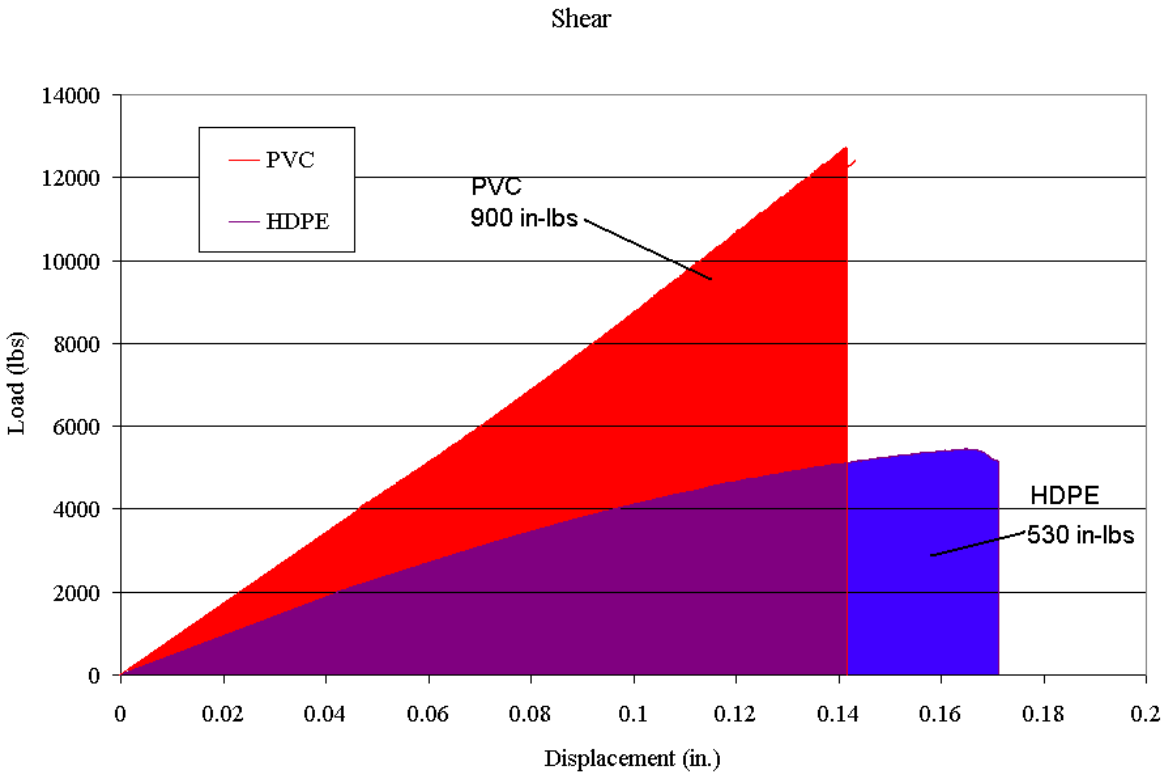

Figure 3.31: Comparison of energy absorbed for HDPE and PVC formulations

3.10 Conclusions

Based upon the experimental tests conducted on WPC sections presented in this chapter, material strength values are established for the design of prototype structural elements for application in demonstration projects. The test results indicate that specimens formulated with the PVC material are stronger and stiffer than those formulated with the HDPE material. However, the PVC specimens exhibited a nearly linear response to failure and with lesser displacement at failure than was obtained with the HDPE specimens. The average compression parallel-to-extrusion strengths were 2243 psi and 8225 psi for HDPE and PVC, respectively, based on net cross-sectional area. The average modulus of rupture (MOR) from the bending

tests for HDPE was 1822 psi and for PVC was 5171 psi. The average compression perpendicular-to-extrusion strengths were 3651 psi for the HDPE and 8033 psi for the PVC, based on net web area. The average shear stresses from bending shear tests were 1133 psi and 2931 for HDPE and PVC, respectively.

CHAPTER 4

PREDICTING BENDING STRENGTH AND BEHAVIOR IN WOOD-PLASTIC COMPOSITE SECTIONS

4.1 Abstract

A Fortran program (MPHIWPC) was developed to analyze wood-plastic composite (WPC) sections under flexural loading. The program determines for beam elements the stress distribution through the depth, the corresponding moment-curvature relationship, and the load-displacement behavior under either 3-point or 4-point bending. Based on comparisons between test results and the predicted results using the program, MPHIWPC provides a very good prediction of the flexural response of both nonreinforced and reinforced WPC sections. The program enabled an improved understanding of the behavior of WPC sections and will in the future assist in the design of WPC flexural members by providing preliminary strength estimates for proposed sections.

4.2 Introduction

In an attempt to further understand the WPC behavior, a Fortran program (MPHIWPC) was developed to analyze WPC beam sections under flexural loading. The program is useful for determining strength and ductility of the sections and for analyzing the distribution of stress though the depth, the shift of the neutral axis as load increases, and the effects of reinforcement on flexural response. The program is able to analyze solid or hollow sections with or without reinforcing, and it incorporates the nonlinear response of the WPC material and the differences in strength and stiffness in tension and compression.

Assumptions in the program include plane sections remain plane (no warping occurs in the member during loading), only axial stresses and strains act in the material (implying pure bending of the member), perfect bond (no slip) between reinforcement fiber and the WPC, and shear deformations are not considered.

4.3 Program MPHIWPC

4.3.1 Program Description

The program develops moment-curvature data points as a function of flexural strain in bending sections. The moment-curvature data is then used to determine load-displacement behavior for two common test setups. Material behavior parameters, cross-sectional shape, and test configuration are required as input to carry out the analysis. The program increments the level of compressive strain, with the increment being specified by the user, and determines moment and curvature for each level of strain. For each increment, the slope of the strain distribution through the depth of the beam is adjusted until equilibrium of axial tensile and compressive forces in the section is reached. Failure is indicated when either the compressive strain capacity or the tensile strain capacity of the WPC material is reached.

With the assumption of a perfect bond between the fiber and WPC, the fiber reinforcing strains, stresses, and forces can be computed, as for the WPC material, using the strain distribution. Load and mid-span displacement data are computed using the moment-area method. The program currently limits the load-deflection calculations to 3-point bending setups with loading at the midpoint and 4-point bending setups with loading at the third points. Appendix C contains a flowchart for the program and the MPHIWPC code.

4.3.2 Program Input

The specific input required for the moment-curvature calculations includes the constitutive stress-strain relationships for both the WPC material and the fiber reinforcement. Previous research developed hyperbolic tangent models to characterize the stress-strain behavior for the HDPE and PVC formulations (Lockyear, 1999). The models were adjusted slightly before use in the program. The constitutive input parameters and maximum strains for the WPC materials are shown in Table 4.1. Figures 4.1 and 4.2 show the tensile hyperbolic tangent models superimposed with coupon test results for the HDPE and PVC materials, respectively. Figures 4.3 and 4.4 show the compressive hyperbolic tangent models along with coupon test results for the HDPE and PVC materials, respectively.

The figures show that the hyperbolic tangent model can characterize the tensile behavior of the material very well. As seen in Figures 4.3 and 4.4, the hyperbolic tangent model characterizes the compressive behavior of the PVC material quite well, but some differences exist between the model and the compression test results for the HDPE material. Based on information from the carbon fiber manufacturer, Zoltek Inc., the tensile stress-strain relation for the carbon fiber is assumed to be linear until failure. Therefore, only the tensile modulus of elasticity (MOE) and strain capacity are required to describe the behavior of the carbon fiber in tension (Table 4.2). Because no data was available on the behavior of the fiber in compression, and for simplicity, the compressive MOE was assumed to be equal to the tensile MOE.

To determine the maximum compressive strain for the reinforcing fiber, a double-box section reinforced with a single layer of fiber on both the top and bottom flanges of the section was instrumented with strain gages and loaded axially in compression. The gages were mounted on the fiber layers at the two ends of a double-box section. Load and strain data were collected

as the specimen was loaded. The results showed that the fiber buckled and failed to hold load after reaching compressive strains between 0.002 to 0.005. As a conservative limit, the 0.002 strain value was used as a maximum strain for the fiber in compression. Table 4.2 shows the MOE and maximum strains for the carbon fiber that were used in the program for reinforced sections.

Additional input for the program includes the shape of the section and the reinforcement configuration. The WPC sections must be divided into layers to capture the shape of the section. The user specifies the height and width of each layer as well as the location and area of each carbon fiber layer.

Table 4.1: Tensile and compressive maximum strains and hyperbolic tangent constitutive parameters (from Lockyear, 1999)

	HDPE			PVC		
Loading	ε_{max}	a (psi)	b	ε_{max}	a (psi)	b
Tension	0.0149	1271	339	0.0073	5396	197
Compression	0.0461	2200	213	0.0112	8750	107

Table 4.2: Tensile and compressive maximum strains and modulus of elasticity for Zoltek reinforcing carbon fiber

	Zoltek Carbon Fiber	
Loading	ε_{max}	MOE
		(Msi)
Tension	0.0167	33
Compression	0.0020	33

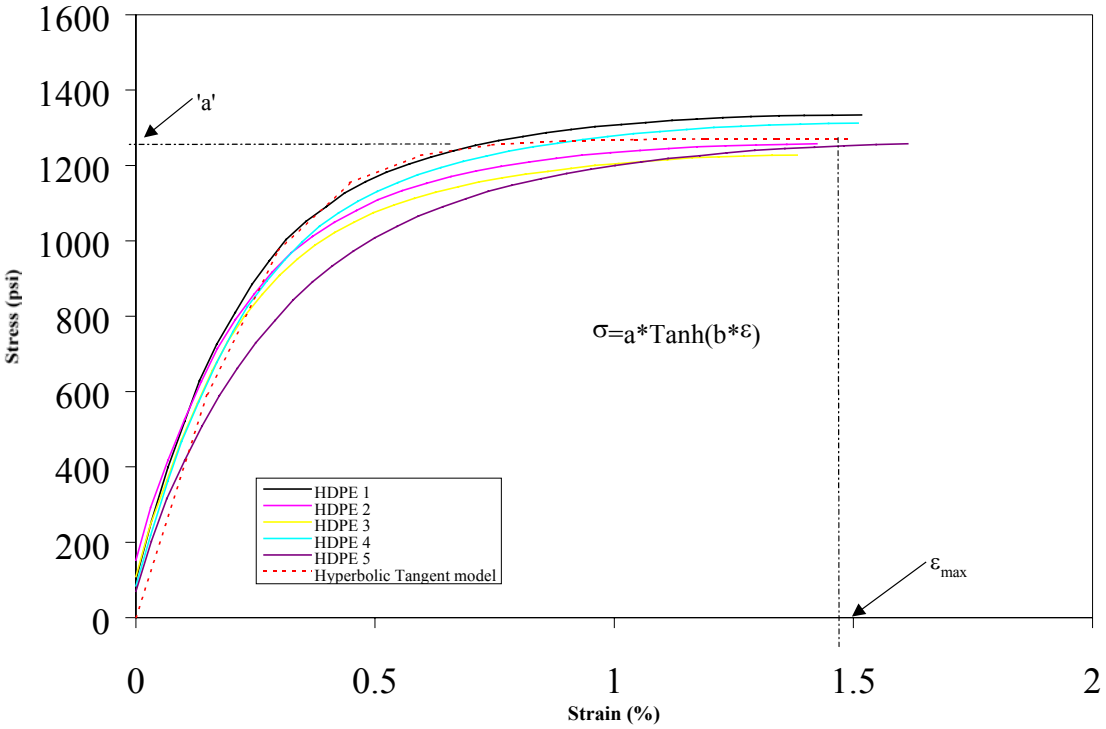

Figure 4.1: Constitutive tensile stress-strain relationship for HDPE

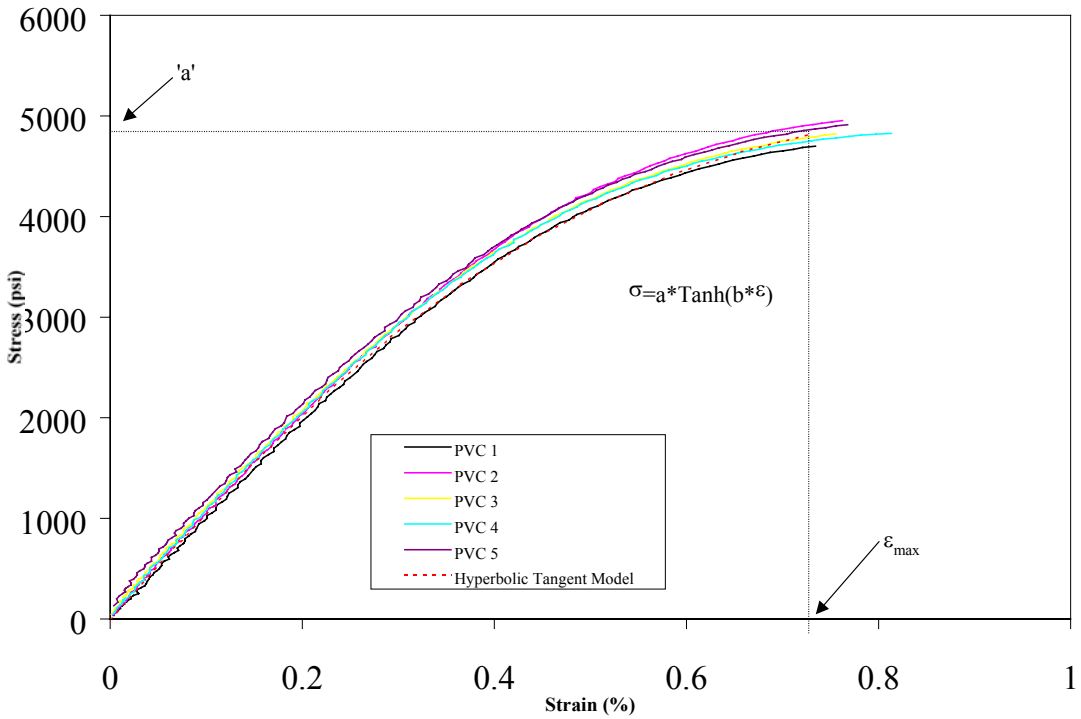

Figure 4.2: Constitutive tensile stress-strain relationship for PVC

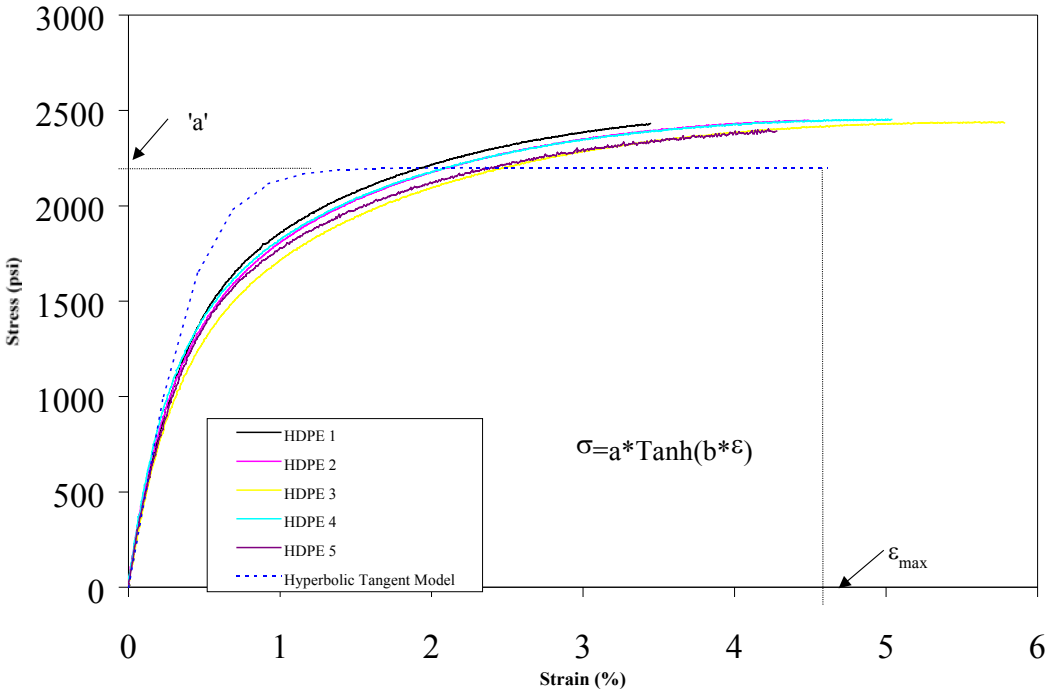

Figure 4.3: Constitutive compressive stress-strain realtionship for HDPE

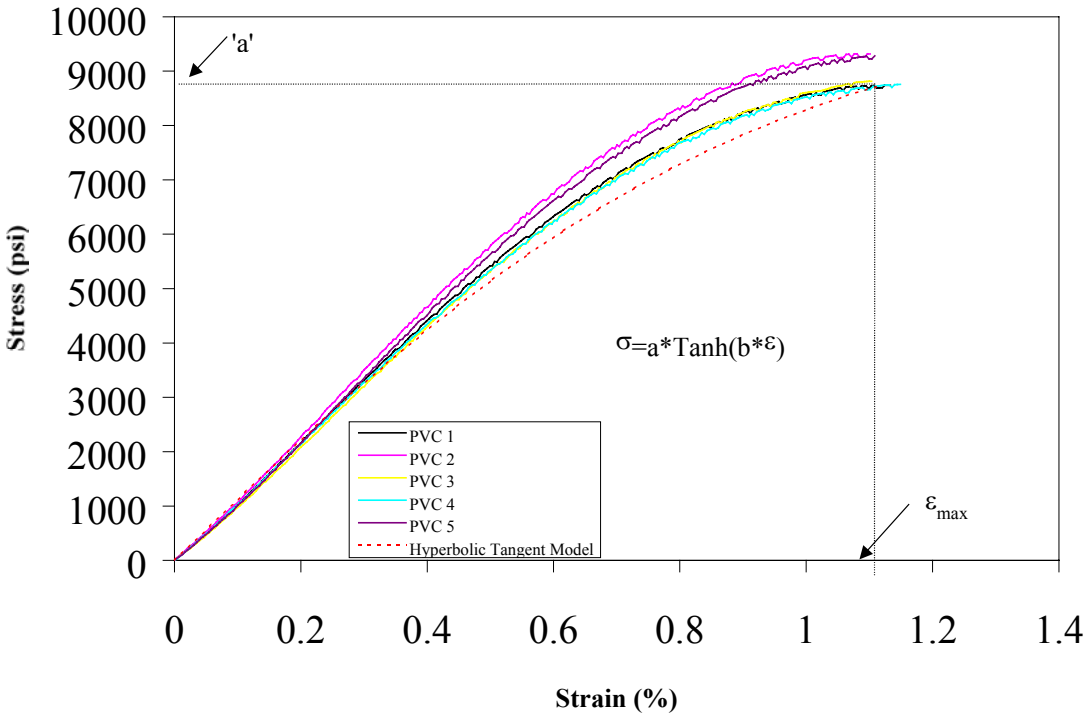

Figure 4.4: Constitutive compressive stress-strain relationship for PVC

4.3.3 Program Output

The output from the moment-curvature calculations for each increment of strain consists of the strain at the top and bottom of the section along with the moment, curvature, and depth of the neutral axis. Load-displacement data are also determined at each strain increment as well as the stress distribution through the depth of the section.

4.4 Comparison of Flexural Test Results to Predicted Results

4.4.1 Comparison of Load-Displacement Results for Near Full-Size Sections

As a means of evaluating the accuracy of the results from MPHIWPC, the triple-box sections previously tested in bending were analyzed using the program. Sections constructed from both WPC formulations were analyzed and compared to experimental results. The HDPE formulation consists of approximately 70% wood and 30% HDPE, and the PVC formulation consists of approximately 50% wood and 50% PVC. The specimens were a rectangular three-cell box section and were tested in both the flat-wise and edge-wise orientations. Figure 4.5 shows the triple-box cross-section. Figures 4.6 and 4.7 show the flat-wise and edge-wise test setups.

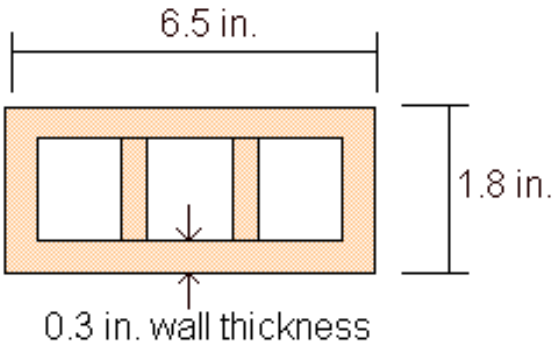

Figure 4.5: Triple-box cross section

The edge-wise specimens were assembled with three side-by-side pieces bolted together at the neutral axis for lateral stability. The specimens were tested in the loading configuration specified in Chapter 2 of this thesis for WPC flexural members. The span lengths were 30 inches for the flat-wise tests and 108 inches for the edge-wise tests. Load and displacement data were collected during each test.

Figure 4.6: Flat-wise flexural test setup

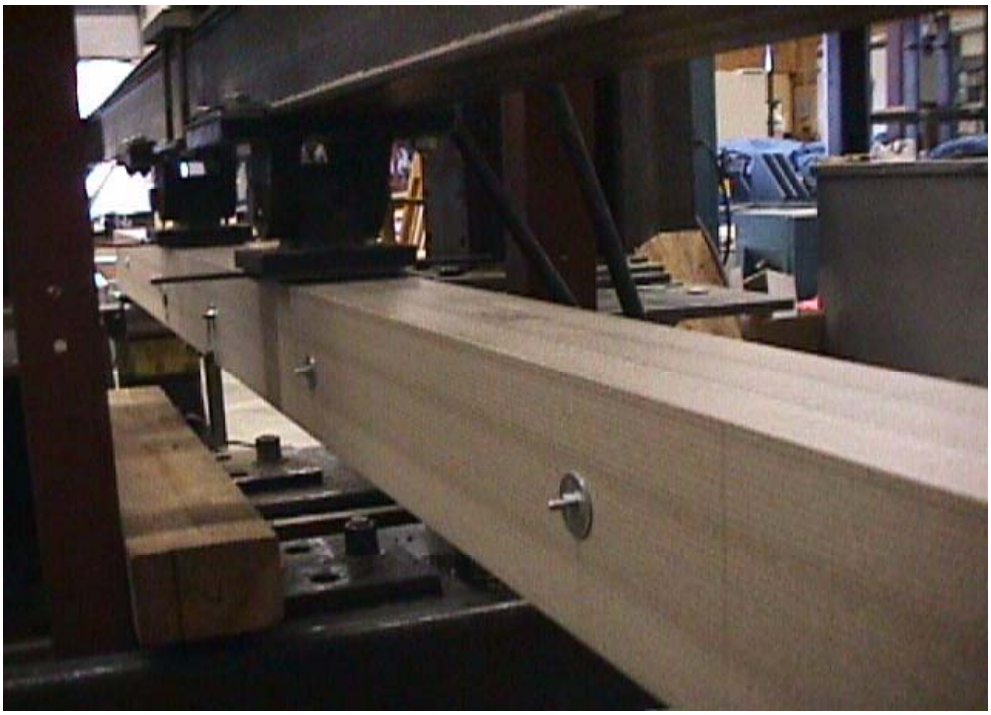

Figure 4.7: Edge-wise flexural test setup

The load-displacement results for flat-wise and edge-wise sections from the program were compared directly to the load-displacement results for the experimental flexure tests for both formulations. Table 4.3 shows a comparison of the maximum loads for the flexure tests and the program output for the tested sections. Figures 4.8 and 4.9 show the flat-wise and edge-wise load-displacement results for the actual bending tests versus the MPHIWPC output for corresponding sections. The results show that the program captures the behavior of sections constructed of both materials very well and provides a good prediction of the maximum loads and displacements.

Table 4.3: Comparison of maximum loads

Section	Maximum Load		
	Flexure Tests (average) (lbs)	**MPHIWPC output** (lbs)	**Percent Diff.** (%)
HDPE flatwise	912	949	(+4)
PVC flatwise	2772	2934	(+6)
HDPE edgewise	2076	2249	(+8)
PVC edgewise	5504	6278	(+14)

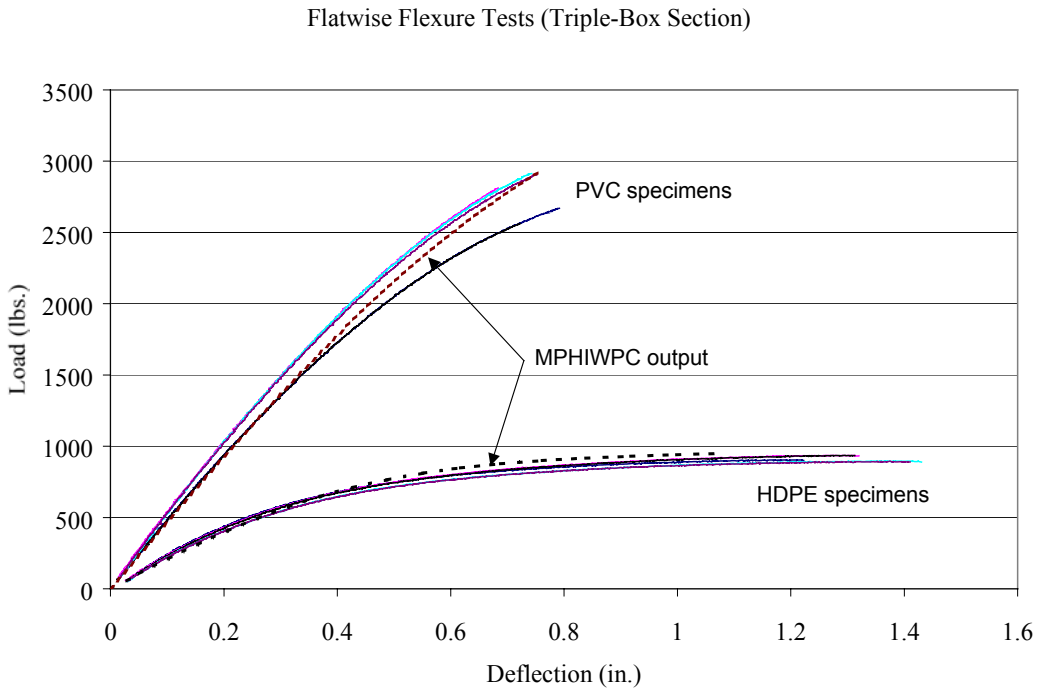

Figure 4.8: Comparison of flat-wise load-displacement results

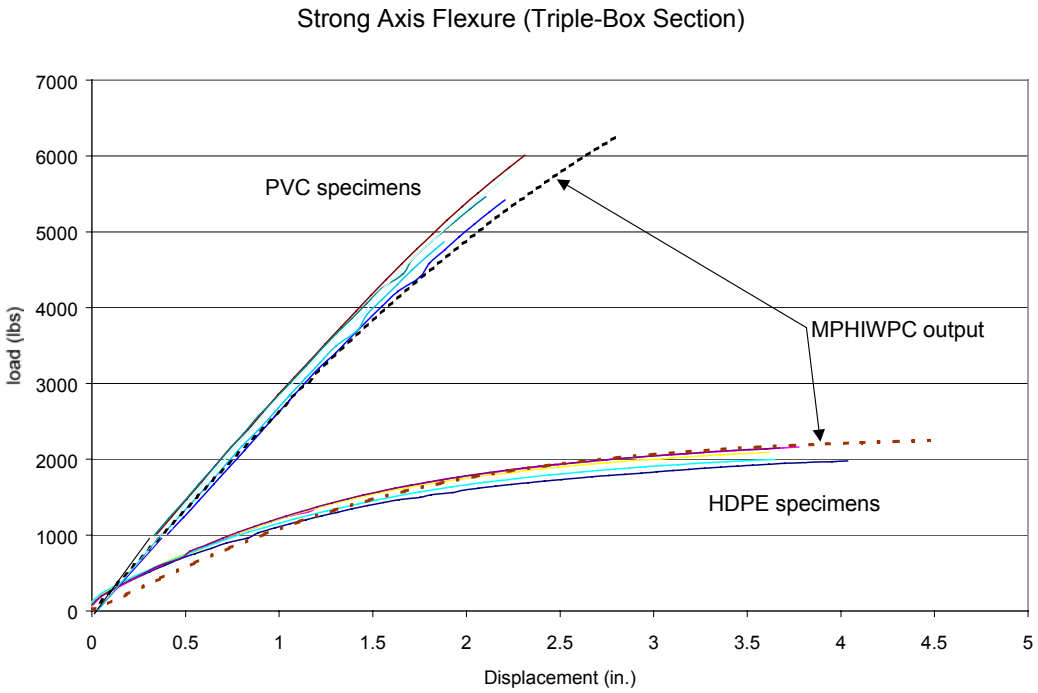

Figure 4.9: Comparison of edge-wise load-displacement results

4.4.2 Comparison of Load-Displacement Results for Coupon Sections

The program was used to analyze coupon sections to make comparisons to coupon test results. The coupon tests were performed by Lockyear (1999) and were conducted in accordance with ASTM D 790, which is a standard test method for flexural properties of unreinforced and reinforced plastics. The dimensions of the test specimens were 6 in. x 0.3 in. x 0.5 in., and the test span was 4.8 inches. The pieces were loaded in 3-point bending using an Instron 4411 testing machine. Figures 4.10 and 4.11 show the results of the MPHIWPC program for a coupon section compared to typical HDPE and PVC coupon load-displacement data. Again, the program captures the general shape of the test results for both formulations. However, the predicted maximum loads and displacements fall short of those observed in the experimental coupon tests.

Previous comparisons of modulus of rupture (MOR) showed similar differences between coupon and near full-size section test results (Paynter, 1998). Differences in the values were, at that time, attributed to sample size (i.e., variations due to the small number of test specimens), scale effects (size effects), and/or to the effect of the bolt holes in the flexure zone of the near full-size section tests. The test results presented in Chapter 3 of this thesis suggest that bolt holes in the flexure zone of the section are not the cause of these differences, as similar MOR's were observed between the flat-wise and edge-wise oriented tests. The results in Chapter 3 of this thesis also suggest that sample size is not the cause of these differences because a larger set of data is now available to establish strength values. The suggestion of size effects of some form between coupon and larger net sections remains a possible cause for the differences in strength. Other factors that may account for the observed differences in the strength of the WPC sections includes shape effects due to the specific geometry of the sections and production effects during extrusion.

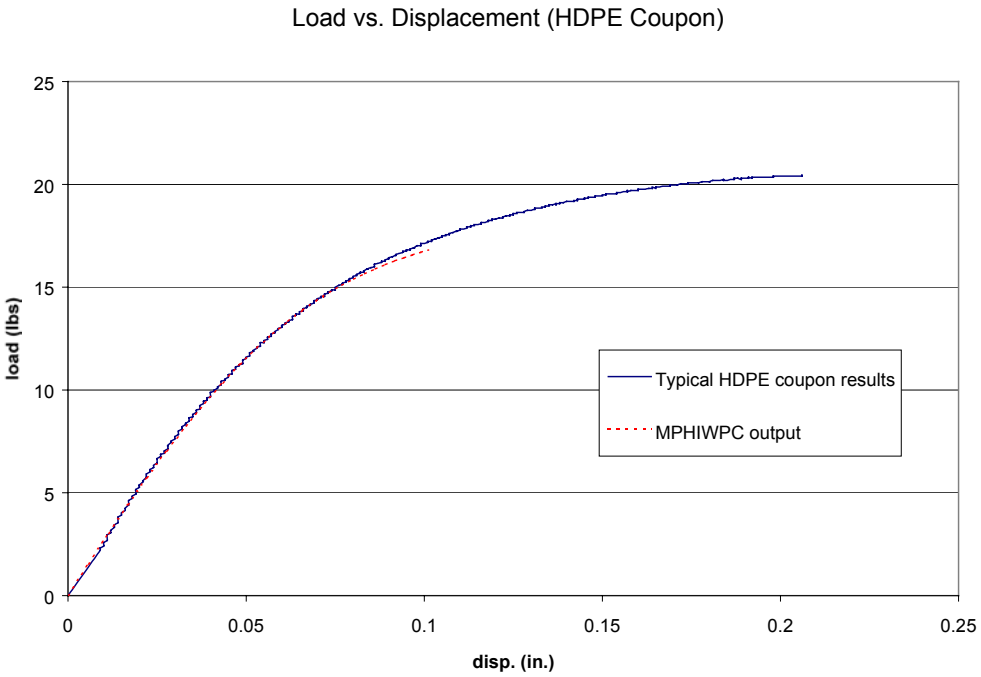

Figure 4.10: Comparison of load-displacement curves for HDPE coupon

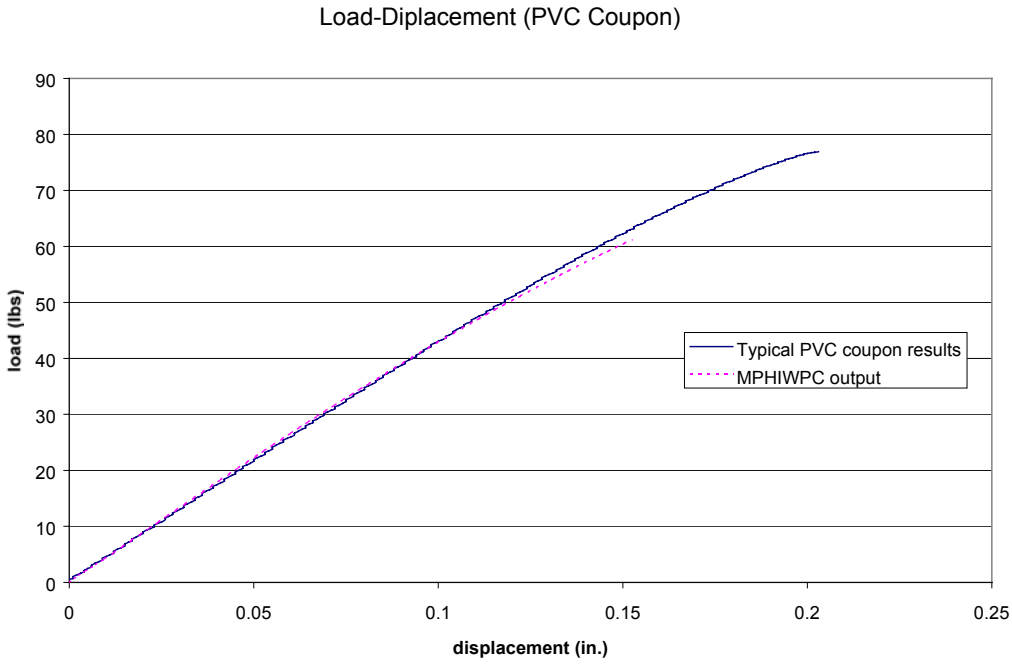

Figure 4.11: Comparison of load-displacement curves for PVC coupon

To investigate size and geometry effects further, the program was modified to permit some additional straining of the material. The WPC materials were allowed to soften in both tension and compression after reaching the maximum strains for the material. This causes a redistribution of the stress in the depth of the section. The softening of the WPC material may be causing the additional load and displacement seen in the experimental coupon tests because the sections are solid.

To characterize the material softening for both materials, the stress-stain relationships after reaching the ultimate strain were assumed to decrease linearly at a slope of 85300 psi.. Figure 4.12 shows an example of the stress-strain curve with the material softening capability. Figures 4.13 and 4.14 show the results for the coupon sections with the modified stress-strain relationships. The results show that the program, with the material softening incorporated, can predict fairly well the behavior of PVC coupon section. However, significant differences remained present between the experimental test data and the program predictions for the HDPE coupon section. This may be due to the apparent yielding and nonlinear behavior of the HDPE material in tension, and the inability of the program to capture the effects of plastic hinge formation in the HDPE material. Because the PVC material exhibits less apparent yielding and nonlinear behavior the program is able to better predict the response of the coupon section compared to the test results.

This allows the section to fail in a more gradual form since the coupon sections are solid. The hollow triple-box net sections would not permit such softening because of the lack of material within the section to redistribute the stress through the depth. This was verified by analyzing the triple-box sections in the modified program with the material softening capability.

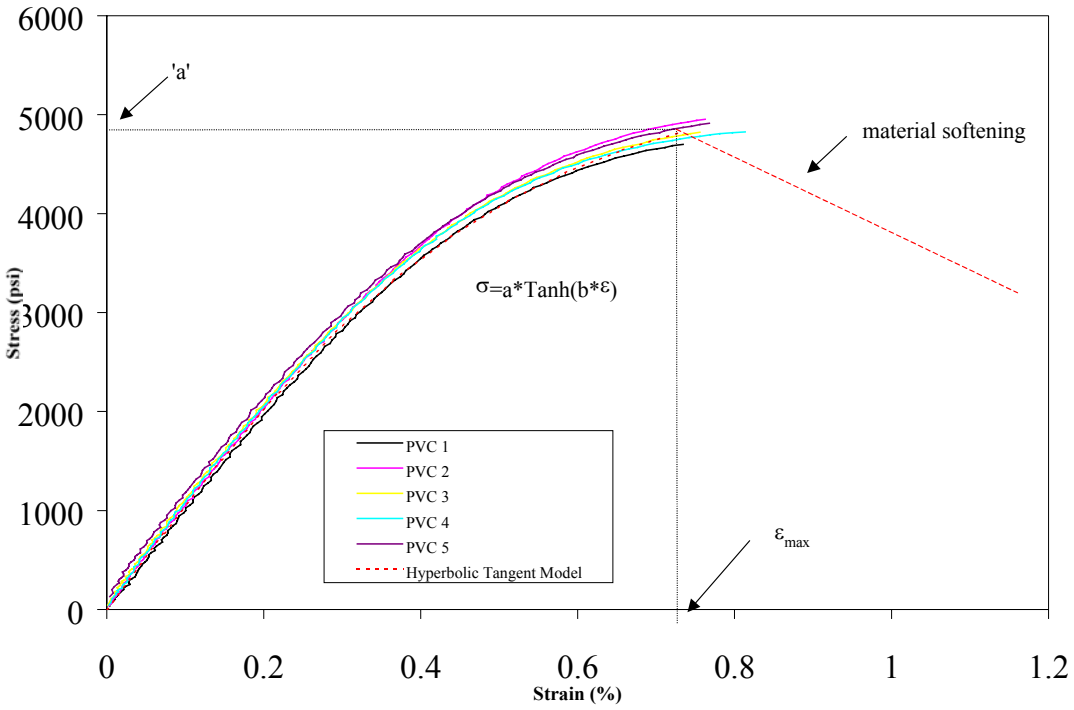

Figure 4.12: Stress-strain curve (tension) with material softening for PVC

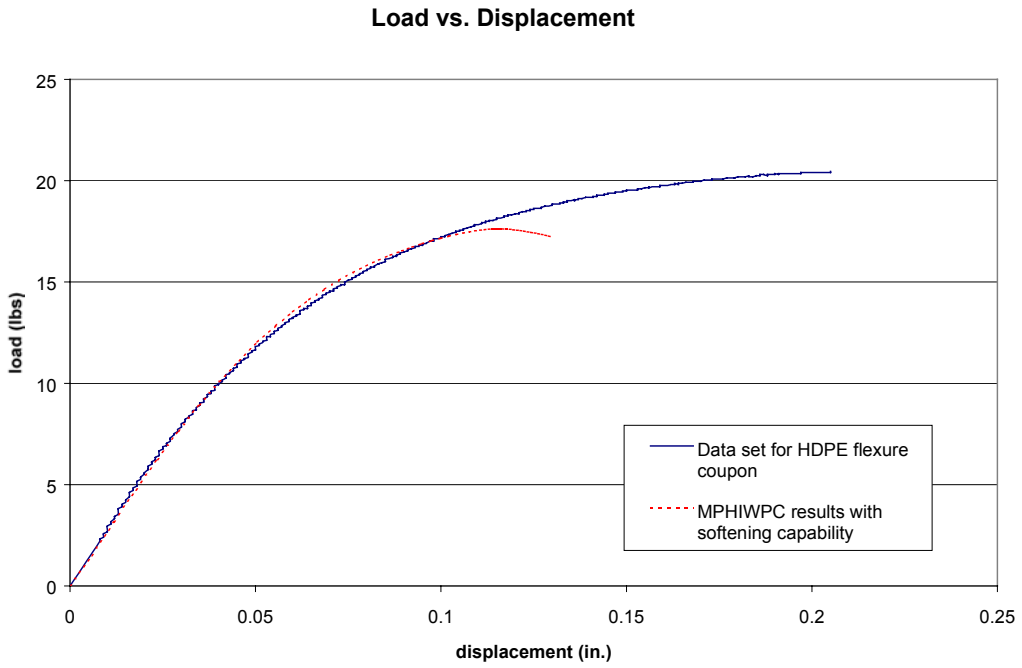

Figure 4.13: Comparison of load-displacement curves for HDPE coupon with material softening incorporated in the program

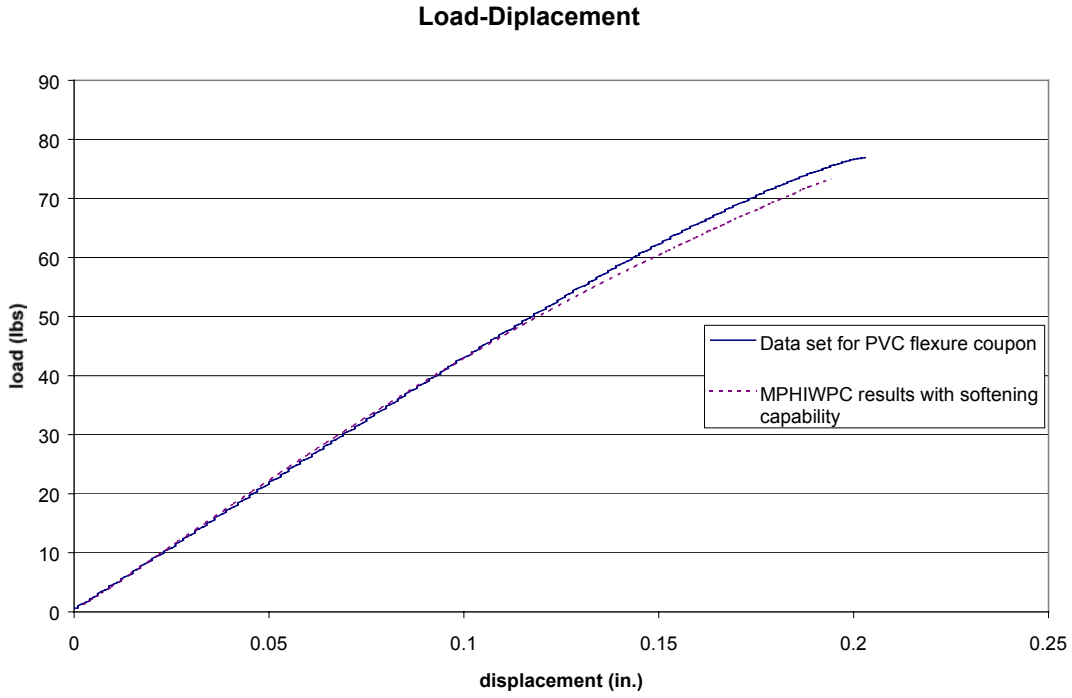

Figure 4.14: Comparison of load-displacement curves for PVC coupon with material softening incorporated in the program

4.4.3 Comparison of Maximum Moments for Single-box and Unsymestric-box Sections

As a means of further evaluating the accuracy of the program, a comparison was made between program MPHIWPC and previously conducted experimental test results for a single-box section and an unsymmetrical-box section for both formulations of WPC materials (Lockyear, 1999). The maximum moments are the only results available for comparison. Each section was cut from a triple-box section to produce the desired section shape. Figure 4.15 shows the triple-box section, the single-box section, and the unsymmetrical-box section.

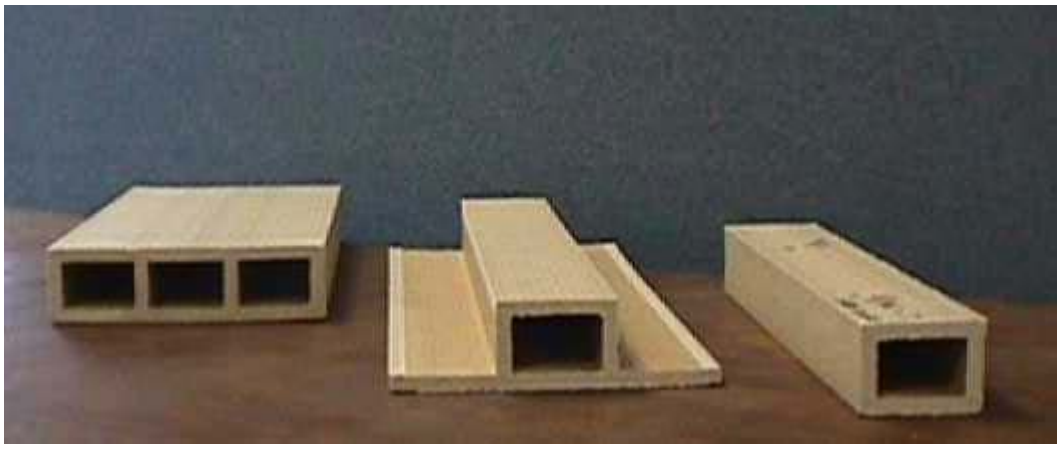

Figure 4.15: Triple-box, single-box, and unsymmetrical-box sections.

The results from the experimental tests and the program are presented in Table 4.4. The comparisons show that the program predicts the strength of the single-box and unsymmetrical-box sections reasonably well. Of note for the PVC unsymmetrical-box section is that the program indicates failure due to crushing at the top of the section rather than tensile failure at the bottom of the section.

Table 4.4: Comparison of maximum moments from experimental tests and MPHIWPC for single-box section and unsymmetrical-box section

Formulation	Section	Experimental test results (Lockyear, 1999) Moment (in.-lbs)	MPHIWPC results Moment (in.-lbs)	Percent difference %
HDPE	single-box	1721	1847	(+7)
	unsym-box	3301	3109	(-6)
PVC	single-box	5539	5570	(+1)
	unsym-box	11661	9109	(-22)

4.4.4 Comparison of Load-Displacement Results for Fiber Reinforced Sections

The strength and behavior of fiber reinforced WPC specimens were evaluated with the program and compared to some limited reinforced section test results. The load-displacement data from a reinforced double-box specimen is shown compared to the MPHIWPC load-displacement output for the same section in Figure 4.16. The results show that the program predicts very well the flexural response of reinforced WPC sections. At this time, the data from the flexural test of the reinforced double-box section is the only reinforced data available for comparison.

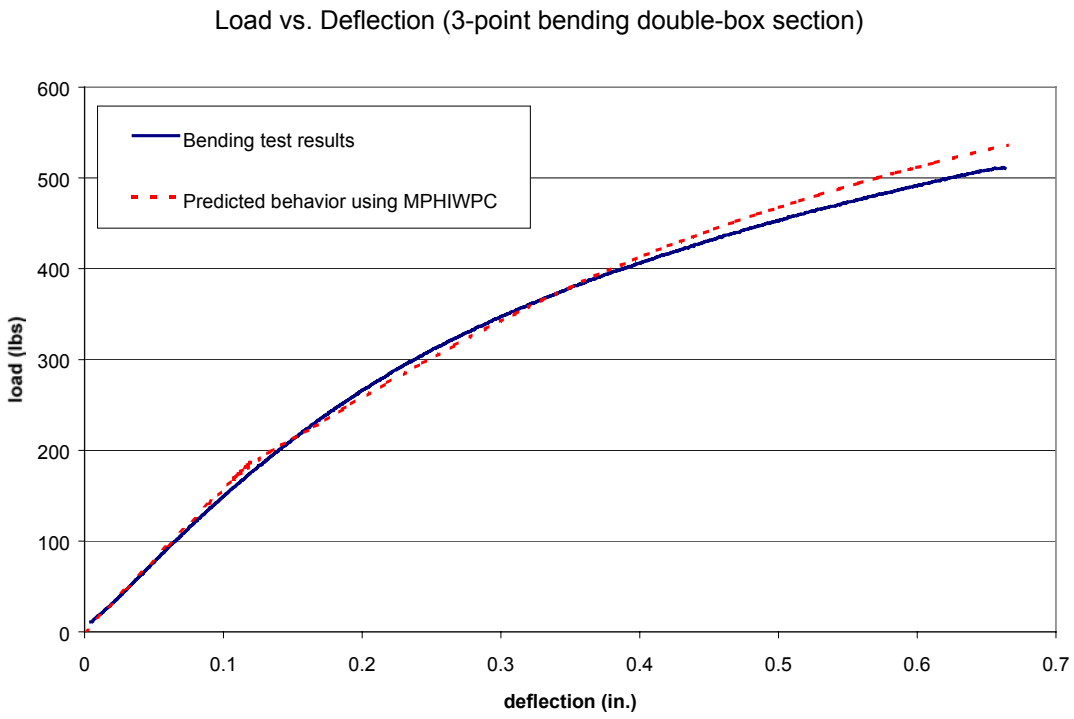

Figure 4.16: Comparison of load-displacement curves for fiber reinforced section

4.5 Shifting of the Neutral Axis in WPC Sections

4.5.1 Unreinforced Near Full-size Sections

Because the WPC material is stronger in compression than tension, it would be expected that the neutral axis would shift toward the top of the member as moment is increased. The MPHIWPC program illustrates this change as a function of moment. Figures 4.17 and 4.18 show the shift of the neutral axis as moment increases for both formulations for flat-wise and edge-wise orientations, respectively. As tensile strains approach maximum values, tensile yielding of the material causes differences in the rate of strain in the outer fibers of the section. This causes the neutral axis to shift upward since the rate of compressive strain will lag the rate of tensile strain due to the higher compressive strength when compared to tensile strength for both WPC formulations.

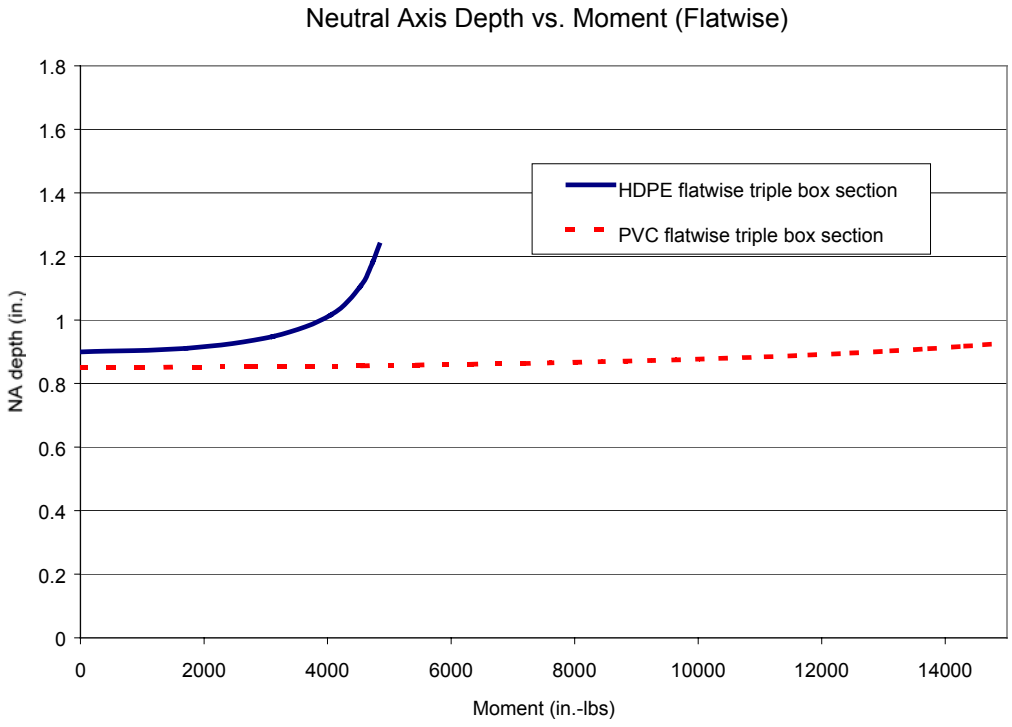

Figure 4.17: Neutral axis shift in flat-wise sections

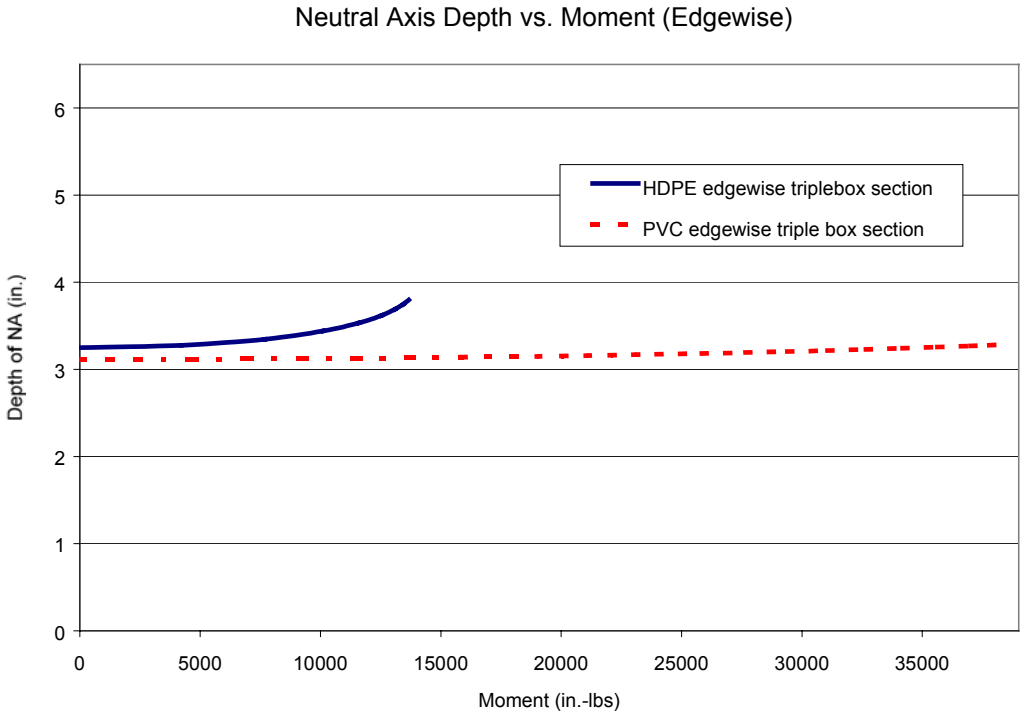

Figure 4.18: Neutral axis shift in edge-wise sections

4.5.2 Fiber Reinforced Near Full-Size Sections

The program was also used to characterize the neutral axis position in reinforced sections. Figure 4.19 shows the neutral axis shift with increase in moment for an HDPE reinforced double-box section. The upward shift of the neutral axis at small moment values is consistent with previous results for the nonreinforced section. This is because equal amounts of compressive and tensile reinforcing are used in the member. The upward shift continues until the compressive fiber reinforcement located near the top of the section buckles. The drop in the neutral axis near 1500 in.-lbs is due to the buckling failure of the compressive fiber reinforcement at this load. The downward trend near the maximum moment is due to the higher total tensile strength with reinforcing now located only at the bottom of the section. This is

similar to the behavior of the unreinforced section near maximum moment where the neutral axis shifts up due to higher compressive strength.

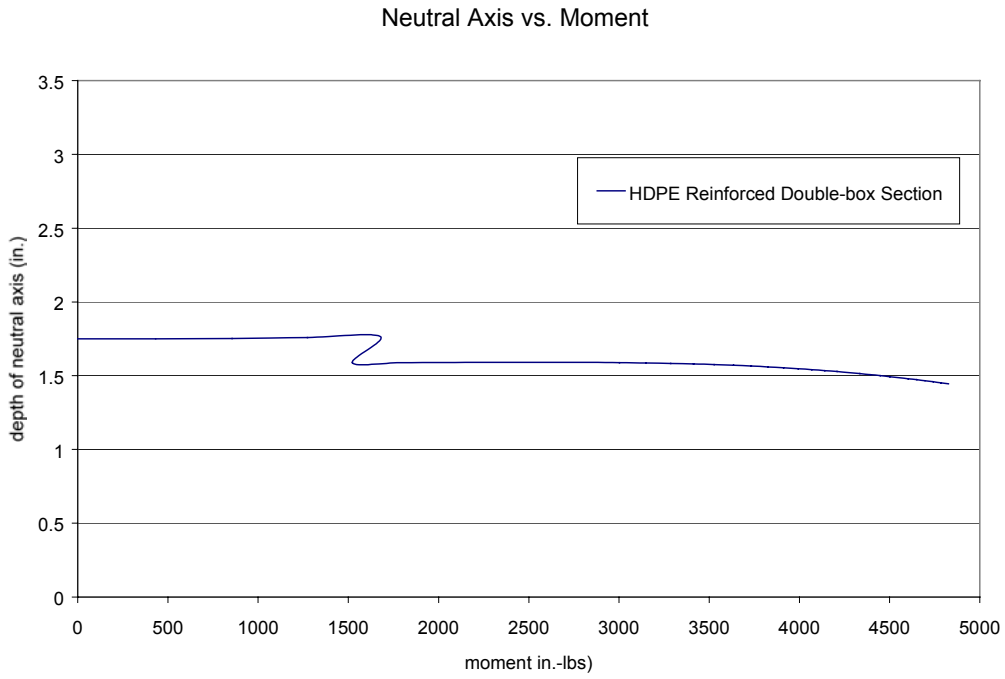

Figure 4.19: Neutral axis shift in reinforced double-box section

4.6 Experimental Bending Tests to Investigate Neutral Axis Shift, Strain Distribution, and Failure Strains in WPC Sections

Experimental bending tests were conducted to further understand the neutral axis shifting, the distribution of strain through the depth, and to compare failure strains in the WPC sections with similar output from the program MPHIWPC. Two flat-wise and two edge-wise triple-box sections of both formulations were instrumented with strain gages and tested in bending. The tests were carried out in accordance with the loading configuration specified in Chapter 2 of this thesis for WPC flexural members. Figures 4.20 and 4.21 show the test setup for the flat-wise and edge-wise tests, respectively. The span lengths were 30 inches for the flat-wise tests and 66

inches for the edge-wise tests. Lateral support was provided for edge-wise pieces to prevent lateral-torsional buckling during loading. Load and displacement data was collected during each test. The edge-wise pieces were loaded using an MTS actuator equipped with a 50-kip load cell. The flat-wise specimens were tested using a United testing machine equipped with a 20-kip load cell. Displacement data was collected using a potentiometer for both flat-wise and edge-wise tests.

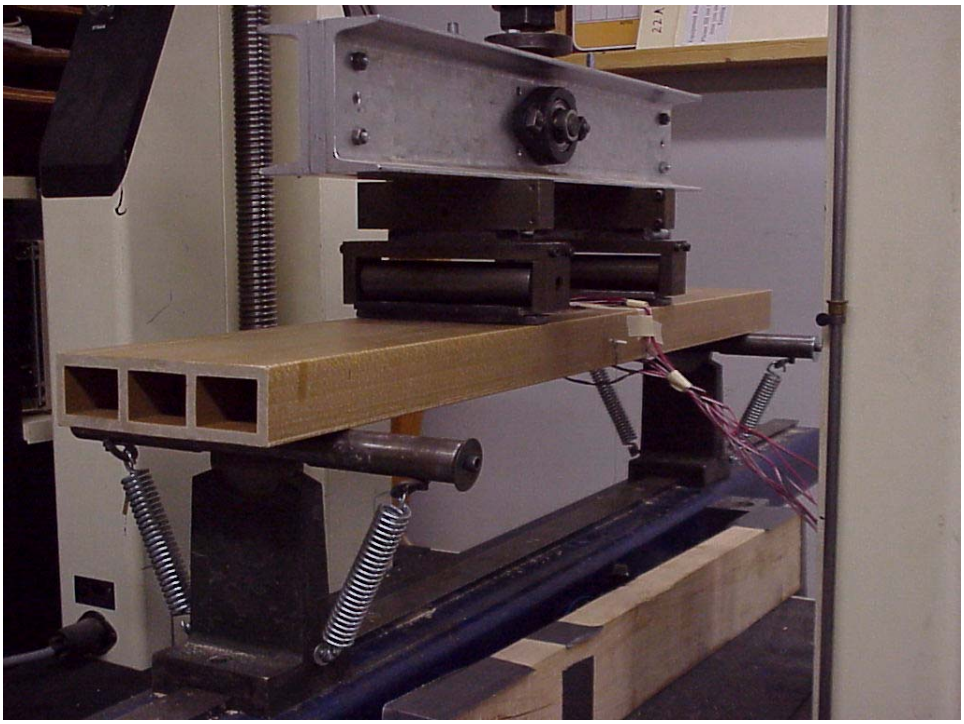

Figure 4.20: Flat-wise bending test setup with strain gages

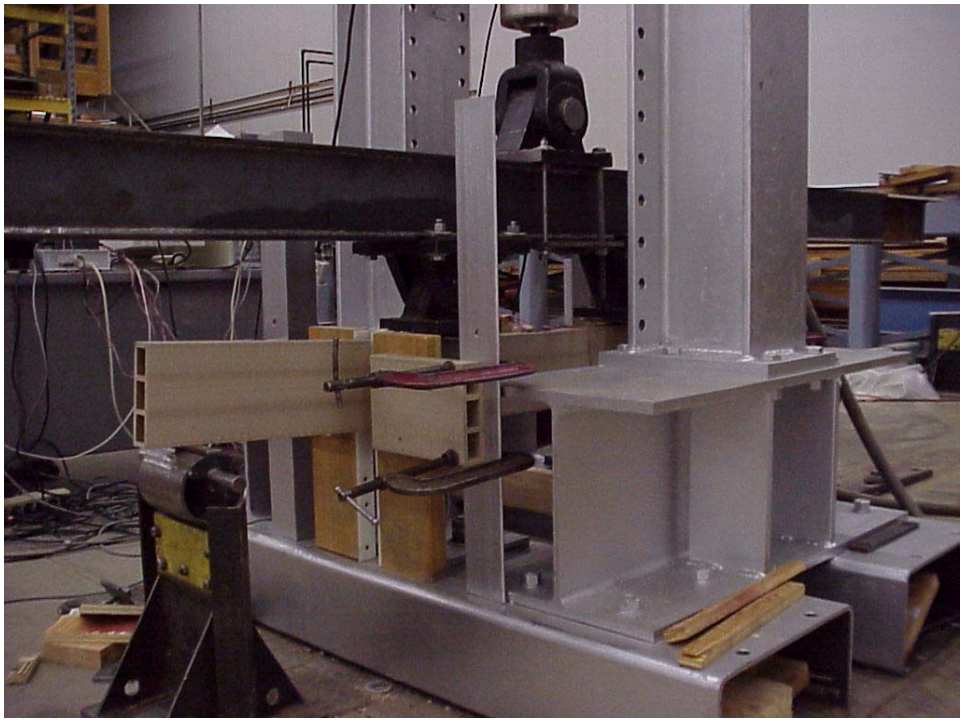

Figure 4.21: Edge-wise bending test setup with strain gages

Strain gages were placed along the depth of edge-wise specimens to characterize the strain distribution through the depth of the sections. Strain gages were also placed across the top and bottom of the flat-wise specimens to characterize variations in strain across the width of the section. Figures 4.22 and 4.23 show the strain gages on flat-wise and edge-wise test sections, respectively.

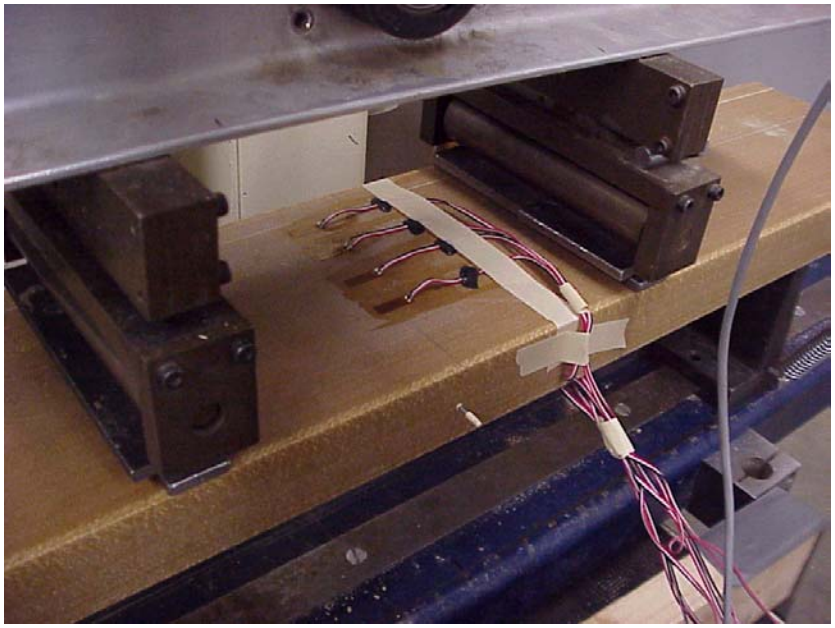

Figure 4.22: Flat-wise mounted strain gages

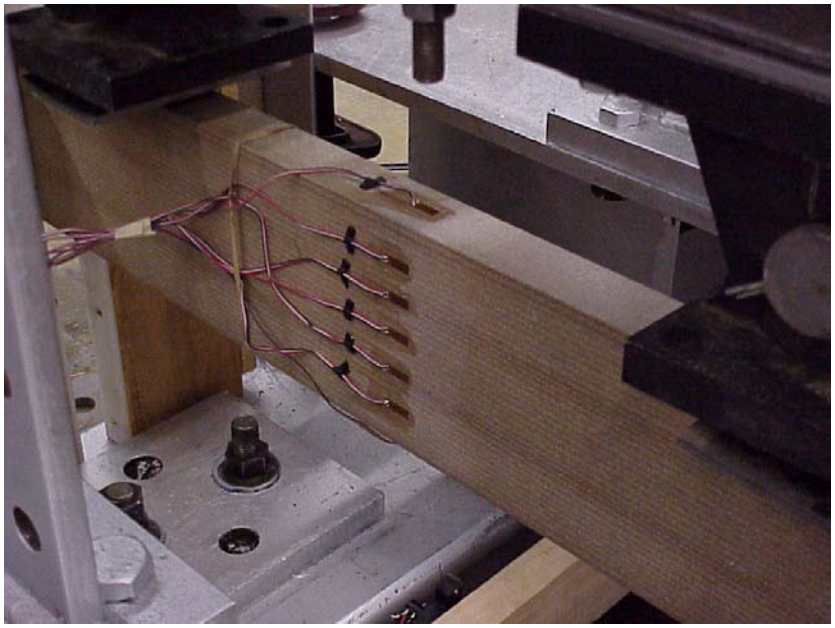

Figure 4.23: Edge-wise mounted strain gages

The strain distributions at failure for each of the edge-wise HDPE and PVC sections are shown in Figures 4.24 and 4.25, respectively. Because of a coarse resolution setting in the data

collection system during testing, there is some question of the accuracy of the intermediate values for strain through the depth of the section for the edge-wise tests. A straight line approximation of the data points shows that the points near the top and bottom fit the approximation fairly well. Figures 4.26 and 4.27 show the strain distribution for each of the flat-wise HDPE and PVC sections. Since gages were only placed on the top and bottom of the section, a straight line is used to represent the strain distribution through the depth of the section.

The results from the flat-wise tests show little variation in strain across the width of the section. Figure 4.28 and 4.29 show the strain distribution at failure for both formulations across the top and bottom of a test specimen, respectively.

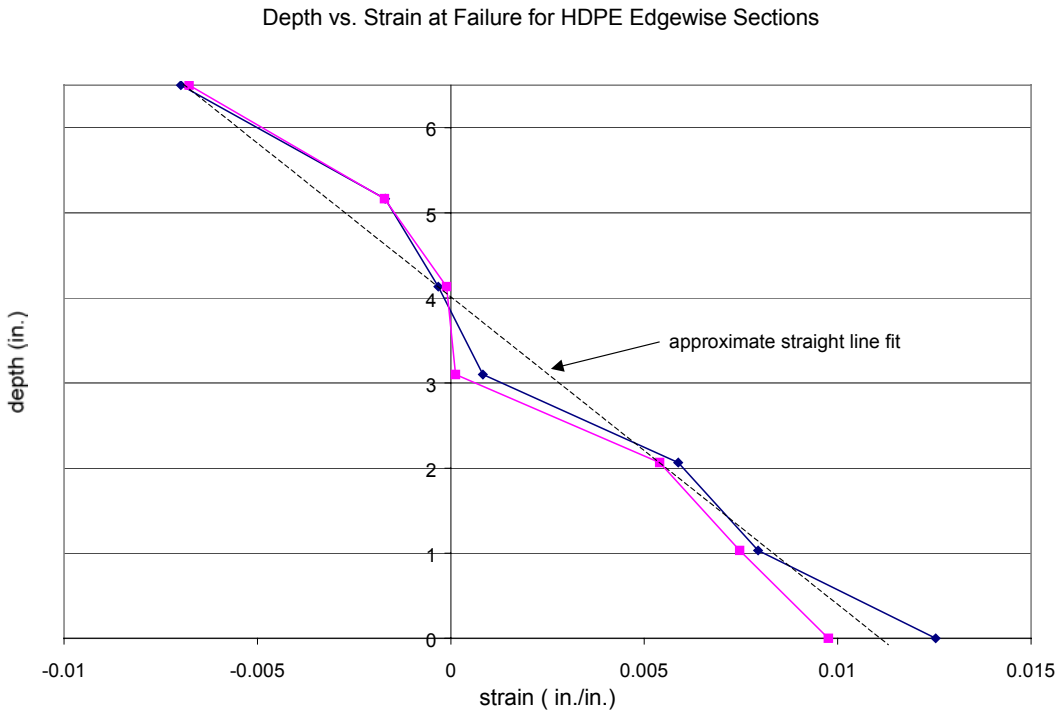

Figure 4.24: Strain distribution at failure for HDPE edge-wise sections

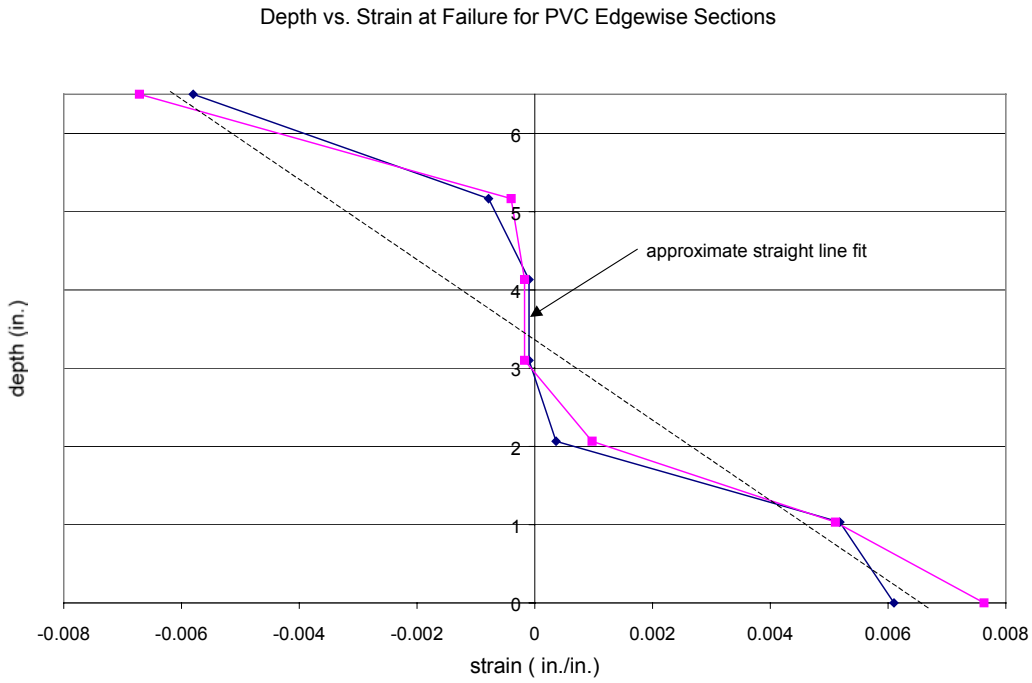

Figure 4.25: Strain distribution at failure for PVC edge-wise sections

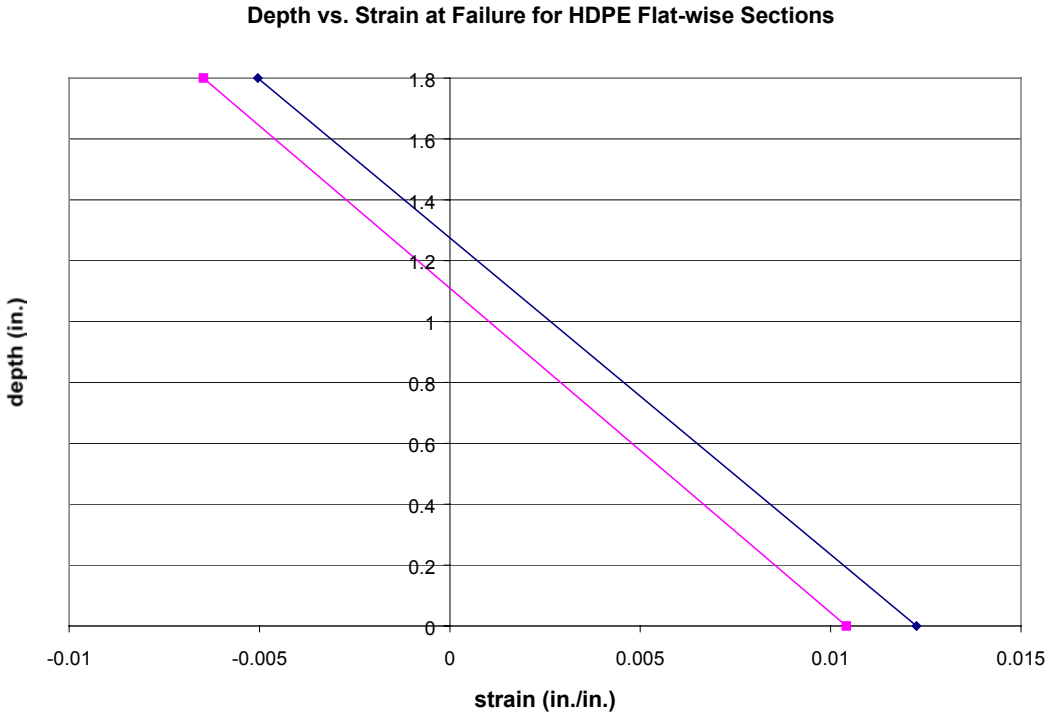

Figure 4.26: Strain distribution at failure for HDPE flat-wise sections

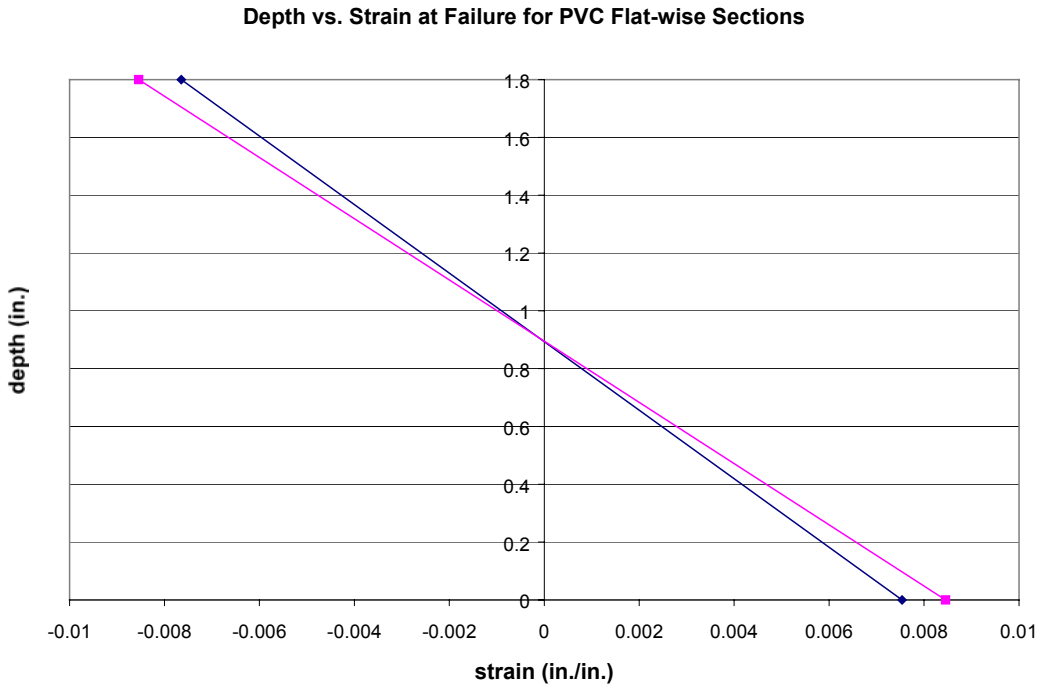

Figure 4.27: Strain distribution at failure for PVC flat-wise sections

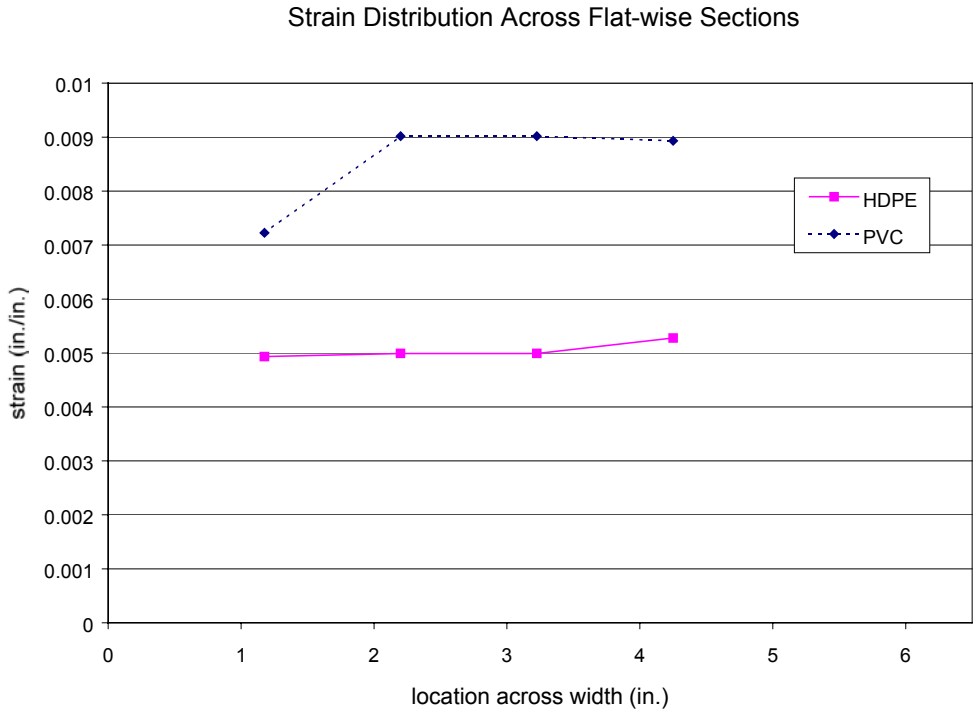

Figure 4.28: Compressive strain distribution at failure across top of flat-wise sections

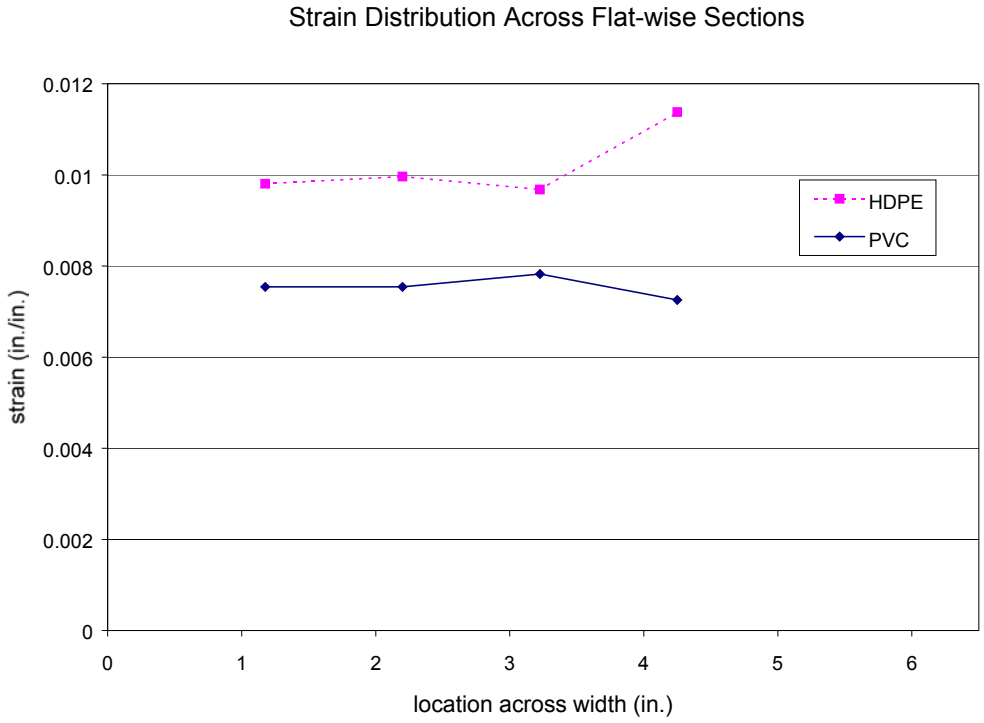

Figure 4.29: Tensile strain distribution at failure across bottom of flat-wise sections

Table 4.5 shows a comparison of the recorded strains at failure for the experimental tests to the maximum strains determined for the WPC material from coupon tests and used as strain limits in the program MPHIWPC. The results show that the strains at failure in the experimental tests are reasonably similar to the limiting strain values set for the WPC material. The difference in maximum strains at failure between the experimental tests and those determined by Lockyear were greater for the HDPE material.

Table 4.5: Comparison of strain at failure for experimental tests to maximum strain for WPC material

		Flexure test results		Maximum strain (Lockyear, 1999)	Percent difference	
		strain at failure (in./in.)		(in./in.)	(%)	
		specimen 1	specimen 2		specimen 1	specimen 2
Flat-wise	HDPE	0.0123	0.0105	0.0149	(-17)	(-30)
	PVC	0.0076	0.0085	0.0073	(+4)	(+12)
Edge-wise	HDPE	0.0099	0.0127	0.0149	(-34)	(-37)
	PVC	0.0062	0.0077	0.0073	(-16)	(+1)

The neutral axis positions were calculated from the experimental test results and are presented in Table 4.6. The neutral axis location at failure was determined by assuming a linear distribution of the strains through the depth of the member. Again, questions existed on the accuracy of the intermediate points for strain through the depth of the section and were not used in the neutral axis location calculations. Only the gages located at the top and bottom of the edge-wise sections were used to determine the neutral axis position. The average strain across the top and bottom of each flat-wise member was used in Table 4.6 for strain values on the top and bottom of the sections. The results show that the program predicts the location of the neutral axis very well for both flat-wise and edge-wise sections.

Table 4.6: Neutral axis shifting results from flexural tests

Orientation	Formulation	Neutral axis position from strain gage tests (in.) from bottom		MPHIWPC Results (in.) from bottom	Percent Difference (%)	
		specimen 1	specimen 2		specimen 1	specimen 2
Flat-wise	HDPE	1.27	1.11	1.23	(+4)	(-10)
	PVC	0.89	0.90	0.93	(-3)	(-3)
Edge-wise	HDPE	3.84	4.18	3.79	(+1)	(+10)
	PVC	3.33	3.46	3.28	(+2)	(+5)

4.7 Stress Distribution Through the Depth of WPC Sections

4.7.1 Unreinforced Near Full-size Sections

The stress distribution in bending members may be characterized using the MPHIWPC program without the softening capability. When equilibrium is reached in the section for each strain step, the stress at each WPC layer is calculated using the constitutive stress-strain relations for the material. Figures 4.30 and 4.31 show the stress distribution at failure for flat-wise and edge-wise bending for both formulations. The plots show the stronger compressive strength for both materials as well as the shifted neutral axis from the center of the section. The HDPE material exhibits more of a shift for the neutral axis compared to the PVC due to larger differences between the tensile and compressive strengths.

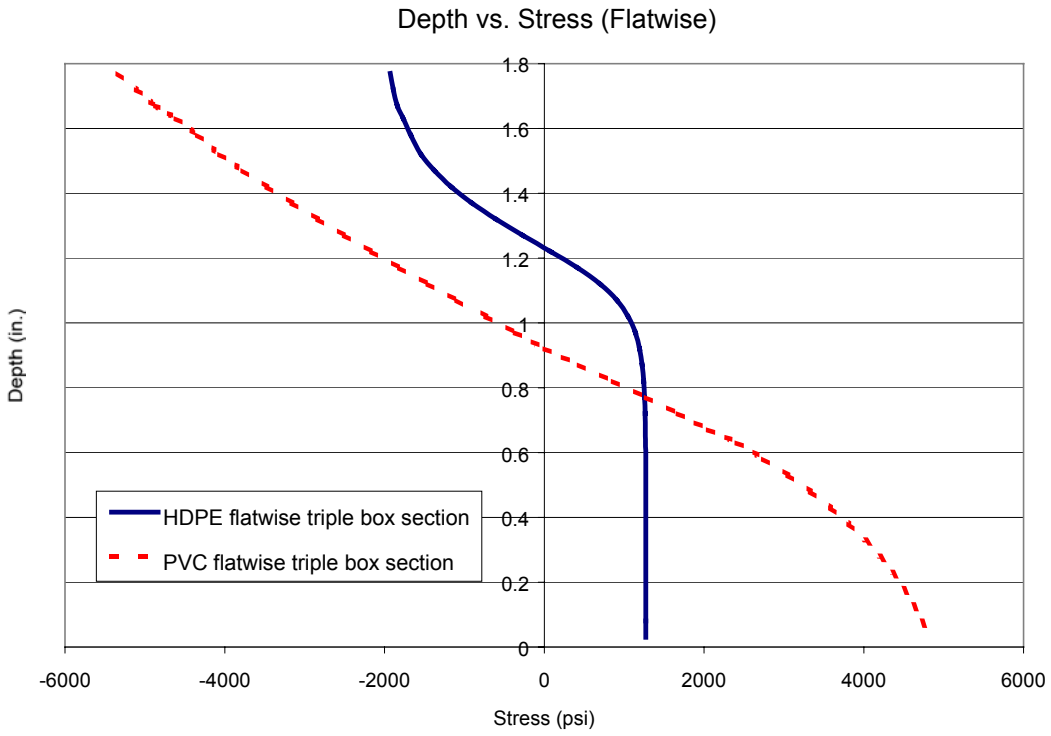

Figure 4.30: Stress distribution for flat-wise triple-box sections

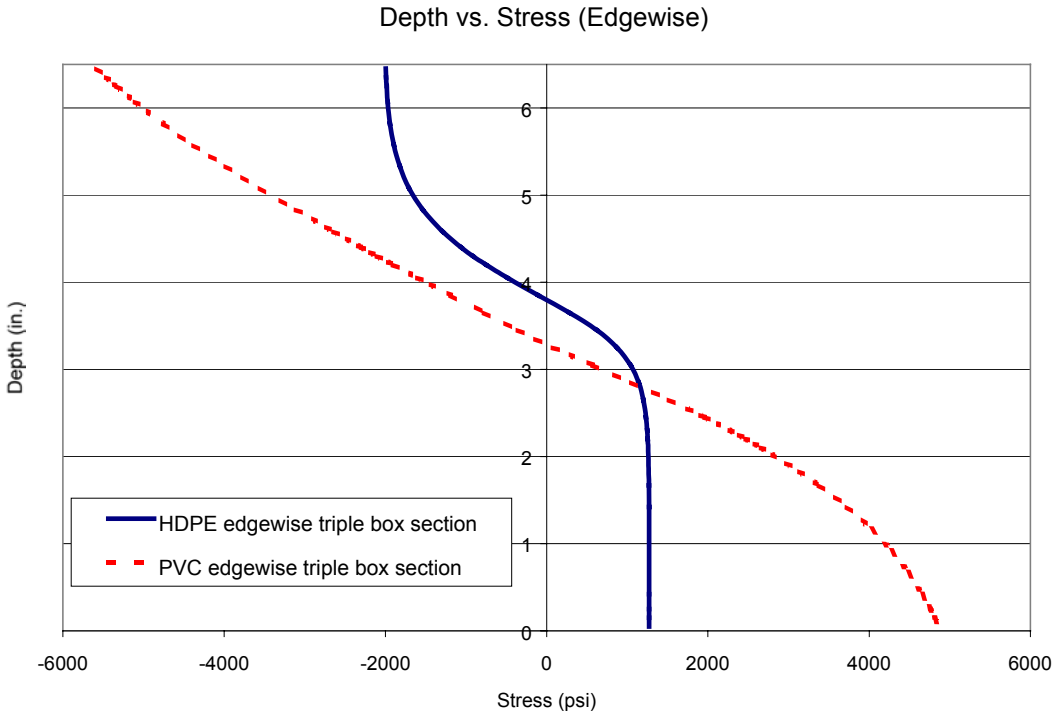

Figure 4.31: Stress distribution for edge-wise triple-box sections

4.7.2 Fiber Reinforced Sections

The stress distribution at failure for an HDPE reinforced double-box section is shown in Figure 4.32. The location of the neutral axis coincides with the position of the neutral axis at failure in Figure 4.19. The downward shift of the neutral axis, as opposed to the upward shift in Figure 4.30 for an unreinforced section, reflects the presence of the tensile reinforcing near the bottom of the section. Because the neutral axis location is below the section centerline at failure the section may be considered over-reinforced. An over-reinforced section is generally stiffer and stronger, but may be considered a less efficient use of the WPC and reinforcing materials because the section will become less ductile. The effects of reinforcement on strength and ductility are discussed further in section 4.8.

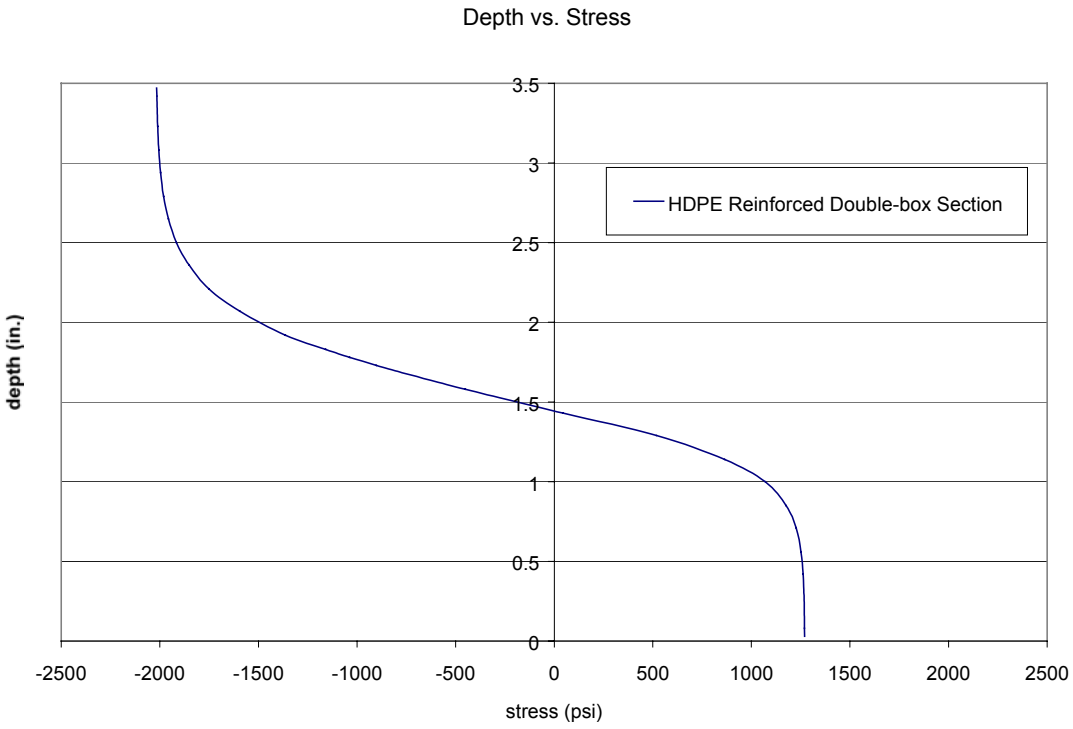

Figure 4.32: Stress distribution in reinforced double-box section

4.8 Effects of Reinforcement Quantity on Strength and Ductility for WPC Sections

The program enables comparison of bending strength and ductility for different quantities of reinforcing in WPC sections. The modified program with the softening capability was used to analyze a double-box section with various amounts of reinforcement for HDPE and PVC formulations. Figures 4.33 and 4.34 show the load-displacement results for the reinforced double-box sections. For an HDPE section, as the amount of reinforcing for both tension and compression is increased from one layer through four layers, the maximum load increases while the maximum displacement decreases. This is because the HDPE material is near the point of tensile yielding with only one layer of reinforcement. With more than one layer of tensile reinforcing the section becomes stiffer and will carry more load, but ductility is lost because a compressive failure at the top of the section occurs and the section is essentially over-reinforced.

For the PVC sections, as the reinforcing area increases the maximum load and maximum displacement also increase. This is expected for the PVC formulation because it exhibits similar stiffness in tension and compression and because the material shows little apparent yielding near failure.

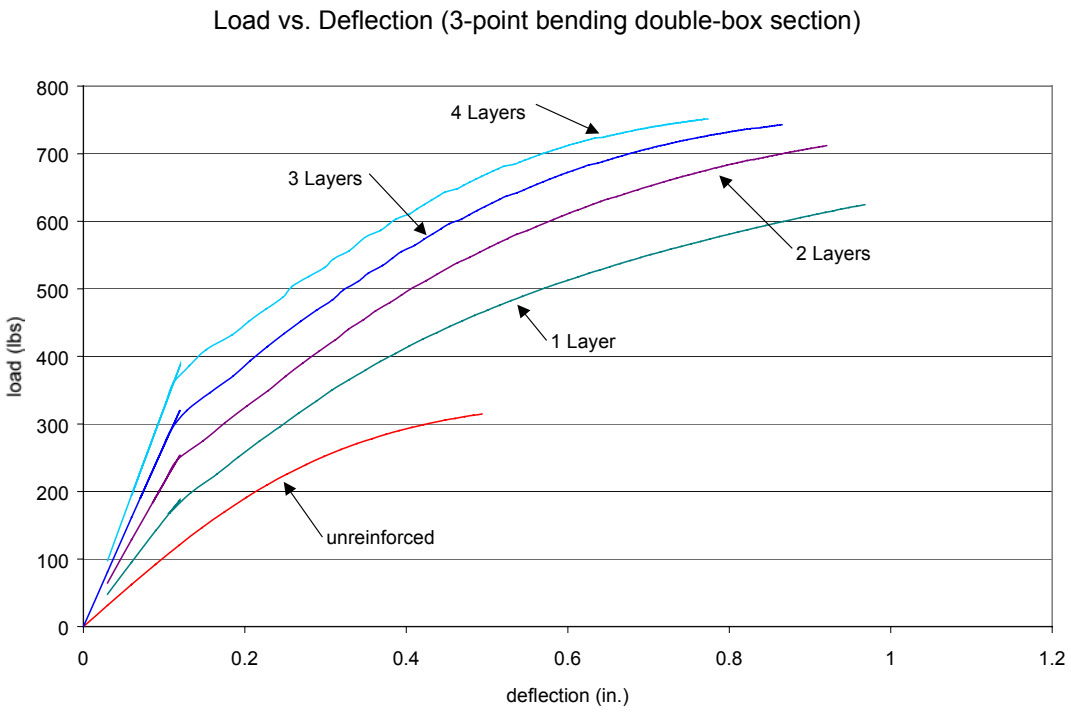

Figure 4.33: Load-displacement for various quantities of reinforcing for HDPE double-box

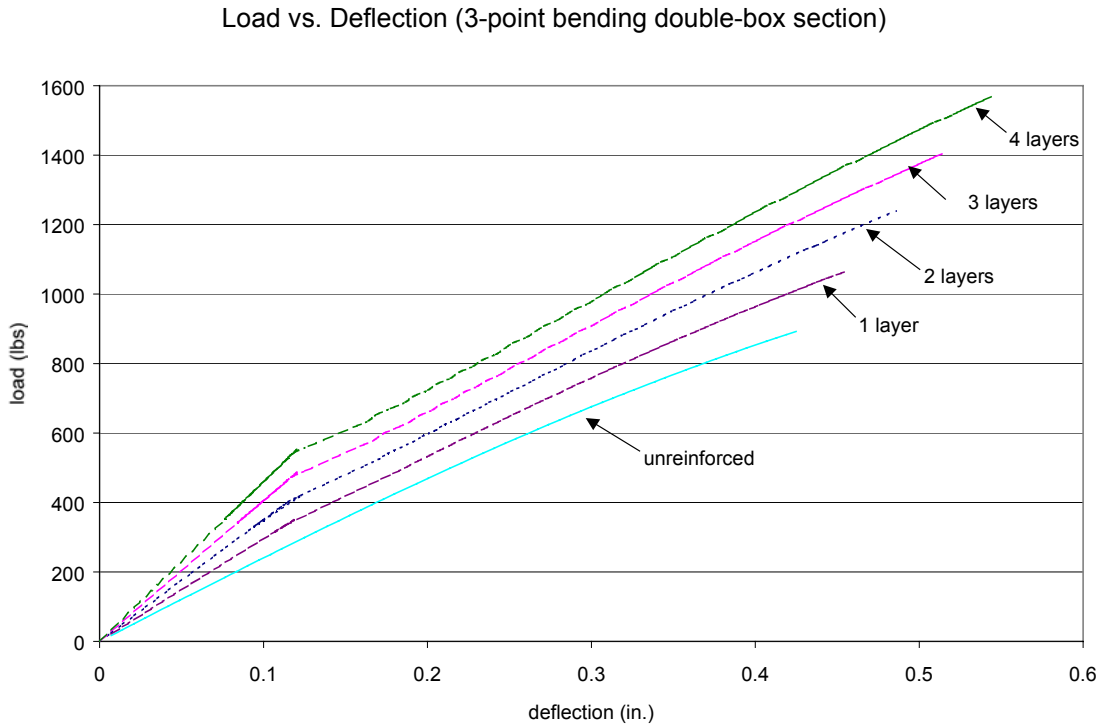

Figure 4.34: Load-displacement for various quantities of reinforcing for PVC double-box

Because WPC sections can be extruded in hollow net section forms, the section shape and configuration may be refined to make efficient use of the tensile reinforcing in the WPC material. One method to accomplish this would be to add compressive area to the section. Figure 4.35 shows the results for the double-box section reinforced with two layers with 15% and 30% more compressive area with respect to the total area of the cross-section. For this HDPE section, increases in maximum load and displacement are obtained with increasing reinforcement. For these applications, the section is no longer over-reinforced. This is evident in Figure 4.36 which shows the neutral axis shift for the two layer reinforced section and the two layer reinforced section with 30% more compressive area. At failure, the neutral axis is located

nearer the center of the section for the piece with the additional compressive area, which indicates a more efficient section in terms of the material strengths.

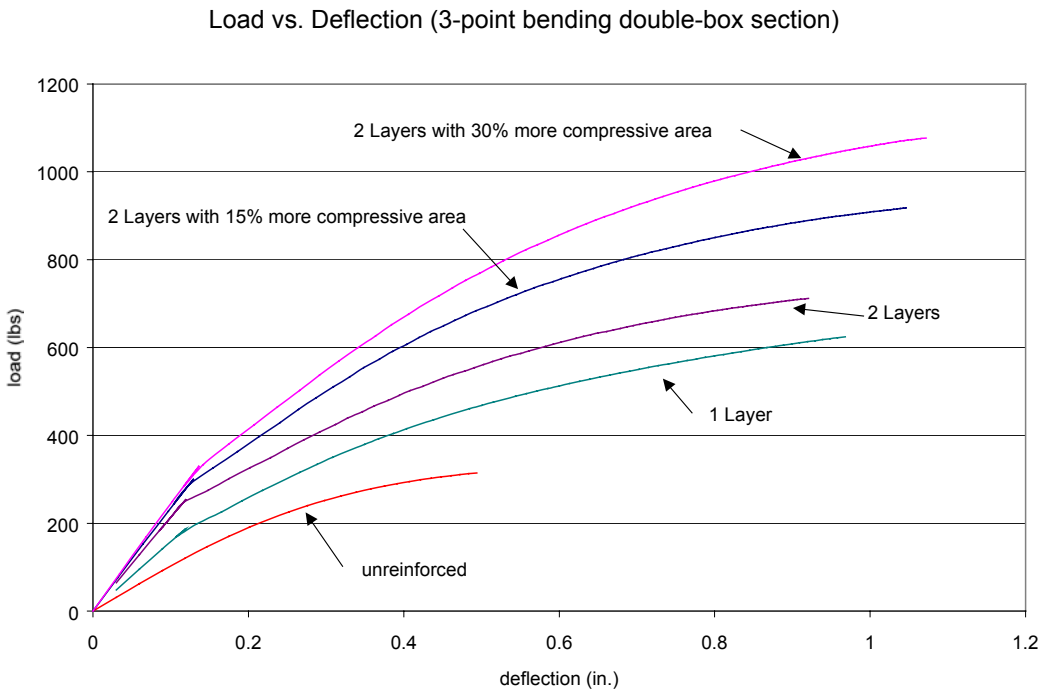

Figure 4.35: Load-displacement for HDPE double-box with additional compression area

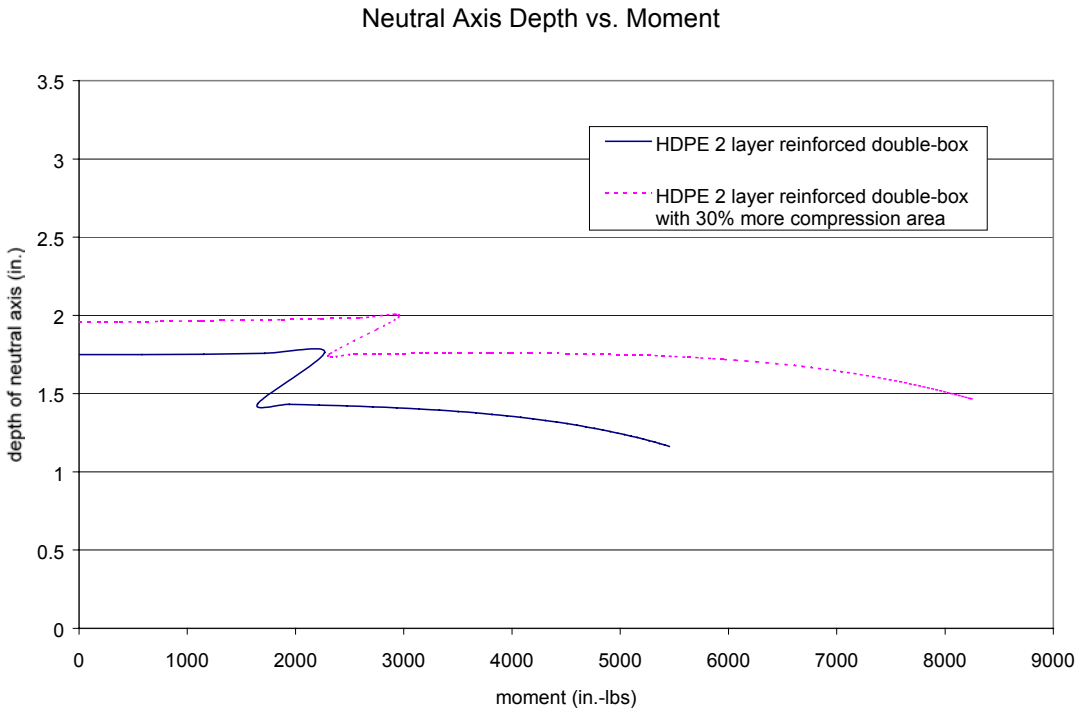

Figure 4.36: Neutral axis shift for 2 layer reinforced sections

4.9 Conclusions

The program MPHIWPC enabled an improved understanding of the WPC material and the behavior of WPC flexural members. The program provides insight into the load-displacement response, the distribution of stress though the depth, the shift of the neutral axis as loading occurs, and the effects of reinforcement on flexural response. Based on the comparisons of test results to predicted results using the program, MPHIWPC provides a very good prediction of the flexural response for both nonreinforced and reinforced WPC sections. In addition, the program enables the comparison of strength and ductility for various section shapes, reinforcement quantity, and reinforcing arrangement. This will aid in the design process for WPC flexural members and allow section configurations to be more easily refined for more efficient structural performance.

The comparison of flexural test results for coupon specimens to program predictions indicates that possible causes for the differences in strength may be due to size effects, shape effects due to section geometry, and production effects during extrusion. To investigate size and geometry effects on strength, the program was modified to allow the WPC material to soften upon reaching the ultimate strains. Since coupon section are solid they may be expected to redistribute stress more than hollow net sections. The results showed that the program can predict fairly well the behavior of solid PVC coupon section with the material softening capability incorporated in the program. However, program results for the HDPE coupon section continued to show significant differences in strength and displacements from the experimental test data. These differences may be the result of the inability of the program to capture the effects of plastic hinge formation in the HDPE material, or they may be due to production effects during extrusion of the sections.

CHAPTER 5

ASSIGNMENT OF ALLOWABLE WOOD-PLASTIC COMPOSITE DESIGN VALUES

5.1 Abstract

This chapter outlines proposed procedures for determination of allowable design values for the design of wood-plastic composite (WPC) structural members. The proposed procedures are applied to experimental results obtained from tests of near full-size WPC specimens to obtain allowable design values for high-density polyethylene (HPDE) and polyvinyl chloride (PVC) formulations. These allowable design values were used in the design of prototype components for the demonstration applications of this project.

5.2 Introduction

Other ongoing activities in this project have included development of a draft set of ASTM standard procedures for assignment of design values for WPC (draft D WPC, 1999) materials. The proposed specifications were adapted from traditional timber design value assignment procedures. Allowable design values were determined for HDPE and PVC formulations using the results of tests performed on a limited number of near full-size specimens. The HDPE formulation consisted of 70% wood and 30% HDPE and the PVC formulation consisted of 50% wood and 50% PVC. The allowable design values established in this chapter were intended for use only in demonstration projects of this research. However, the procedures used to develop the allowable design values do provide guidance for future use in determining design values for use in the design of WPC components.

5.3 Characteristic Design Values

The proposed standard suggests using a nonparametric lower fifth percentile tolerance limit, with 75 percent confidence as a characteristic design value, and requires a minimum of 28 test specimens (ASTM D 2915 section 3.4.3.1). Using this method the lower fifth percentile is estimated as the smallest or weakest value from the 28 test specimens. To obtain a lower fifth percentile tolerance limit for a fewer number of tests, a parametric one-sided tolerance limit method may be used with an assumption of normally distributed data (ASTM D 2915 section 3.4.3.2). This method varies from the proposed procedure in that the characteristic design value, B, is affected by the variance observed in the material. Using the parametric one-sided method, the characteristic design values for bending (F_b), shear (F_v), compression perpendicular to extrusion ($F_{c\text{-}perp}$), and compression parallel to extrusion ($F_{c\text{-}par}$) may be calculated using the following equation:

$$B = x - x\left(k\left(\frac{s}{x}\right)\right) \qquad (1)$$

Where:

B = Characteristic design value;

x = mean value of specimen tests;

k = confidence level factor (ASTM D 2915 Table 3); and

s = standard deviation of specimen values

5.4 Method for Allowable Design Value Assignment

The proposed standard specifies the allowable design values, F_a, be calculated according to the following formula:

$$F_a = BC_aC_tC_mC_v \qquad (2)$$

Where:

B = Characteristic design value;

C_a = property adjustment from Table 5.1;

C_t = temperature adjustment factor;

C_m = moisture adjustment factor; and

C_v = volume adjustment factor in accordance with Annex A1 of ASTM D 5456

5.5 Property Adjustment

The property adjustment factors given in Table 5.1 include factors for both safety and load duration. These factors were originally developed for the assignment of structural lumber allowable design values. Research is currently underway to define the load duration response for WPC members. Pending the results from this effort, it is proposed that the same property adjustments as those used for wood be used for WPC members.

Table 5.1: Property adjustment factors

Property	Adjustment factor C_a
Apparent Modulus of Elasticity	1.000
Bending Strength	0.476
Tension Strength Parallel to extrusion	0.476
Compression Strength Parallel to extrusion	0.526
Compression Strength Perpendicular to extrusion	0.599
Shear Strength	0.317

5.6 Temperature Adjustment

The temperature adjustment factor was estimated from available test data for HDPE specimens. A limited number of bending tests were conducted at the Washington State University Wood Materials and Engineering Laboratory (WMEL) at various temperatures to evaluate temperature effects in wood-plastics. The data and results were used to evaluate the changes in strength with respect to room temperature (68 degrees Fahrenheit). Based on these tests, a 25% loss in the modulus of rupture (MOR) was observed at 122 degrees, and a 30% increase in MOR was observed for specimens tested at 6 degrees. Figure 5.1 shows a plot of data and the trend of the temperature effects taken from the results obtained from tests conducted at WMEL. Three specimens were tested at each temperature for each formulation.

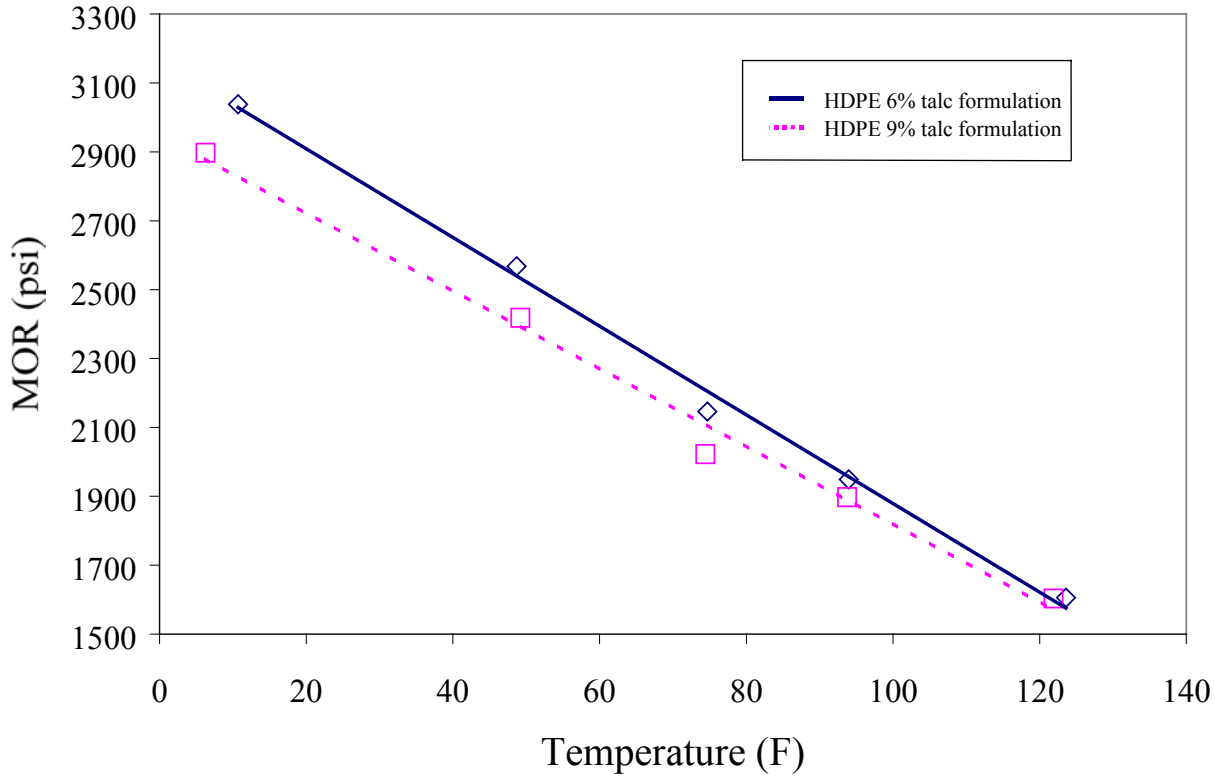

Figure 5.1: Temperature effects on modulus of rupture.

Table 5.2 lists proposed factors for adjusting strength due to temperature effects for various ranges of temperatures expected in service. The draft standard maintains that the adjustment factor found for bending strength may be used for all strength properties for which design values are to be assigned. Of note is the fact that the 25 percent loss in strength at high temperature is similar to the adjustment factor used for wood members at similar temperatures.

Table 5.2: Temperature adjustment factors for strength

Temperature Adjustment, C_t	
In Service Expected Temperature Exposure (Degrees F)	C_t
$T \leq 100$	0.85
$100 \leq T \leq 130$	0.75
$130 \leq T \leq 150$	0.6

5.7 Moist Service Adjustment

Currently, it is the judgement of other researchers involved in the materials development portion of this project that moisture effects in the above-water components of a WPC fendering system will be minimal. Hence, no moisture factor was applied to the characteristic design values of this report.

5.8 Volume Adjustment

No volume factor was applied to the characteristic design values since the tested specimens were approximately equivalent to the expected size of the prototype fendering components. Volume effects may be better characterized with further research currently being conducted to model the behavior of hollow WPC beam sections.

5.9 Allowable Design Values

The characteristic design values for both HDPE and PVC materials were determined from tests using five near full-size sections for each test and are reported in Chapter 3 of this thesis. These values must then be adjusted by a series of factors prescribed by the draft standard, which account for load duration, safety, temperature effects, moisture effects, and volume effects in the material.

Allowable design values for bending (F'_b), shear (F'_v), compression perpendicular to extrusion ($F'_{c\text{-}perp}$), and compression parallel to extrusion ($F_{c\text{-}par}$) were calculated for the PVC and HDPE formulations that were tested and are presented in Table 5.3.

Table 5.3: Allowable design values

Property	HDPE	PVC
Bending Strength	597 psi	1544 psi
Shear Strength	261	545
Compression Strength Parallel to extrusion	801	2660
Compression Strength Perpendicular to extrusion	1473	3421

5.10 Conclusions

Allowable design values for HDPE and PVC material formulations were established using test data from tests conducted on near full-size WPC specimens. The proposed nonparametric lower fifth percentile tolerance limit procedure, with 75 percent confidence as a characteristic design value, was substituted with a parametric one-sided tolerance limit method with an assumption of normally distributed data. This was done due to an insufficient number of test specimens to fully carry out the proposed procedures.

Characteristic design values for strength were determined using the substitute procedure and were adjusted for safety, load duration, and temperature. No adjustments were made for moisture or volume effects. The allowable design values are presented in Table 5.3. These allowable design values were used in the design of prototype components for demonstration applications of this project.

CHAPTER 6

ANALYSIS AND DESIGN OF WOOD-PLASTIC DECKBOARD SECTION

6.1 Abstract

This chapter is a summary of the analysis and design of the decking system at the Newport Naval Undersea Weapons Center (NUWC) Pier 171. The deck is to be replaced as a demonstration project for the wood-plastic composite (WPC) material. The objectives were to analyze the decking and the support system while subjected to specific load requirements then, using design values determined from material testing and design value assignment procedures, provide information needed for the deckboard section design.

6.2 Introduction

Appropriate structural models were developed to determine the demand expected for the deckboards. Figure 6.1 shows the pier deck and some of the supporting structural elements. The boards were modeled as beam elements using the computer program COSMOS/M version 2.00 to account for shear effects in the material (Figure 6.2). As a means of verification, a plane stress analysis was also performed and conveyed results within ten percent of the beam element model. The plane stress model was also done using COSMOS/M version 2.00 (Figure 6.3). The material properties of the polyvinyl chloride (PVC) wood composite material were used in the analysis since this is the most likely candidate material for the deckboards.

The load requirements for the deck surface are as follows:

- 600 psf anywhere on the deck surface; and
- 16000 lbs single wheel load from a forklift.

- The support structure is 6 in.x12 in. treated timbers spaced about 24 in. on center with a variance of a few inches. This results in an average clear span of about 18.5 in.

Figure 6.1: Pier deck and support elements

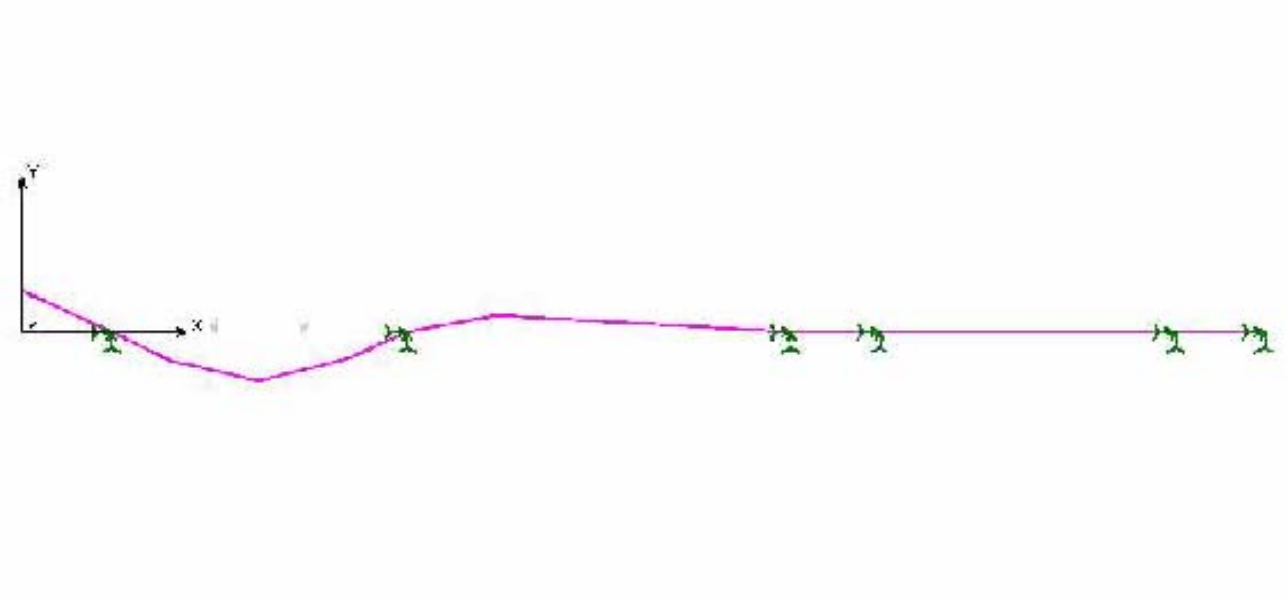

Figure 6.2: Cosmos beam element model deflected shape

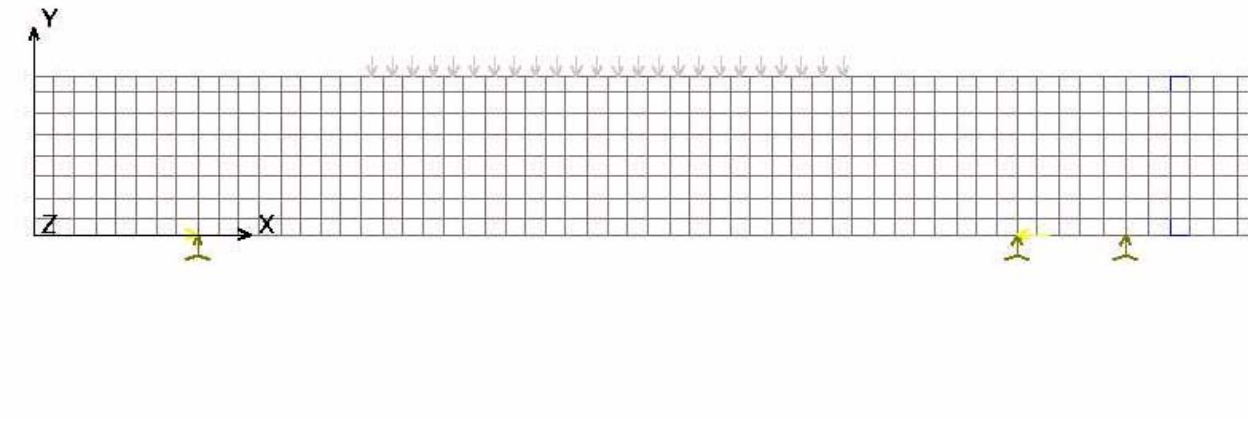

Figure 6.3: Cosmos plane stress model

6.3 Analysis

The critical load case for compression was with the 16000-lb wheel load located directly over a single stringer. The critical load case for bending and shear occurred with the 16000-lb wheel load located at the center of an end-span. Figure 6.2 shows the deflected shape of the Cosmos beam element model. As a simplified and slightly conservative approach, the 16000-lb load was assumed to act on a single 12-in. wide deckboard. This creates a 12-in. square contact area with a required tire pressure of 110 psi. Since the demonstration deckboard is expected to have a 6 in. width to meet current production capabilities, this reduces the load to a maximum 8000 lbs on a single board. The plane stress model and the deflected shape are shown in Figure 6.3 and Figure 6.4, respectively.

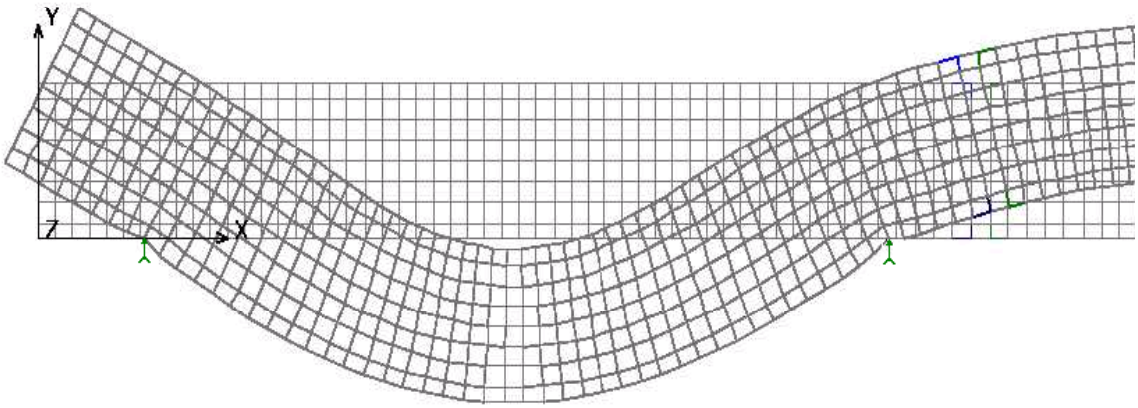

Figure 6.4: Plane stress model deflected shape

Analyses were conducted for wheels on a single span and consecutive spans in the event of a loaded forklift straddling a stringer. A clear spacing of 20 in. rather than the 18.5 in. was

used to account for variability in the spacing of the stringers. The stringers were modeled as two pin supports 6 in. apart to simulate the bending of the planks over the stringer corners. However, since the spikes used to fasten the deckboards to the stringers are not expected to provide uplift resistance, the deckboard was not restrained with pin supports at exterior stringer edges of the loaded span (See Figure 6.2). The maximum loads and stresses from the analysis are shown in Table 6.1. Figure 6.5 shows the normal stresses from the plane stress analysis and Figure 6.6 shows the shear stresses from the plane stress analysis.

Table 6.1: Loads, stresses, and allowable design stresses

	Load	Stress	Allowable Design Stress
Moment	21,000 in.-lbs	1706 psi	1747 psi
Shear	4000 lb	506 psi	580 psi
Comp. Perp.	8000 lb	484 psi	1985 psi

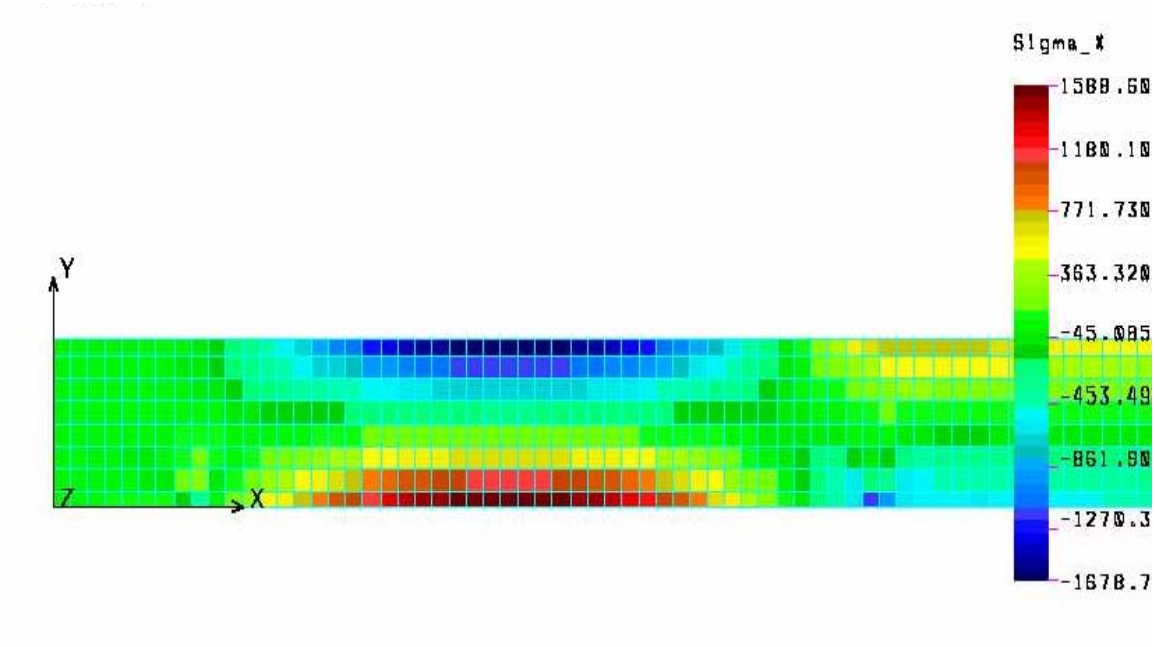

Figure 6.5: Flexural stresses from plane stress model

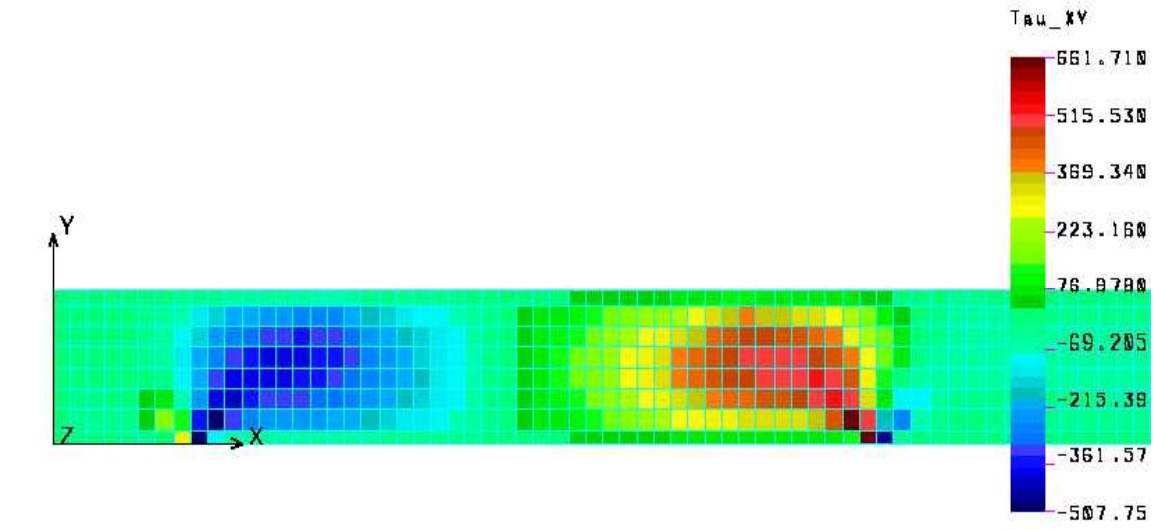

Figure 6.6: Plane stress model shear stresses

6.4 Deckboard Section Design

For the determination of design values, a draft ASTM standard for assignment of design values for wood-plastic composites was used (draft D WPC, 1999). The specification was used to determine design values for the PVC material considering the deckboard application. Allowable design values for bending (F'_b), shear (F'_v), and compression perpendicular to extrusion ($F'_{c\text{-}perp}$) were calculated and are presented in Table 6.1 along with the loads and stresses from the analysis. These design values are slightly different from those for PVC material presented in Chapter 5. This is due to limited data available for assigning an adjustment factor for temperature at the time of the deckboard design. However, the differences in the allowable design values are very small.

6.5 Conclusions

Based upon calculated service stresses and utilizing proposed allowable design values, the design of the deckboard cross-section of the NUWC Pier 171 was performed. A goal of the design was to minimize the amount of material required in the section. This resulted in a minimum moment of inertia (I) of 23.5 in^4 and a minimum net web thickness (t) of 2.5 in. The final deckboard design, developed by the other researchers in this project, is shown in Figure 6.7.

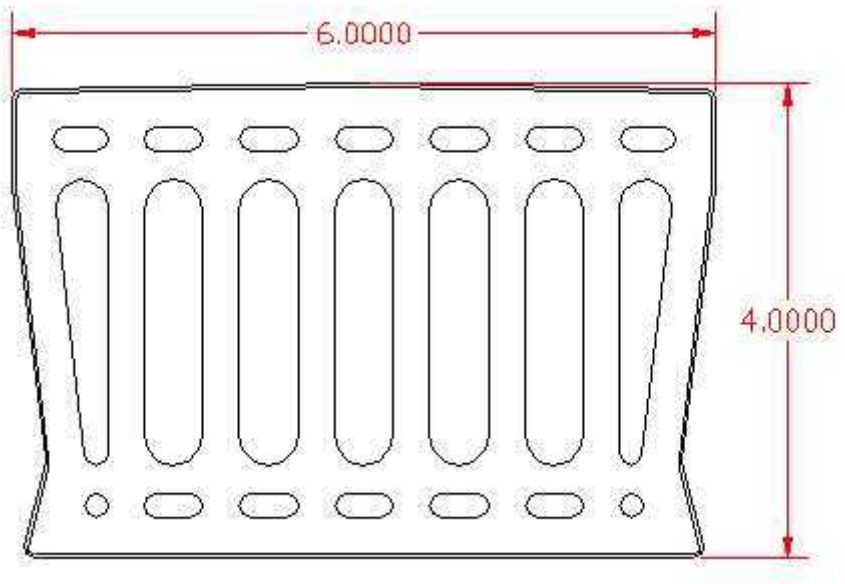

Figure 6.7: Deckboard section design

CHAPTER 7

CONCLUSIONS

7.1 Summary

The purpose of this research was to characterize the performance of wood-plastic composites (WPC) for use in fender system component design. The specific goals of this research included determining adequate test procedures for WPC materials, characterizing material behavior and strengths, and determining allowable design values for use in designing WPC prototype fender system components. The goals of this research also included developing a method for analyzing and predicting flexural strength and behavior to aid in the design of WPC prototype fender system components such as chocks, wales, and piles.

Test procedures were developed for testing WPC members and determining strength properties for the material. The specific strength properties considered were modulus of rupture (MOR), compression parallel-to-extrusion strength, compression perpendicular-to-extrusion strength, beam shear strength, shear strength parallel and perpendicular to extrusion, shear strength by Iosipescu shear fixture, puncture strength, and resistance to impact by a falling weight.

Based on the proposed test procedures, tests were conducted on near full-size WPC sections to determine strength for prototype WPC structural elements. The specimens were selected to be representative of the components expected to be used in fendering systems. Two WPC formulations were evaluated: an HDPE formulation consisting of approximately 70% wood and 30% HDPE, and a PVC formulation consisting of 50% wood and 50% PVC. The specimens consisted of a rectangular three-cell box section and were tested in both the flat-wise and edge-wise orientations.

A Fortran program (MPHIWPC) was developed to characterize behavior for WPC beam sections. The program uses constitutive stress-strain relationships for the WPC and reinforcing materials to predict strength and ductility for various nonreinforced and reinforced cross-sections. The program provides insight into the load-displacement response, the distribution of stress though the depth, the shift of the neutral axis as loading occurs, and the effects of reinforcement on flexural response. The program has also enabled an improved understanding of the general behavior of WPC sections and will in the future assist in the design of WPC flexural members.

Allowable design values were determined for HDPE and PVC formulations using a draft set of ASTM standard procedures for assignment of design values for WPC materials (draft D WPC, 1999). The design values were used in the analysis of a decking system at the Newport Naval Undersea Weapons Center (NUWC) Pier 171 to provide information needed for deckboard section design. The design values may also be used for design of prototype fender system components such as chocks, wales, and piles.

7.2 Conclusions

Based on the experimental tests of wood-plastic composite members presented in this thesis, material strength values were established for the design of prototype fender system components. The test results provide a basis for comparison of strength, apparent stiffness, and the energy dissipated during loading between the HDPE and PVC formulations. The comparison of behavior for each test for the two formulations shows that the PVC formulation is from 2 to 4 times stronger and from 2 to 3 times stiffer than the HDPE formulation. The comparison of

energy absorbed for each test for the two formulations shows that the PVC formulation will absorb from 1 to 1.5 times more energy than the HDPE formulation.

The comparisons between near full-size section test results and predicted results using program MPHIWPC indicate that the program provides a very good prediction of the flexural response of nonreinforced and reinforced WPC sections. The program will aid the design process for WPC flexural members by enabling the comparison of strength and ductility for different section shapes, reinforcement quantity, and reinforcing arrangement. This may ease the refinement of WPC sections for more efficient structural performance.

Some differences in apparent strength existed between hollow section and solid coupon test results. Previous studies have attributed these differences to size and/or geometry effects. The program, MPHIWPC, was modified to investigate size and geometry effects on strength by allowing the WPC material to soften upon reaching the ultimate strains. Since coupon sections are solid, they may be expected to redistribute stress more than hollow net sections with softening of the material. Results with softening showed that the program can predict fairly well the behavior of solid PVC coupon. Program results for the HDPE coupon section, however, continued to show significant differences in strength and displacements from the experimental test data. These differences may be the result of the inability of the program to capture the effects of plastic hinge formation in the HDPE material.

7.3 Recommendations

The following recommendations are provided as possible further refinement for the MPHIWPC program:

1. Provide more comparisons between program predictions and physical test results for fiber reinforced specimens. Currently, only the double-box reinforced section test results are available for comparison.
2. Modify the program to incorporate more load scenarios. At present, the program can only analyze bending for 3-point and 4-point load cases. Fender systems are subject to various load cases and the capability to analyze these would be beneficial in the development of prototype components.

REFERENCES

American Society of Testing Materials, 1998. Standard test methods of static tests of lumber in structural sizes. ASTM D 198. ASTM. Philadelphia, PA.

American Society of Testing Materials, 1998. Standard test methods for flexural properties of unreinforced and reinforced plastics and electrical insulating materials. ASTM D 790. ASTM. Philadelphia, PA.

American Society of Testing Materials, 1998. Standard methods of testing small clear specimens of timber. ASTM D 143. ASTM. Philadelphia, PA.

American Society of Testing Materials, 1998. Standard test method for compressive properties of rigid profiles. ASTM D 695. ASTM. Philadelphia, PA.

American Society of Testing Materials, 1998. Standard test method for shear properties of composite materials by the v-notched beam method. ASTM D 5379. ASTM. Philadelphia, PA.

American Society of Testing Materials, 1998. Standard test method for shear strength of plastics by punch tool. ASTM D 732. ASTM. Philadelphia, PA.

American Society of Testing Materials, 1998. Standard test method for impact resistance of polyvinyl chloride rigid profiles by means of a falling weight. ASTM D 4495. ASTM. Philadelphia, PA.

American Society of Testing Materials, 1998. Standard practice for evaluating allowable properties for grades of structural lumber, Sections 3.4.3.1 and 3.4.3.2 ASTM D 2915. ASTM. Philadelphia, PA.

American Society of Testing Materials, 1998. Standard specification for evaluation of structural composite lumber products. ASTM D 5456. ASTM. Philadelphia, PA.

Draft ASTM standard, 1999. Standard specification for establishing design values for wood-plastic composites. Designation: D WPC.

Hoyle, R. J., Jr. and Woeste, F. E. 1989. Wood Technology in the Design of Structures, fifth edition, Iowa State University Press, Ames, Iowa 50010.

Lockyear, Scott, Masters Thesis Chapter 3 and Appendix B. *Mechanical Analysis of Transversely loaded Wood/Plastic Sections*, 1999.

Paynter, Monique, Master Thesis Chapter 5. *Wood Based Composite Members for Waterfront Fendering Systems*, 1998.

Rammer, D.R.; Soltis, L.A. 1994. Experimental shear strength of glued-laminated beams. Research Paper. FPL—RP—527. Madison, WI: U.S. Department of Agriculture, Forest Service, Forest Products Laboratory.

Zoltek, (1999) Internet web page, URL: http://www.zoltek.com/carbon_fiber_products/continuous_fiber.shtml

Appendix A

Method for determining span length for flexural tests

The displacement equations below are for four-point bending with loading at the third points and characterize the displacement at the midspan:

$$\Delta_b = \frac{23PL^3}{1296EI} \qquad (1)$$

$$\Delta_s = \frac{PL}{6GAk} \qquad (2)$$

Where,

I = Moment of inertia of the cross section about horizontal axis

L = Total length of the beam

P = Applied load

E = Modulus of elasticity

G = Shear modulus

k = shape factor

A = Gross cross section area

D_b = Displacement due to bending (moment)

D_s = Displacement due to shear

r = least radius of gyration

Setting shear displacements equal to five percent of the bending displacements (Hoyle and Woeste 1989) and simplifying yields:

$$\Delta_s \leq 0.05\Delta_b \qquad (3)$$

$$\frac{PL}{6GAk} \leq 0.05\frac{23PL^3}{1296EI} \qquad (4)$$

$$\frac{1}{GAk} \leq 0.05\frac{23L^2}{216EI} \qquad (5)$$

Now, substitute equation 6 into equation 5 and solve for l/r:

$$I = r^2 A \qquad (6)$$

$$\left(\frac{4320}{23}\frac{E}{Gk}\right)^{1/2} \leq \frac{l}{r} \qquad (7)$$

The E/Gk ratio must be determined from procedures outlined in ASTM D 198 (1997) Appendix X4. When a value for E/Gk is unavailable a conservative value of 30 may be used to determine a span length for testing. This may be done as follows:

$$\left(\frac{4320}{23}\frac{30}{1}\right)^{1/2} \leq \frac{l}{r} \qquad (8)$$

$$\left(\frac{4320}{23}\frac{30}{1}\right)^{1/2} r \leq l \qquad (9)$$

Appendix B

Alternate method for determining span length for 5-point shear test given section properties and estimates for shear strength, τ, and bending strength, σ.

$$\tau = \frac{V_{\max} Q}{Ib} \quad (1)$$

$$V_{\max} = \frac{11P}{32} \quad (2)$$

$$\sigma = \frac{M_{\max} y}{I} \quad (3)$$

$$M_{\max} = \frac{3PL}{64} \quad (4)$$

Where,

τ = Bending shear strength of the material

σ = Bending strength of the material

V_{max} = Maximum shear in the beam

Q = First moment of area of the cross section about horizontal axis

I = Moment of inertia of the cross section about horizontal axis

b = Total width of the specimen at the location of interest

M_{max} = Maximum moment in the beam

y = Distance from neutral axis to extreme tensile fiber

L = Total length of the beam

P = Total load on the beam

Substituting equation 2 into 1, and equation 3 into 4, and solving for P in equation 1, and solving for L in equation 3 yields:

$$P = \frac{32\tau Ib}{11Q} \qquad (5)$$

$$L = \frac{64\sigma I}{3Py} \qquad (6)$$

Given values for τ, σ, and section properties, the load P to produce a shear failure may be calculated from equation 5. This value of P is then substituted into equation 6, which gives the maximum span length to ensure a shear failure rather than a bending failure. The equation for span length can be simplified as follows:

$$L < \frac{22\sigma Q}{3y\tau b} \qquad (7)$$

Appendix C: Program MPHIWPC

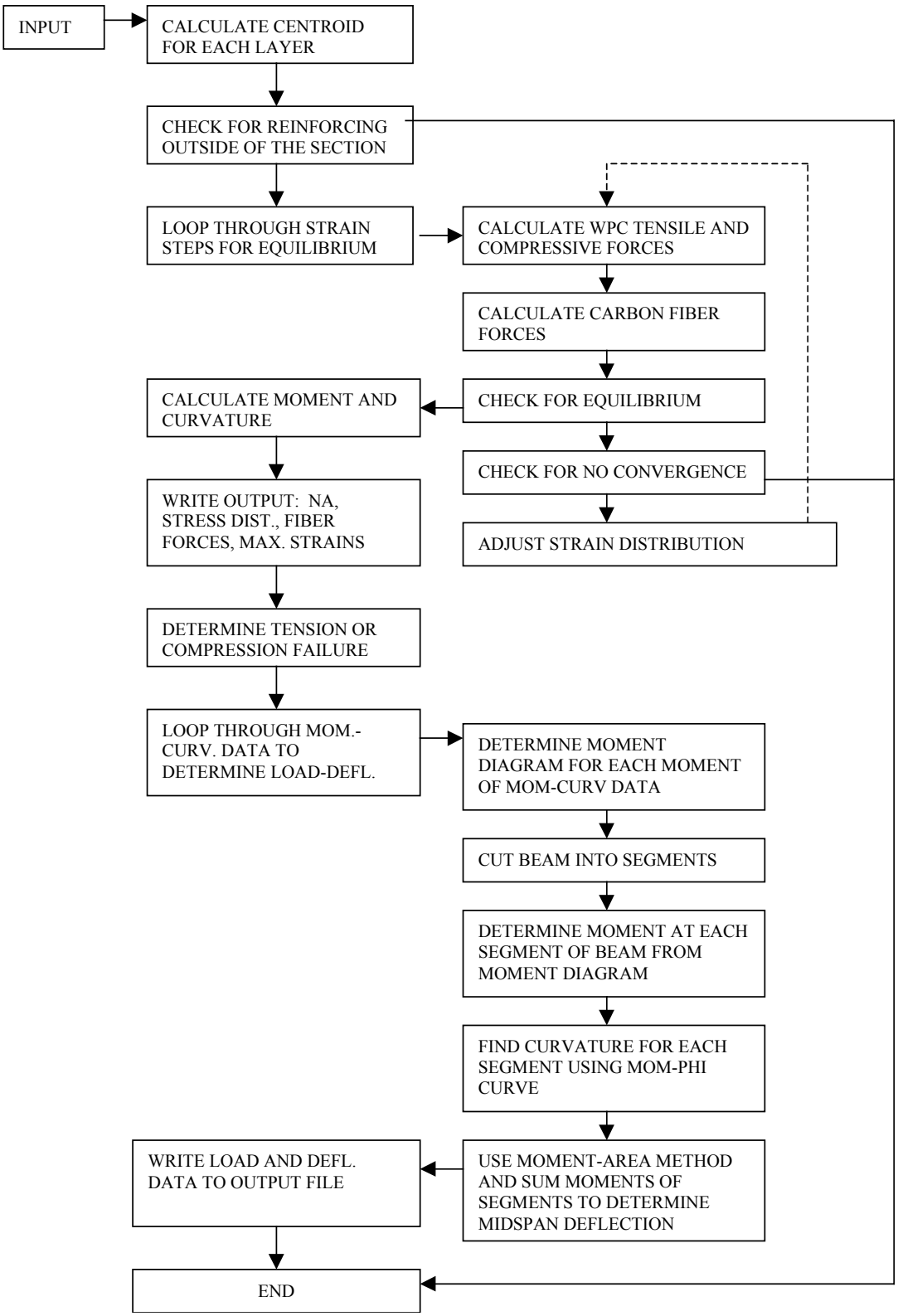

```
PROGRAM MPHIWPC
C
C  ************************************************************
C
C  MOMENT-CURVATURE    KEVIN HAIAR  01/27/2000  WASH. STATE UNIV.
C
C
C   VERSION 1.0       MOMENT-CURVATURE, STRESS DISTRIBUTION AND
C                      LOAD-DEFLECTION FOR VARIABLE SPAN 4-POINT
C                      BENDING OR 3-POINT BENDING, FOR WPC MEMBERS
C                      WITH OR WITHOUT CARBON FIBER REINFORCING
C
C  THIS PROGRAM GENERATES THE POINTS FOR A PLOT OF MOMENT VS.
C  CURVATURE FOR A WOOD-PLASTIC COMPOSITE (WPC) CROSS-SECTION
C  SUBJECTED TO MONOTONICALLY INCREASING MOMENT.
C
C  CROSS SECTIONS MAY BE ANY SHAPE AND SIZE, BUT MUST BE MANUALLY
C  CUT INTO LAYERS AND EACH LAYER HEIGHT AND WIDTH MUST BE
C  DETERMINED AND STATED IN THE INPUT FILE
C
C  THE BEHAVIOR OF THE WPC IS BASED ON A HYPERBOLIC TANGENT
C  STRESS-STRAIN RELATIONSHIP FOR BOTH TENSION AND COMPRESSION
C
C  THE INPUT IS READ FROM A FILE ASCRIBED TO 'WPCIN' AND THE OUTPUT
C  IS READ INTO FILES ASCRIBED TO 'WPCOUT' AND 'DATA'.
C
C  EACH LAYER IS ASSIGNED A STRAIN FOUND FROM A SET STRAIN AT THE
C  OUTERMOST COMPRESSIVE FIBER AND AN ASSUMED SLOPE OF THE STRAIN
C  DISTRIBUTIONS.  CARBON FIBER REINFORCING IS ASSIGNED A STRAIN
C  ACCORDING TO LOCATION IN THE DEPTH.
C
C  FROM THESE STRAINS THE LAYER FORCES ARE FOUND. AN EQUILIBRIUM
C  CHECK
C  IS PERFORMED AND THE SLOPE OF THE STRAIN DISTRIBUTION IS ADJUSTED
C  UNTIL EQUILIBRIUM IS SATISFIED.  THEN THE MOMENT AND CURVATURE ARE
C  CALCULATED AND STORED.  THE STRESS DISTRIBUTION IN THE WPC AND THE
C  STRESS, STRAIN, AND FORCE IN THE FIBER LAYERS ARE WRITTEN TO THE
C  WPCOUT
C  OUTPUT FILE FOR EACH STRAIN INCREMENT. THE OUTER FIBER COMP. STRAIN
C  IS
C  THEN INCREMENTED AND THE PROCESS IS REPEATED UNTIL ALL STRAINS
C  BETWEEN
C  0.0 AND ULTIMATE ARE ACCOUNTED FOR.
C
C   INPUT VARIABLE DEFINITION:
C
```

```
C  BP-BENDING PARAMETER (3-POINT OR 4-POINT BENDING)
C  A1-COMPRESSION PARAMETER FOR TANH
C  B1-COMPRESSION PARAMETER FOR TANH
C  A2-TENSION PARAMETER FOR TANH
C  B2-TENSION PARAMETER FOR TANH
C  ECULT-COMPRESSION FAILURE STRAIN
C  ETULT-TENSION FAILURE STRAIN
C  NL-NUMBER OF LAYERS INTO WHICH THE BEAM IS CUT
C  NSTEP-NUMBER OF STEPS (STRAIN INCREMENTS) TO CONSIDER
C  HL(I)-HEIGHT OF LAYER I (TOP TO BOTTOM)
C  WL(I)-WIDTH OF LAYER I
C  L-SPAN LENGTH OF BEAM IN BENDING
c  AFL(I)-AREA OF FIBER LAYER I
C  TENE-TENSILE MOE FOR FIBER
C  COMPE-COMPRESSIVE MOE FOR FIBER
C  MAXTEN-MAXIMUM TENSILE STRAIN FOR FIBER
C  MAXCOMP-MAXIMUM COMPRESSIVE STRAIN FOR FIBER
C  DCFL(I)-DEPTH TO CARBON FIBER LAYER I
C  NCFL-NUMBER OF CARBON FIBER LAYERS
C  CF-FIBER REINFORCING PRESENT (1) OR NOT (0)
C
C  ***************************************************************
C
C
     CHARACTER*80 TITLE
          REAL A1,A2,B1,B2,ECULT,ETULT,HL,WL,DCL,M,TH,QTOP,QBOT,TF,
          .QCHANGE,SLOPE,PHI,NA,E,F,S,L,MM,PHIPHI,MINIL,DIST,MOMAREA,
          .MSLOPE,MB,P,PHIB,FBRSTN,AFL,FBRSS,FFORC,TENE,COMPE,MAXTEN,
          .MAXCOMP,DCFL,QTOPW,FAILSLOPE
          Integer NL,NSTEP,COUNT,FLAG,I,J,K,COUNTER,NCFL,CF,BP,DNSTEP,
          .FLAGG,SOFT
     DIMENSION HL(200),WL(200),DCL(200),E(200),S(200),F(200),
          .MM(200),PHIPHI(200),PHIB(200),AFL(200),FBRSS(200),FBRSTN(200),
          .FFORC(200),DCFL(200)
C
     OPEN (UNIT=10,STATUS='OLD',FILE='wpcin')
     OPEN (UNIT=11,STATUS='unknown',FILE='wpcout')
          OPEN (UNIT=12,STATUS='unknown',FILE='data')
C
C
C  ***************************************************
C
C
C  READ THE INPUT DATA FILE
C
C
```

```
C  READ THE NUMBER OF LAYERS, ULTIMATE COMP AND TEN STRAINS,
C  NUMBER OF STRAIN INCREMENTS, AND HYPERBOLIC TAN PARAMETERS
C
        Read (10,1) Title
1    Format (A80)
        Read (10,*) NL,L,BP
        READ(10,*)ECULT,ETULT,NSTEP,SOFT
        READ(10,*)A1,B1,A2,B2
C
        Write (11,*) Title
        WRITE (11,*)
C
C  READ IN REINFORCING INFORMATION; IF NO REINFORCING PRESENT
C  THEN SKIP TO WPC LAYER DIMENSIONS
C
    READ (10,*) CF
        IF (CF.EQ.0) THEN
        GOTO 5
        END IF
C
C
    READ (10,*) NCFL,TENE,COMPE,MAXTEN,MAXCOMP
C
        WRITE (11,*) 'Fiber Reinforcement Information'
    WRITE (11,*) 'NO.LYRS  TEN.MOE   COMP.MOE   MAXT STRN  MAXC STRN'
        WRITE (11,3) NCFL,TENE,COMPE,MAXTEN,MAXCOMP
3       FORMAT (1X,I3,2X,F14.2,2X,F14.2,1X,F6.4,2X,F6.4)
    WRITE (11,*)
        WRITE (11,*)
C
C READ IN CARBON FIBER LAYER DEPTHS AND AREAS
C
    DO 4 I=1,NCFL
        READ(10,*) DCFL(I), AFL(I)
4       CONTINUE
c
c Read in  WPC layer dimensions
c
5    DO 6 I=1,NL
        READ(10,*) HL(I), WL(I)
6       CONTINUE
C
C  CALCULATE DEPTH TO CENTROID FOR EACH LAYER (FROM TOP)
C
    DO 8 I=1,NL
          IF(I.EQ.1) THEN
```

```
            DCL(I)=(HL(I))/2
          ELSE
            DCL(I)=DCL(I-1)+((HL(I-1)+HL(I))/2)
          END IF
8       CONTINUE
C
        WRITE (11,10) L
        Write (11,11) NL
        Write (11,12) ECult
        Write (11,13) Etult
        Write (11,14) NSTEP
        Write (11,15)
        Write (11,15)
        WRITE (11,17)
10      FORMAT (1X,'Span length of beam',F6.2)
11    Format (1x,16HNumber of layers,I5)
12    Format (1x,'Maximum Compressive Strain (WPC)',F8.4)
13    Format (1x,'Maximum Tensile Strain (WPC)',F8.4)
14    Format (1x,'Number of compressive strain increments',I5)
15    Format (1x)
17      FORMAT (4x,'Moment',5x,'Curvature',5x,'Depth of N.A.',1x,
        .'Top Strain',2x,'Bottom Strain')
C
C  INITIALIZE MOMENT AND TOTAL HEIGHT
C
     M=0.0
    TH=0.0
C
C
     STEPSIZE=ECULT/NSTEP
C
     DO 18 I=1,NL
        TH=TH+HL(I)
18      CONTINUE
C
C  CHECK FOR FIBER REINFORCEMENT OUTSIDE OF THE SECTION; IF SO THEN
C  GET OUT AND PRINT ERROR MESSAGE
C
     DO 19 I=1,NCFL
          IF (DCFL(I).GT.TH) THEN
          WRITE (11,*)
          WRITE (11,*) 'REINFORCEMENT OUTSIDE OF SECTION...'
          WRITE (11,*) 'HAVE SOME MORE COFFEE AND TRY AGAIN'
          GOTO 1001
          END IF
19      CONTINUE
```

```
C
    QTOPW=STEPSIZE*(-1)
    QBOT=(-1)*QTOPW
C
        DNSTEP=2*NSTEP
        FAILSLOPE=(1271)/(.0149)
        FLAGG=0
C
C  START LOOPING THROUGH NSTEP STRAIN INCREMENTS TO FIND
C  MOMENT AND CURVATURE AT EQUILIBRIUM FOR EACH EXTREME
C  COMPRESSION FIBER STRAIN
C
    QCHANGE=STEPSIZE/1000
C
    DO 100 I=1,DNSTEP
        COUNT=0
C
        QTOP=I*STEPSIZE*(-1)
        FLAG=0
        TF=0.0
        M=0
C
20    DO 30 J=1,NL
c
c Calculate slope of strain (curvature) and strain at each layer
C HERE THE SOPE IS THE CHANGE IN STRAIN/DEPTH OF THE BEAM
c
    SLOPE=(QBOT-QTOP)/TH
        E(J)=SLOPE*DCL(J)+QTOP
          IF (E(J).GT.0.0) THEN
              IF (E(J).LT.ETULT) THEN
              S(J)=A2*TANH(B2*E(J))
              END IF
              IF (E(J).GT.ETULT.AND.SOFT.EQ.1) THEN
              S(J)=A2-(FAILSLOPE*(E(J)-ETULT))
              END IF
           END IF
          IF (E(J).LT.0.0) THEN
             IF (E(J).GT.((-1)*ECULT)) THEN
              S(J)=(-1)*A1*TANH(B1*(ABS(E(J))))
             END IF
              IF (E(J).LT.((-1)*ECULT).AND.SOFT.EQ.1) THEN
              S(J)=(-1)*(A1-(FAILSLOPE*((ABS(E(J)))-ECULT)))
              IF (S(J).GT.0) THEN
              GOTO 45
              END IF
```

```
            END IF
          END IF
        F(J)=S(J)*HL(J)*WL(J)
        TF=TF+F(J)
30      CONTINUE
C
C  NOW COMPUTE CARBON FIBER STRAINS AND ADD TO TOTAL TEN AND COMP
C  FORCES
C
C  IF NO CARBON FIBER PRESENT THEN SKIP TO EQUILIBRIUM CHECK
C
    IF (CF.EQ.0.0) THEN
        GOTO 41
        END IF
C
    DO 40 K=1,NCFL
        FBRSTN(K)=SLOPE*DCFL(K)+QTOP
          IF (0.0.LT.FBRSTN(K).AND.FBRSTN(K).LT.MAXTEN) THEN
          FBRSS(K)=FBRSTN(K)*TENE
          GOTO 38
          END IF
            IF ((-1*MAXCOMP).LT.FBRSTN(K).AND.FBRSTN(K).LT.0.0) THEN
            FBRSS(K)=FBRSTN(K)*COMPE
            ELSE
            FBRSS(K)=0.0
            END IF
38      FFORC(K)=FBRSS(K)*AFL(K)
        TF=TF+FFORC(K)
40      CONTINUE
C
C
C  NOW CHECK IF EQUILIBRIUM IS SATISFIED AND ADJUST SLOPE
C  IF NECESSARY
c
41       IF (ABS(TF).LT.1.0) THEN
            GOTO 50
       END IF
C
          IF (TF.LT.0.0) THEN
             QBOT=QBOT+QCHANGE
             TF=0
             GOTO 45
           END IF

                IF (TF.GT.0.0) THEN
            QBOT=QBOT-QCHANGE
```

```
            TF=0
            GOTO 45
          END IF
C
C
45          FLAG=1
        Count = Count +1
              If (count.eq.100000) then
                Write (11,*)
                Write (11,*) 'No convergence... Program terminated'
                WRITE (11,*)
                WRITE (11,*) 'TRY INCREASING NO. OF STEPS (NSTEP)'
                Goto 130
              End if
            GOTO 20
c
C  CALCULATE MOMENT, CURVATURE, NUETRAL AXIS DEPTH, AND
C  EXTREME FIBER STRAINS
C
50      DO 55 J=1,NL
            M=M+F(J)*DCL(J)
55        CONTINUE
C
      IF (CF.EQ.0) THEN
          GOTO 57
          END IF
C
          DO 56 J=1,NCFL
          M=M+FFORC(J)*DCFL(J)
56        CONTINUE
C
57      PHI=SLOPE
          NA=(-1)*QTOP*(1/SLOPE)
          Write (11,58) M,PHI,NA,QTOP,QBOT
58        FORMAT (1X,F10.1,8X,F6.5,8X,F6.4,6X,F8.5,6X,F8.5)
C
    MM(I)=M
        PHIPHI(I)=PHI
c
C  WRITE THE STRESS DISTRIBUTION AND FIBER STRESSES FOR EACH MOMENT
C  TO THE DATA FILE
C
    WRITE (12,*)
        WRITE (12,75) M
75      FORMAT (1X,F10.4)
        Write (12,*) 'Layer Number   Layer Depth   Stress'
```

```
          Do 80 J=1,NL
      Write (12,82) J,DCL(J),s(J)
80     Continue
82    Format (1x,i5,6x,F10.2,8x,F10.2)
C
C
     WRITE (12,*)
         WRITE (12,*) 'LAYER   DEPTH     STRAIN      STRESS        FORCE'
         DO 90 J=1,NCFL
         WRITE (12,92) J,DCFL(J),FBRSTN(J),FBRSS(J),FFORC(J)
90       CONTINUE
92       FORMAT (1X,I3,2X,F8.4,2X,F8.4,4X,F12.2,2X,F12.2)
C
C  CHECK FOR TENSION FAILURE.  IF TENSION FAILURE OCCURS
C  THEN ITERATION IS halted and program terminated
C
C
           COUNTER=I
       IF (QBOT.GT.ETULT.AND.FLAGG.EQ.0) THEN
             Write (11,*)
             Write (11,*) 'TENSION FAILURE'
             WRITE (11,*)
                   FLAGG=1
                  ELSE
                  GOTO 95
            END IF
            IF (QTOP.LT.((-1)*ECULT).AND.FLAGG.EQ.0) THEN
              WRITE (11,*)
              WRITE (11,*) 'COMPRESSION FAILURE'
              WRITE (11,*)
              FLAGG=1
            ELSE
            GOTO 95
            END IF
C
95        IF (SOFT.EQ.0) THEN
          IF (QBOT.GT.ETULT) THEN
                   GOTO 130
                   END IF
      END IF
C
           IF (SOFT.EQ.0) THEN
                IF (QTOP.GT.ECULT) THEN
                     GOTO 120
                     END IF
           END IF
```

```
C
      IF (QBOT.GT.(8*ETULT)) THEN
          GOTO 130
          END IF
C
          IF (QTOP.LT.((-2)*ECULT)) THEN
          GOTO 120
          END IF
C
100     CONTINUE
C
C
C
120     WRITE (11,*)
          WRITE (11,*) 'COMPRESSION FAILURE'
C
C
C
C  LOAD-DEFLECTION CALCULATIONS
C
C  CURVATURE IS DEFINED ALONG THE LENGTH OF THE BEAM AND THE
C  MOMENT AREA METHOD IS USED TO FIND THE MIDSPAN DEFLECTION
C
C
130     DIST=0
          P=0
          MOMAREA=0
          MSLOPE=0
          MB=0
          PHIB=0
          MINIL=L/60
          WRITE (11,*) 'LOAD (LBS)     DEFLECTION (IN)'
          WRITE (11,*)
            DO 150 I=1,COUNTER
              IF (BP.EQ.4) THEN
              P=6*MM(I)/L
              END IF
              IF (BP.EQ.3) THEN
              P=4*MM(I)/L
              END IF
C
C  THE BEAM IS CUT INTO 60 SEGMENTS AND CURVATURE IS CALCULATED
C  FOR EACH SEGMENT
C
               DO 140 J=1,30
               DIST=L*(J)/60
```

```
                IF (BP.EQ.4) THEN
                  IF (DIST.LT.L/3) THEN
                  MSLOPE=P/2
                  MB=DIST*MSLOPE
                  ELSE
                  MB=P*L/6
                  END IF
                 END IF
                 IF (BP.EQ.3) THEN
                  IF (DIST.LE.L/2) THEN
                  MSLOPE=P/2
                  MB=DIST*MSLOPE
                  END IF
                 END IF
C
C  STEP UP MOM-PHI CURVE TO FIND PHI AT EACH SEGMENT BY INTERPOLATING
C  BETWEEN THE NEAREST TWO POINTS
C
          DO 135 K=1,200
           IF (MB.GT.MM(K)) THEN
              GOTO 135
           ELSE
           GOTO 133
133        IF (K.EQ.1) THEN
           PHIB(J)=(MB/MM(K))*PHIPHI(K)
           GOTO 140
           ELSE
           PHIB(J)=PHIPHI(K-1)+((MB-MM(K-1))/(MM(K)-MM(K-1)))*
          .  (PHIPHI(K)-PHIPHI(K-1))
           GOTO 140
           END IF
          END IF
135       CONTINUE
C
C
140    CONTINUE
C
C
C  NOW SUM MOMENTS TO DETERMINE DEFLECTION AT MIDSPAN
C
     DO 145 K=1,30
         MOMAREA=MOMAREA+PHIB(K)*MINIL*MINIL*(K)
145   CONTINUE
C
     WRITE (11,146) P,MOMAREA
146   FORMAT (1X,F10.2,6X,F8.4)
```

```
C
      P=0
           MOMAREA=0
           MSLOPE=0
           MB=0
           DIST=0
           PHIB=0
C
150   CONTINUE

C  ***********************************************
 1001 STOP
      END
```